Fall 12-16-2016

Design of a Modified Stewart Platform Manipulator for Misalignment Correction

Adekunle Ayoko
Bowling Green State University

DESIGN OF A MODIFIED STEWART PLATFORM MANIPULATOR FOR MISALIGNMENT CORRECTION

Adekunle Adeyinka Ayoko

A Master's Thesis

Submitted to the Graduate College of Bowling Green

State University in partial fulfilment of

the requirements for the degree of

Master of Technology Management

December 2016

Committee:

Dr. Mohammed Mayyas, Chair

Dr. Todd C. Waggoner

Dr. Christopher Kluse

ABSTRACT

This thesis work is about the design of a modified Stewart platform manipulator for misalignment correction. The common version of the Stewart platform uses six actuators. The traditional Stewart platform of this kind has a moving top plate and a fixed base plate. However, in this research, the modified design of the traditional Stewart platform is studied. It is designed to be an easy connect-disconnect platform that can wrap around different structures with different cross sections and symmetrically designed. It is able to adjust position easily by using four identical but independent linear actuators populated evenly in two parts fastened to the top and bottom base by ball joints with each part been symmetrical to the other.

To design two symmetrical parts and an adjustable clamp are a major objective of the thesis. One symmetrical part flipped upside down produces the other. The adjustable clamp was printed in 3D and can be used to align regular structural shapes especially circle of various diameter. To correct the misalignment, a failure study was carried out to determine the two equal but opposite loads required to correct misalignment in two plastic beams. Five loads were applied which showed that the smaller the load, the better the misalignment. This study showed that it is better to fix the base at a location where it does not move. To investigate that the modified Stewart platform can resist structure stiffness, the actuator assembly was analyzed using ANSYS software. The results showed that the deformation and maximum stress is less that the structure stiffness, which proves why the assembly can resist structural stiffness. The results support that the modified Stewart platform can be used for misalignment correction.

ACKNOWLEDGEMENT

My immeasurable appreciation and deepest gratitude goes to God almighty who saw me through the completion of this thesis.

I would like to express my sincere appreciation to all for those who extended help, support and contribution in making this research work in one way or another a success. Many thanks to my parents, Johnson and Christianah Ayoko for their interests in me from an early age and for their generous financial support towards my education.

I would also like to thank sincerely my advisor, Dr. Mohammed Mayyas for his advices, guidance, constant supervision and provision in completing this thesis.

My thanks also go to my thesis committee members, Dr. Todd C. Waggoner and Dr. Christopher Kluse for their patience, critical advice and guidance towards the completion of this study.

Not forgetting the faculty, staff and students of the College of Technology, Architecture and Applied Engineering for their support particularly the research team: Mikhail Shilov, Mohammed Almajed, Ahmad Alzayer and Hadi Aqeel for their expertise and cooperation towards the success of this thesis.

Finally, I would like to extend my sincere appreciation to my family and friends, Seun Ayoko, Bukola Ayoko, Bodunde Agboola for providing words of encouragement throughout the research work. My Inestimable thanks also goes to Kehinde Bola for her tremendous support from the start of the thesis to the end, I cannot thank you enough.

NOMENCLATURE

List of symbols

a	position of the structure
B	base of the platform
B_{R_T}	rotation matrix of platform
F_{XB}	force applied to the base on X-axis
F_{XB}	force applied to the base on Y-axis
GT_i, B_i	position vector
k	number of linear actuators
L	relative length of the actuator
l	length of structure to be aligned
l_o	length of Stewart platform
$\dot{L}$ and $\dot{X}$	Velocities of the leg and moving platform respectively
P	Force applied on the structure.
r_{base}, r_p	base and moving platform radii
$\vec{r}_{desired}$	Position of the measured points after alignment
$\overrightarrow{r_m}$	Relative position measured on the misaligned structure
$\vec{r}$	Relative misalignment position measured between two structures
$R_X(\alpha), R_Y(\beta), R_Z(\gamma)$	Rotation matrix for roll, pitch and yaw respectively
$S_{corrected}$	Corrected structure curve
S	Structure
X_{p-o}	Position and orientation of the moving platform
$\vec{V}_{T_J}$	The generalized velocity of the platform connection point of the leg
δ_m	Maximum deflection
θ	Bending angle
θ_p, θ_b	Separation angle between top and base platforms
u_i	Unit vector along the axis of the prismatic joint of link *i*
J_{IB}, J_{IIB}	First and second Jacobian matrix
E	Young modulus
I	Area moment of inertia

TABLE OF CONTENTS

LIST OF FIGURE

Figure page

LIST OF TABLE

Table page

CHAPTER 1: INTRODUCTION

1.1 Context of the Problem

Precision automatic assembly is playing a major role in all sectors of manufacturing industry, the introduction of flexibility and automation are becoming crucial to reduce production time and cost with specified production tolerances. Stewart platforms remain the best known manipulators basically used for precision positioning and vibration control (Hanieh, 2003). They have been that widely studied with several 6-degrees-of-fredom (DOF) parallel manipulators already proposed (Majid, Huang, & Yao, 2000). A manipulator is one of the most commonly used and important mechanism used in industrial applications. Other applications include flight landing control, flight simulator, structure stabilizers, medical fixators and lots more. It is also present in space applications significantly for the use of vibration control of space structures while connecting them rigidly (Hanieh, 2003). It is used to correct misalignment in structures and enables precision positioning of structures in 6D-space. Its high load capacity, high rigidity, high stiffness and high accuracy make them one of the most popular manipulators used both in the commercial and industrial fields. These manipulators are flexible and applicable in most fields.

Coupled with the fact that precision positioning of structures is important, the determinants for operation may put the device to various fault conditions, hence leading to device break down and causing vibrations in mechanical systems. Wrongly aligned equipment such as a bent building structure in construction project, motor shaft alignment will most definitely lead to excessive wear and sudden equipment shutdown due to increased stresses on its parts. In the motor shaft alignment, correct alignment allows for smooth and efficient power transmission while misalignment produces noise, shaft failure, excessive vibration, etc. (Dept. of Energy. Office of Scientific and Technical information, 2005) The Stewart platform manipulator is a possible solution to achieve the required alignment. It is a very important task for industries to stay away from breakdowns. If this task is to be achieved, the manipulator has to be continually monitored to detect faults; vibrations/misalignment in early stages. Detection of this misalignment beforehand enables both the designer and maintenance personnel to take necessary corrective actions at fast pace. The main types of misalignment are found in closed-end and open-end structures. The post processing after alignment could be fastening, welding, etc. Misalignment is the most frequent cause of machine malfunction. They can cause increased vibration and load machine parts for which they have not been initially designed. As a result, it becomes mandatory for both the maintenance and engineering professionals to comprehend misalignment, which results in machine malfunction.

In the past, industrial automation is known for constant change in its design methods with this change linked to the global economics. One of these methods is the design of a precision mechanism which is a conceptual approach to designing precision mechanisms like manipulators, precision equipment, etc. and basically focuses on the mechanical aspects in a mechatronic system context. The use of industrial robots is considered the latest trends in the automation of the manufacturing process (Craig, 1986). As a result, there is a need to develop an assistive robotic mechanism that is easy to install. An assistive robot performs a physical task for the well-being of a person with a disability (Jaffe, Nelson, & Thiemer, 2012). This mechanism will be helpful for elderly and disabled people to support their independent life and in situations of limited care professionals. The mechanism is also seen in the medical industry. For example, robotic nursing assistant, walking assist robots, wheel chair robots and also the Mckesson PROmanager-Rx which is used in the pharmacy stores to dispense solid medications to maximize efficiency and most importantly accuracy.

The current state of the art of Stewart platform is limited to certain applications. However, this new mechanism is aimed to be proposed, released and possibly adopted by industries. Its application generates lots of attention in the industry, as well as the robotic communities. Some of the applications extend to the manufacturing industry, automobile industry, and machine tool technology as in high speed machine tools, car suspensions, medical field including skull and orthopedic surgery and in crane technology. It is also applicable in the automobile industry, for example, in shaft alignment where two or more shafts are aligned together within a tolerated margin. The proposed modified Stewart platform manipulator can provide stability reduce vibration, fault correction, self-alignment especially when wrapped around a deformed structure in a building due to vibrations. This manipulator will consist of reduced actuators (four instead of the usual six), an assembly of two symmetrical parts with the orientation of one flipped upside down, one part base produced and replicated for the other three parts, a spring loaded clamping device that can be used for several cross sectional area unlike other parallel manipulators with predefined specific sizes. It will also be used in closed-end and open-end structures. This modified Stewart platform can be programmed autonomously to reduce the vibrations, improve the stability and even detect a possible fault. The current state of the art cannot be used for some of these applications. As a result, a connect and disconnect platform is to be proposed.

1.2 Statement of the Problem

In this study, the approach for flexible automated assembly mechanism for precision positioning of large structures will be presented by modifying a Stewart platform manipulator. Often structures suffer from slight misalignment due to loading or failure. There is need to develop a mechanism that can accommodate several structural shapes. Such mechanism would undergo a series of automatic correction to adjust position and oriented in 6D-space. Examples of assembly of such large structures include positioning and then welding two misaligned structural beams. In this work, we will focus on the development of a generic prototype fixture automated holding and positioning process of large structures. The automatic process for holding and correcting the position include misalignment measurement, grasping adjustment, 6D-position adjustment and shape adjustment, etc.

1.3 Significance of the Project

This study developed a modular parallel manipulator to correct misalignment in closed structures. The study suggests modifying the design of Stewart platform such that it can be easily reconstructed on the site. This would reduce cost of installing and makes it affordable. In addition, we design a spring loaded clamp that can be adjusted to hold several cross sectional area unlike the other parallel manipulators which are predesigned for specific size. The state of the art Stewart platform have fixed design. Our proposed mechanism is designed to be an easy connect-disconnect platform that can wrap around different structures with different cross sections and also symmetrically designed.

This study finds application in general construction alignment especially in metal construction and vibration reduction. It is also applicable in the medical industry for example, correction of broken bones (Ganem, 2000). In this study, the modified Stewart platform manipulator will be capable of being used in both open-loop and closed-loop structures and will be able to adjust position easily by using four linear actuators.

1.4 Objective of the Study

This paper aims to present the analysis of the dynamic formulation of a modified 6 DOF Stewart platform manipulator by means of a Lagrangian method with the analysis of the rigid body dynamics of both the mechanism and the actuators included in the dynamic model (Bingul & Karahan, 2012). The objectives are defined below.

- To design a modified Stewart Platform manipulator that can be firmly mounted around a cross sectional area (which is as universal as possible) without losing the grip while adjusting the relative position between the two ends of the Stewart platform.
- To define the usage of the modified Stewart platform manipulator for closed-end and open-end structure applications.
- To list the characteristics of the modified Stewart platform for misalignment problems.
- Apply the concept of Stewart platform manipulator to the modified version in order to correct misalignment.
- Study the performance of the proposed modified Stewart platform in comparison to the original Stewart platform.
- To define the significance and importance of the development of analytical tools for such mechanical manipulator.

1.5 Description of the product

In this study, a modified Stewart platform manipulator, which is similar to the traditional Stewart platform manipulator, was designed. This modified Stewart platform manipulator shown in **Figure 1** will have a six DOF parallel mechanism consisting of two platforms, a moving top plate and a fixed base plate. The top and base plates are connected through four identical but independent linear actuators populated evenly in two parts fastened to both the moveable top and fixed base plates by universal joints with each part been identical to the other. Each of the legs contains a precision ball-screw assembly and a DC-motor attached to the end of each leg. These legs have changing combination of leg-platform connections. The length of each leg is variable and can independently control the motion of the top moving platform.

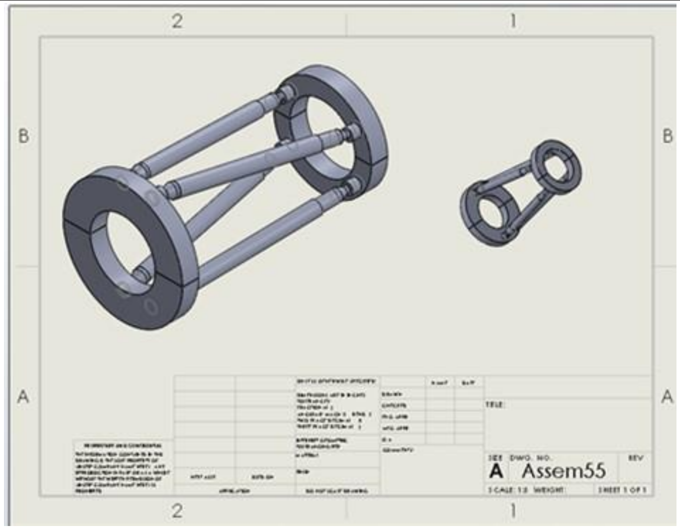

Figure 1: Drawing of the modified SP manipulator.

1.6 Thesis Overview

Chapter one is an introduction to precision automatic assembly and the robotic industry. It introduces the context of the problem, statement of the problem, significance of the project, objective of the study and the product description.

Chapter two gives an overview of the existing literature and history of the Stewart platform, and its application in correcting positioning and accuracy. The first section describes the historical perspective and uses of the Stewart platform, the theoretical topics are described in section two. Finally, the third section describes the current technology.

Chapter three covers the methodology, problem restatement and the mathematics which describes the positions and orientation in 6D-space. This chapter introduces the geometry and numerical algorithm. It deals with the kinematics and kinetics of the speed of the parallel manipulators. Finally, the chapter proposes the theory and mechanism of the modified Stewart platform.

Chapter four addresses the Simulation, experiment and findings. It covers the implementation of the proposed theories in chapter three. This includes testing the rigidity of the structure under static and dynamic loading.

Chapter five covers the results, discussion, and conclusion. This chapter also introduced the future work.

Definitions

1. Angular Constraint: assigning an angular value between any of the following; two points, a point and a line, a point and a plane, or two lines.
2. Actuator: A mechanism that puts something into automatic motion.
3. Distance Constraint: assigning a distance value between any of the following; two points, a point and a line, a point, and a plane, or two lines
4. DOF: Degree of Freedom, is the possible number of independent ways that a dynamic system can move without infringing the imposed constraints and still completely define the position of the system.
5. Finite Element Analysis (FEA): is a numerical technique for performing engineering analysis or finding approximate solutions to boundary value problems for partial differential equations.
6. Inverse Kinematics are kinematic equations used in robotics to determine the joint motion that provides the position and orientation of the end-effector. It is a method back solving for the forces and moments of an object based off of the kinematics of the system
7. Manipulator: A manipulator in robotics is a tooling device that gives a lift assist to help pitch, roll or spin parts in an appropriate placement.
8. MSP: Modified Stewart platform with four actuators
9. SP: Stewart Platform is a type of parallel robot that has six prismatic actuators. A 6 DOF positioning system that uses 6 actuators in parallel to achieve the positioning.

CHAPTER 2: LITERATURE REVIEW

2.1 Historical Perspective of Stewart Platform

The origin of the Stewart platform can be traced back to Stewart's article (Doug, 1965) where he outlined a mechanism with six degrees of freedom (DOF) controlled in any combination by six motors with each motor having a ground abutment. Stewart later proposed that the mechanism can be used for a flight simulator for training helicopter pilots (Plessis, 1999). With Stewart platforms often termed as parallel devices or manipulators, Stewart was not the original source of this type of mechanism as it only had a different configuration of Gough's six linear jack system developed in 1947 (Wang & Gosselin, 1997). Gough's review of Stewart's article indicated that a similar tire machine was designed in 1949 which was later built and was in operation in 1954 – 1955 (Mikrolar, 2016). Stewart stated that Gough's tire test machine is similar to his flight simulation mechanism except for the design approach which was different.

Ironically, Gough is also not recognized as the original inventor of this type of mechanism. Merlet stated that manipulators have been in existence for a long time and that the actual invention of parallel manipulators is a trait of Cauchy, the mathematician, who wrote an article on the possible motion and rigidity of an "articulated octahedron" in 1813 (Mikrolar, 2016). Merlet's was of the opinion that the most appropriate name for this mechanism would have been "Gough's platforms" even though Stewart platform is the most reckoned name for the mechanism.

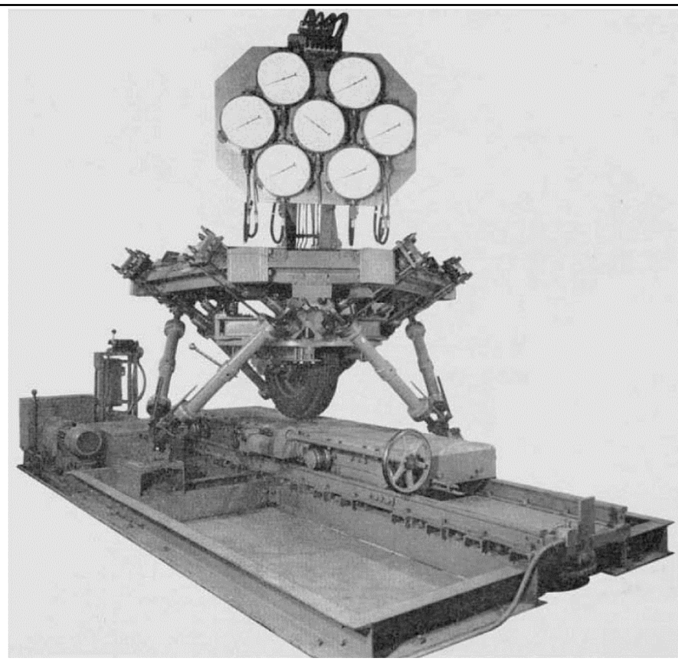

Figure 2: Gough's Six DOF Tire Test Machine. Source: Mikrolar Inc. **(Mikrolar, 2016)**

However, the present recognition of the parallel manipulator is as a result of Stewart's re-discovery in 1965. He reports that this type of robots fully developed interest around 1987 where it recorded a drastic increase in the number of papers on this subject (Plessis, 1999). Following this increase, data records it that in the area of robotic manipulators, the research and development of parallel devices is currently the most popular topics (Duffy & Crane, 1997). A solid model of the modern 6-6 Stewart platform having prismatic actuators is shown in **Figure 3.**

Figure 3: Solid model of the modern 6-6 Stewart platform having prismatic actuators. Source: Stewart-Gough Platform **(Christensen, 2014)**

2.2 Industrial Application of Stewart Platforms

The other uses of this mechanism apart from it been used as a flight simulator as proposed by Stewart includes:

- Been used as an automatic assembly (Furqan & Suhaib, 2014). An example of such mechanism is an assembly machine for automatically inserting blade-like foil in a torque converter turbine drum.
- A platform fixed in space mounted on a vessel such as ship subjected to the random movement of the sea (Furqan & Suhaib, 2014). The assembly can serve as a stabilizing platform which balances the ship especially during rough sea conditions where the wave-excited motion of the ship generates dangerous movement of the cargo hoisted by an offloading/loading crane (Madsen & Kristensen, 2012). A Stewart platform can help

counteract the induced wave from the unworkable sea conditions with the platform ensuring that the crane is steady and not relative to the sea to minimize motion in the crane cargo (Madsen & Kristensen, 2012).

- A new form of machine tool called hexapod which is a machine tool that uses Stewart platform mechanism for positioning. The Stewart platform can be applied in a flexible manufacturing environment as a hexapod milling machine for positioning. One advantage of this hexapod is that several interchangeable head units can be used to perform milling, welding, cutting and assembly operations (Houdek II, 1997).

However, based on some reviewers, another possible use of the platform devices was suggested with G.H. Meier stating that these platforms are more applicable in machine tools and medical fields (Doug, 1965). He went on to explain that the device is used in particularly machine tool industry due to its inherent stability of the platform. The platform had a working table mounted and a 360-degree rotatable table also mounted to the platform. He later suggested that it is a stabilizing platform which could be used to eliminate rotational motions and damp linear motions (Plessis, 1999). J. Tindale also reviewed Stewart's article, which yielded an improvement from the machine tools point of view by designing a universal mill, and oil drilling rig where the platform is supported on a tripod comprising six telescopic legs (Merlet, 1994). Gough's review of Stewart's article improved his tire test machine by attaching digitally controlled motor devices to the screw jacks and electronic instrumentation to study tire-to-ground forces and movement (Plessis, 1999).

Since three decades ago, there has been a continuous development of platforms for flight simulation and amusement park rides with the reason behind the major interest in these platforms due to its high nominal load-to-weight ratio as explained by Merlet (Szatmari, 1999). The weight of the load is approximately equally distributed to the links with the stress in each link mostly of a traction-compression nature appropriate for linear actuators which contribute to the rigidity of the platforms (Plessis, 1999). Merlet also stated that Stewart platforms are ideally suited for assembly lineups due to the position of the moving platform being less sensitive to the errors in the articulated sensors in comparison to serial link robots (Plessis, 1999).

2.3 Medical Fixators Based on Stewart Platform

Various types of bone disorders such as broken or fractured bones, ruptured body parts are commonly known. They are usually as a result of accidents, twists, dislocation, etc. The medical field is one vast industry applying the mechanism of the Stewart platform.

Figure 4: External fixator. Source: University Hospitals, Case Medical Center **(Raymond, n.d.)**

The Stewart platform medical fixators for backbone fixation is an example of a fixator device. It uses the principles of the traditional Stewart platform. These devices are fastened into bones ensuring the reduced movements between the fixed stages (Ganem, 2000). The movements can be a slipped bone, distractions or bone reversals relative to their initial position. A fixator is a device consisting of one or more metal bars and rings connected via metal pins and wires that allow precise control of a bone (Raymond, n.d.). Correcting inner bones and joints is achieved by mere manipulating the fixator on the outside. This device is often used for everyday bone correction until the desired bone position is obtained irrespective of how long it takes to heal. Despite the many orthopedic surgeries performed with internal or implanted device, bones are usually corrected using external devices in cases where the bone is too short and/or has too much of deformity and when the soft tissues cannot allow for correction at once (Raymond, n.d.). This device is able to withstand gentle contact and is attached tightly to the bone or any position of the body in such a way that it is tight enough to pick up the broken body part.

Spine deformity is one major problem the medical industry, particularly the physicians are faced with now **Figure 5**. A spine external fixator is a device that corrects this deformity and is applied in a field hospital under robotic guidance (Gitlin, 2010).

Figure 5: Spine external fixator. Source: Comsol and Mouser Electronics **(Gitlin, 2010)**

The Octopod external fixator is another application of the Stewart platform model that is used in the medical industry. This device is designed to treat bone fractures and deformities with the Adam frame external fixator being a type of the Octopod external fixator **Figure 6**.

Figure 6: Adam frame external fixator. Source: ResearchGate **(Paley, 2011)**

This proposed study relates to a minimally invasive orthopedic device to treat and/or assist the surgical operation of spinal cord injuries, backbone injuries, etc. which is externally mounted on the back, supported and screwed into bones. Such injuries may require one or some of the following: correction, stabilization, adjustment or fixation of the spinal column. Treating these injuries requires that force or pressure is applied to the surfaces to be put together thus keeping them in close contact and promoting bone growth (Howland, Richard, & Kenneth, 1996).

2.4 Application Driven Design

Depending on the design, there is a varying number of Stewart platforms introduced for different purposes. The mechanism of each design differs by using various combinations of prismatic, spherical and universal joints. One design type is based on the distance between points on the top and base platforms (Gao, Lei, Liao, & Zhang, 2003). This is called the generalized or traditional Stewart platform. This design type stated above is believed to be the most popular type of parallel manipulators with 6D-space and a distance constraint. It consists of two rigid bodies linked to six distance and/or angular constraints between six pairs of points in the movable top and the fixed base platform (Gao, Lei, Liao, & Zhang, 2003). This movable top is driven by the six constraints values. Modifying the Stewart platform by adding extra sensors to it produces another design that helps to find a specific position of the platform.

A parallel manipulator first came into existence in a robotics assembly cell in 1979 with the manipulator used as six component force sensors (Szatmari, 1999). The ability to calculate the resulting force and torque acting in the mobile platform is possible due to it been able to measure the traction-compression stress in the links. This feature is why manipulators can be used as assembly units. The paper on the review of Stewart platform defined a parallel manipulator as a closed-loop mechanism that connects the end-effector to the base by at least independent kinematic chains actuated by a prismatic actuator (Plessis, 1999). Merlet, 2006, states in the article that there are a lot of many possible parallel manipulator designs, all having a low cost. The actuator connection points of the general manipulator at any position on both the fixed and moving plates. The two types of manipulators are planar and spatial manipulator.

2.4.1 Planar Manipulator

Planar manipulator is a closed loop type of parallel manipulator. The closed loop manipulator investigated by (Wang & Gosselin, 1997) is when one, two and three DOF respectively have revolute actuators. Merlet described the above mechanism as not parallel manipulators since two linear dependent kinematic chains connect them to the ground. Many designs of the planar manipulator with the three DOF were considered. However, Le et al. designed an equilateral moving platform which is the most stable optimum model (Plessis, 1999) Merlet went further to study the different achievable workspaces of a planar Stewart platform having a triangular moving platform and also described the number and type of kinematic chains used in connecting the moving platform to the ground. Three identical chains with a revolute joint fastened to the ground connect the moving platform to the base. An actuated prismatic joint is then connected to the platform by a revolute joint (Kumar, 1992).

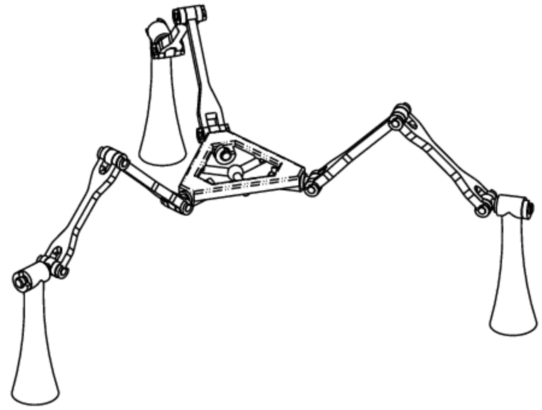

Figure 7: Three DOF parallel manipulator. Source: ParallelMic **(Dimiter Zlatanov, 2002)**

2.4.2 Spatial Manipulator

This type of parallel manipulators usually have degrees of freedom of three to six. Manipulators with three and four DOFs are sometimes applicable in flight simulation while that with five DOF are often available in situations that require the use of tools that are symmetrical around their axis. The number of connecting points on the base and moving bodies often determines how a spatial manipulator is labeled (Plessis, 1999) Spatial parallel manipulators are also dependent on the kinematic chains that connect the fixed and moving bodies with this type of connection also an important design factor to be considered. Just like in planar manipulators, rotary actuators can also be used in the design of the spatial parallel mechanism. The current technology is a combination of a traditional 6-6 Stewart platform with prismatic actuators and a 6-6 parallel manipulator with a revolute actuator (Wang & Gosselin, 1997). This is different from the traditional Stewart platform manipulator in that it has a six firmly fixed linear actuators, i.e. there is no change in the position and orientation of the platform. The mechanism can achieve high speed and good accuracy capabilities (Plessis, 1999).

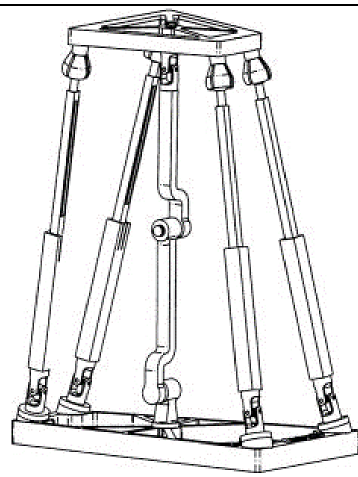

Figure 8: The spatial five DOF parallel mechanism. Source: ASME **(Zhang & Gosselin, 2000)**

2.5 Current Technology

The current state of the Stewart platform consists of two platforms, namely, the fixed plate and the movable top plate connected together by six linear actuators rotatable in 6D-space. These actuators are fastened to both the fixed base and mobile top plate by universal joints positioned at the end of each actuator links which allows for changing leg-platform combinations. The actuator links are variable because of it being designed to have an adjustable upper and lower body connected by a cylindrical joint. Having considered the spatial and planar parallel manipulators, for this thesis, the spatial parallel manipulator is employed. The current design for the Stewart platform will be changed. The main contribution of this thesis is to design the parallel manipulator such that it can easily be assembled around various structural shapes that need an alignment.

Most of the work presented in this thesis will be based on the idea of the Stewart platform. It finds applications related to misalignment correction in the automobile industry, health organizations, flight simulations, robotic industries, machine tool technology, particularly in areas that require high accuracy. The proposed modified Stewart platform manipulator in this thesis consists of four linear actuators populated evenly in two parts with each part being identical as the other as shown in **Figure 15** made from the assembly of two symmetrical parts (part 1 and part 2) that constructs a rigid platform, where the orientation of one part is flipped upside down. The end of each base has a pair of snap-fit mechanism to fasten the assembly. We propose to use simple peg-n-hole structures with a release mechanism as shown in **Figure 15.** Finally, each part base will have an adjustable clamping mechanism consisting of a spring loaded adjustable clamp attached to a lead screw. The analysis of the stiffness and load carrying capacity of the proposed manipulator is analyzed with the modeling and simulation used to quantify the manipulator. The proposed modifies Stewart platform manipulator can be utilized to achieve a range of cross-sectional area, which is to be as universal as possible, without losing the grip while adjusting the relative position between the two ends of the manipulator. The manipulator kinematics and kinetics will be simulated using MATLAB Simulink and finite element analysis (FEA).

Table 1 below shows the comparison between traditional Stewart platform manipulator and the modified Stewart platform manipulator;

Table 1 Stewart platform vs. Modified SP

Traditional SP	Modified SP
Fixed base and movable plate connected via six linear actuators	Fixed base and movable plate connected via four linear actuators
Suitable for closed-loop structure	Suitable for open-loop and closed-loop structures.
The assembly parts are not symmetrical.	The mechanism is made from the assembly of two symmetrical part flipped upside down.
Does not use a peg-n-hole structure and has no release.	Uses a simple peg-n-hole structures with a release mechanism.
Does not have an adjustable clamp.	Each part base has a spring loaded adjustable clamping mechanism.

2.6 Summary

In this chapter, a review of the literature was provided. Precision positioning remains one reason why the Stewart platform was designed. The applications and many designs approach have been addressed ranging from different actuator requirements and design. The approach used in this proposed study is to modify Stewart platform by designing one with four actuators (and not the usual six) and to incorporate an adjustable clamping device to the base. The historical perspective of Stewart platform, industrial applications, medical fixators based on Stewart platform and the application driven design were discussed. Parallel manipulators were critically looked into, discussing the functions and types of parallel manipulators, making a comparison between both and also the design of each type. The spatial parallel manipulator was further discussed since it is the type employed in this thesis.

Current technology used in the Stewart platform design and the modified Stewart platform manipulator was discussed and the reason for the change explained. A comprehensive study of the new technology to be employed in this thesis, modified Stewart platform manipulator, was carried out. Overall, this review of literature clarified several aspects of position control and made comparisons to arrive at the modified Stewart platform mechanism.

CHAPTER THREE: PROCEDURES

3.1 Restatement of the Problem

In this Study, we present a novel approach to correct misalignment by using modified Stewart platform for precision positioning of large structures. The modified Stewart platform is first designed to correct the spatial misalignments applicable to open and closed structures via guided alignment process. Secondly, the clamping mechanism should be adjustable to different cross sections without losing the grip while adjusting the relative position between two ends of the fixator.

- **Problem illustration**

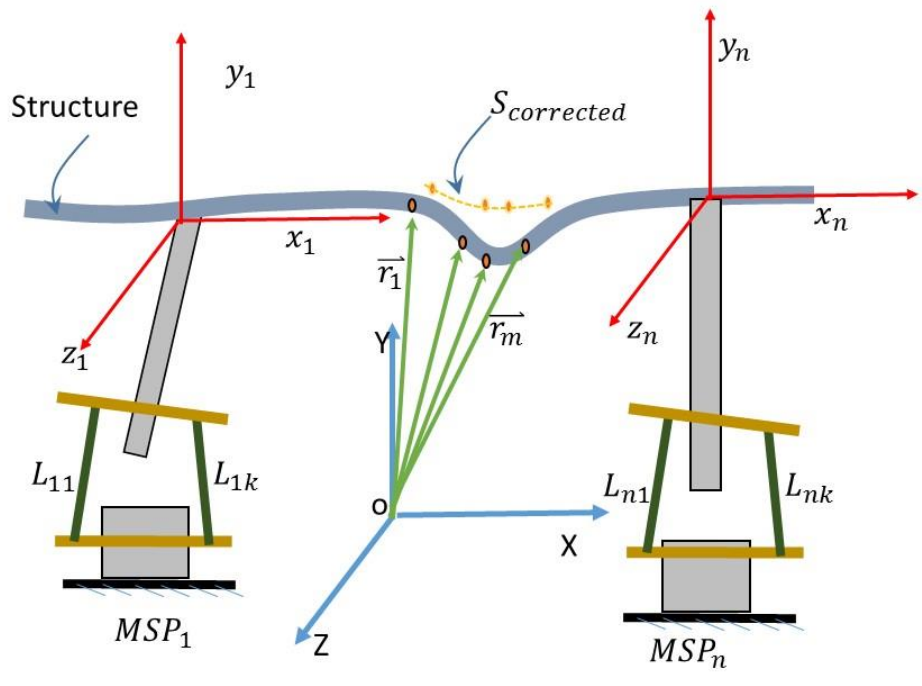

Figure 9: Structural alignment using *n* number of distributed platform.

The illustration above is a misalignment problem of a bent structure with unleveled surfaces which can be corrected using *n* number of distributed modified Stewart platform (**Figure 9**). MSP_1, MSP_n are the modified Stewart platform to be fixed to the unleveled surface along their respective coordinates with MSP_1 having k linear actuators ($L_{1_1}L_{1_2}$ ... L_{1_k}) and MSP_n with k linear actuators ($L_{n_1}L_{n_2}$ ... L_{n_k}) where L is the relative length of the actuator measured at a given time. The resultant $\overrightarrow{r_1}\,\overrightarrow{r_2}$ ... $\overrightarrow{r_m}$ of the relative misalignment is measured along the bent structure from the origin relative to the coordinate.

Mathematically,

Suppose ∃ *n* number of MSP is supporting the large structure.

Let $\overrightarrow{r_i}$ be the absolute position measured on the misaligned structure.

Where $\overrightarrow{r_i}$ {i= 1, 2…m} constructs the misalignment curve $S_{incorrected}$

The objective is to adjust MSP_1 ... MSP_n such that $\vec{r} \longrightarrow \vec{r}_{desired}$. Also, where the $\vec{r}_{desired}$ is the position of the measured points after alignment which together construct the corrected curve $S_{corrected}$.

Let the number of the linear actuator in each Stewart platform be *k* = 6. We want to find the optimal length of each actuator in the distributed system:$\{L_{1_1}L_{1_2} \dots L_{1_6},\ L_{2_1}L_{2_2} \dots L_{2_6} \dots L_{m_1}L_{m_2} \dots L_{m_6}\}$ Such that the location of the measured points, defined by $\overrightarrow{r_1}\,\overrightarrow{r_2}$ ... $\overrightarrow{r_m}$, follow the $S_{corrected}$

- **Special case**

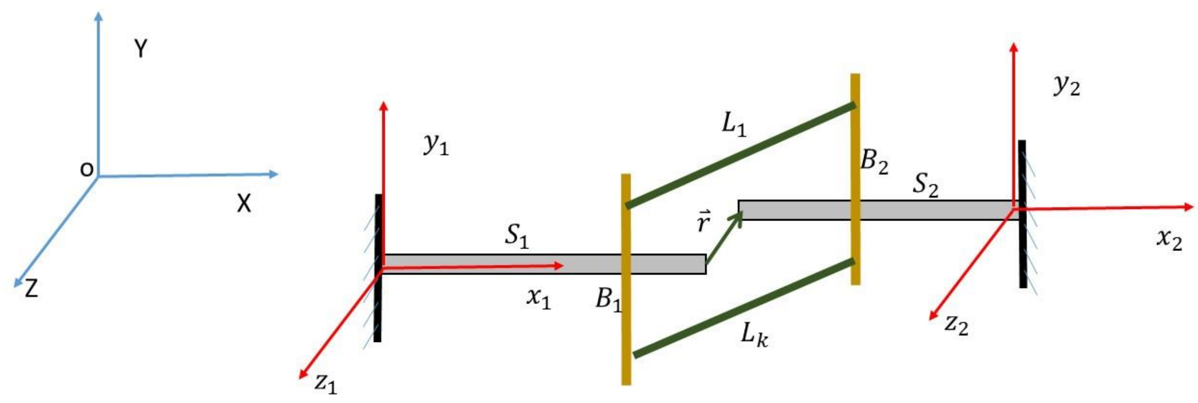

Figure 10: Misalignment correction in closed structure.

The modified Stewart platform is used to correct misalignment in a closed structure such as a broken frame in a car, bone fracture or broken beam in a factory (**Figure 10**). In this case, two structures $S_1 S_2$ are to be aligned using one modified Stewart platform with base $B_1 B_2$ and k linear actuators $L_1 L_2 \dots L_k$. The vector $\vec{r}$ is the relative misalignment position measured between the centers of the two structures' end.

Mathematically,

$\vec{r}$: measure the relative misalignment between the two structures

Objective: $\vec{r} \longrightarrow 0$

Let the number of actuator in this Stewart platform be k = 6, i.e. $\overrightarrow{L_1}\,\overrightarrow{L_2}$ ... $\overrightarrow{L_6}$. The length of each linear actuator can be measured relative to two local coordinates $\{x_1y_1z_1, x_2y_2z_2\}$. The goal is to find ($\overrightarrow{L^*{}_1}\,\overrightarrow{L^*{}_2 \ldots}\overrightarrow{L^*{}_6}$) such that $\vec{r} = 0$

3.2 Design Specification Requirements

The design process is similar to that of a Stewart platform. The origin of Stewart platform, which consists two plates attached to six adjustable legs, can be traced back to when it was first modeled as an aircraft simulator, which is applicable to space vehicle emulator, hand vehicle maintenance, shipbuilding, machine tool technology, automotive, etc. (Gong, 1992). This manipulator has generated lots of design research and study with this research yielding some design specifications including but not limited to load capacity, work space requirements, that is, the range of rotation about axes, the range of motion (vertical and horizontal). Six geometrical parameters just similar to six degrees of freedom were determined according to these design considerations. Sometimes, considering these specifications, the designed platform could not perform at an acceptable standard. A further study of the Stewart platform should be examined for its design in order to ensure that the performance is satisfactory. The stiffness of the platform is another element which should be part of the design considerations. If the direction of the platform is to be designed to be as rigid as possible, a thorough study of the static loading attribute should be done in order to select the most suitable parameters. The requirements for the modified Stewart platform design are:

- The platform should enable precision positioning of structures in six-dimensional (6D) space.
- It should be easily used in closed-end and open-end structures **Figure 11.**
- The platform should be an adjustable manipulator that is inherently rigid with Stewart platform as one candidate mechanism.
- It should be firmly mounted around a range of cross-sectional area as universal as possible without losing the grip while adjusting the relative position between two ends of the platform.
- The Modified Stewart platform design should have load and position range capability that are adequate for correcting the structure misalignment.
- It should be able to adjust position easily either by using screw-lead mechanism or linear actuators.
- The modified Stewart platform must be affordable, be conducive to manufacturability and easy to use.

3.3 Suggested Mechanism

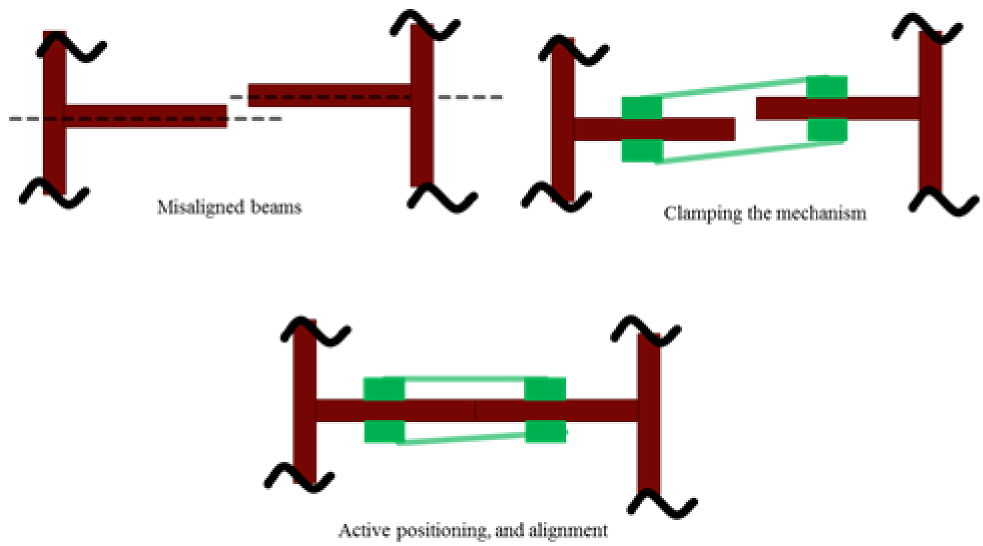

Figure 11: Fixator used to align closed-end structures.

3.3.1 How the device works as a whole:

Position control is one of the many important characteristics of a mechanical design and it can be found in different application such as stabilizing the helicopter landing assisted by a Stewart platform. The proposed modified Stewart platform is a preparatory step that facilitates assembly where it can be used to align two structural beams relative to each other. The post processing after alignment might be fastening, welding, etc.

The full assembly of a Stewart platform consists of a parallel mechanism with two platforms, a movable top plate which is connected to a fixed base plate and is defined by three static points on the fixed base fastened to six independent linearly actuated legs (Zhang B. , 2005). The modified

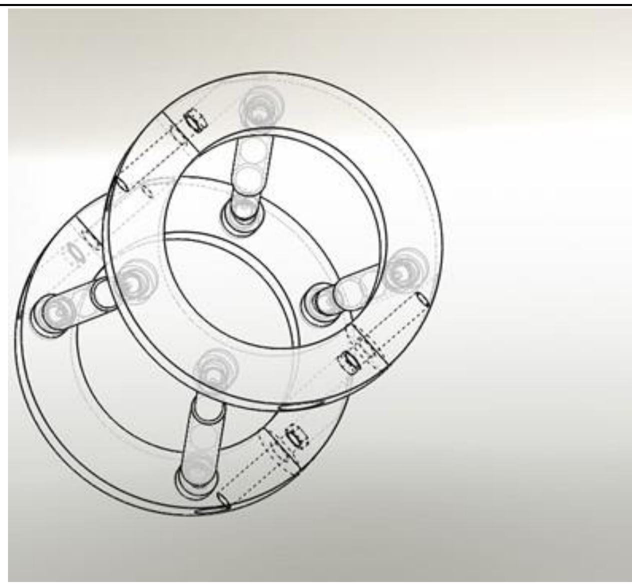

Figure 12: Solid model of the Modified Stewart Platform

Stewart platform manipulator in this study has four legs, unlike most parallel manipulators that have six linearly actuated legs with changing combination of leg-platform connections with these legs fastened to both the fixed base and mobile top plate by universal joints positioned at the end of each leg. The fixed and mobile bases are easy connect and disconnect mechanism. A complete platform is constructed from two mirror image parts with one inverted upside down. The length of each leg is variable because of it being designed to have an adjustable upper and lower body connected by a cylindrical joint.

The extent to which the legs can be adjusted varies in order to determine the position and direction of the movable platform due to its unusual range of motion and accuracy. The positioning of the platform offers controllability in six-degree space with the first three-dimensional space being in rotational degrees and the other three in translational degrees. The top plate is rotated from the base platform at 60 degrees causing the six actuated legs to be at equal distance from one another with the movement of each leg independent of the others (Zhang B. , 2005). For a given structural mass, the platform plays a significant role in positional certainty due to its high rigidity or stiffness characteristics. The accurate position characteristics are preferred over that of individual actuators because it is a parallel manipulator with forces spread across the six links.

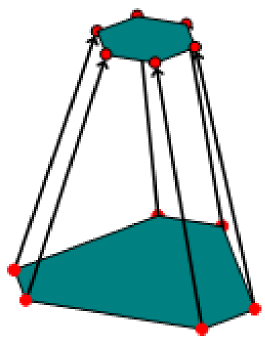

Figure 13: Schematic of Stewart platform.

The proposed modified Stewart platform will differ from the Stewart platform in the sense

- It will consist of four linear actuators populated evenly in two parts. Each part is identical to the other as shown in **Figure 15**.
- The mechanism is made from the assembly of two symmetrical parts (part 1 and part 2) that constructs a rigid platform, where the orientation of one part is flipped upside down as shown in **Figure 15**. The end of each base has a pair of snap-fit mechanism to fasten the assembly. We proposed to use simple peg-n-hole structures (P1, H1, P2, and H2) with a release mechanism as shown in **Figure 14**.
- Each part base has an adjustable clamping mechanism and it consists of a spring loaded adjustable clamp attached to a leadscrew.

Figure 14: Solid model of the two symmetrical parts

3.3.2 Innovation of this Manipulator Mechanism

- Reduced number of actuators; four linear actuators is used instead of the usual six
- Assembly of two symmetrical parts with the orientation of one flipped upside down.
- One part base is produced and replicated for the other three part base
- A spring loaded adjustable clamp for each part base

3.3.3 Merits of the proposed Modified Stewart platform Manipulator

The modified Stewart platform offers many significant advantages to its end users. These advantages range from mechanical simplicity, higher load and position range capacity, higher accuracy, great dynamic properties, higher stiffness, reduced installation requirements and more so a simpler inverse kinematics for position control, some of the merits particularly identified with the proposed manipulator are:

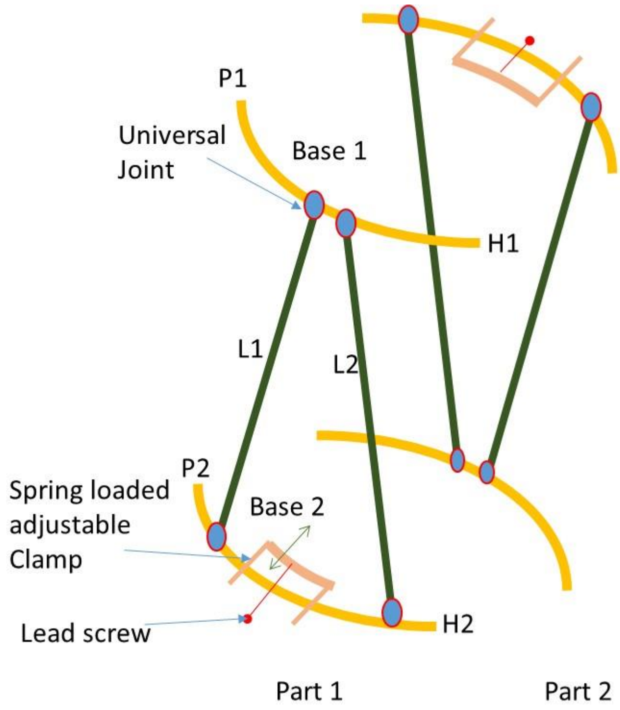

Figure 15: Proposed mechanism with four actuators (*k* = 4).

- It can be used in open-end and closed-end structures.
- The adjustable clamping mechanism will allow for different cross-sectional areas of structures.
- It is easier to manufacture since just one part base is to be produced and then replicated for the other three parts.
- Since it requires simpler and fewer parts i.e. four actuators, the cost of production is reduced and is less difficult to install each part.
- This device is applicable in most industries such as automotive, health, manufacturing and many more.

The attributes of this mechanism allow for a possibility to change the current manipulator design.

3.3.4 Impact of the Proposed Manipulator

Stewart platform is one of the most studied and researched parallel manipulators. As a result, lots of research on the development of parallel manipulator design particularly the Stewart platform, have been published. The modified Stewart platform offers an important role in all industries particularly the robotics industry and further foster the academic research on the development of parallel manipulators as a whole. This study also has an impact in the academia as follows: provides an easy connect and disconnect platform that can be used in the laboratory environment to teach students the kinematics and kinetics of parallel manipulators. The device will give students learning experience in the control theory, position analysis and the ease of manufacturing it since it is simple to make.

This parallel manipulator is an addition to the many different manipulator designs used to correct misalignment in structures.

3.4 Specific Objectives

3.4.1 Project Objective 1:

- To develop a mechanism that corrects misalignment for small millimeter scale misalignment and high accuracy without sensor feedback.

Hypothesis:

To test the hypothesis that a modified Stewart platform design can be used to achieve misalignment within the 2 cm range and high accuracy.

Approach (Test)

- Four linearly actuated struts used with a dc motor
- The inverse kinematics and modified actuators/dimensions achieve required specification

3.4.2 Project Objective 2:

- To develop a mechanism provides a force that resists the structure stiffness.

Hypothesis:

To test the hypothesis that the developed mechanism can provide the force required to resist the structure stiffness.

Approach (Test)

An optimized combination of a design and linear actuators capable of resisting stiffness which enables the platform to manipulate loads of up to 20 kN will be developed.

3.4.3 Project Objective 3:

- To test that the developed mechanism can be used in closed and open structures.

Hypothesis:

To test the hypothesis that the developed mechanism can be mounted on structures using two symmetrical parts.

Approach (Test)

To predict that the developed mechanism can be used in close structures. A finite element model is built and simulated using ANSYS finite element software. This model will be dependent on the use of element technique, retaining the most important degrees of freedom (DOF) of each component to reduce the total number of DOF of the system (Hanieh, 2003).

3.4.4 Project Objective 4:

- The developed mechanism can hold beam cross section ranging from 3 cm to 5 cm.

Hypothesis:

To test the hypothesis that the proposed Stewart platform manipulator can hold cross section from 3 cm to 5 cm with the use of the spring loaded adjustable clamp. This clamp is attached to each base and can be expanded and contracted to accommodate for proper grasping of the beam.

3.5 Structure Description

The modified Stewart platform manipulator shown in **Figure 1** is a six-DOF parallel mechanism, which consists of two platforms, a moving top plate and a fixed base plate connected through four identical but independent kinematics legs that are linked to both the moveable top and fixed base plates by universal joints. These legs have changing combination of leg-platform connections. The length of each leg is variable and can independently control the motion of the top movable platform.

3.5.1 Actuators

Linear actuators are important components of the structural fixator. The motion needed in this device is the linear motion which is derived when rotary motion is converted to linear motion or from linear electrical motors. These manipulators can be actuated open loop when used as a rotary stepper motor (Lazarevic, 1997). A linear motion transmitted from rotary motion is required if a rotary motor is used as an actuator. Conversion of rotary motion into linear motion is often by ball-screw transmission and rack-and-pinion transmission. Although the rack-and-pinion transmission seems to offer more advantages compared to the ball screw, each of them has different applications. The rack-and-pinion can allow for easy adjustment, take less space, more appropriate for attaining higher speed and is more efficient, the ball screw can achieve zero backlashes more allowing the platform to stop in the case of shutdown (Lazarevic, 1997). However, the ball screw system will be used by this device although it at the expense of speed since it is a slow and less efficient system.

For the proposed modified Stewart platform, four prototyped feedback rod linear actuators were used with each of them having a built in potentiometer that helps to determine the actuator position at any point in time. The actuators have 12 inches stroke, 12 volts input and are 200 Lbs. dynamic force linear actuators. Each actuator is weighted 3.85 lbs. with a retracted and extended length of 17.9 inches and 29.9 inches respectively (Firgelli Automations, 2016). The table below shows the specification of the actuator.

Table 2. Specifications for Actuators

Dynamic force	200 lbs.
Static force	400 lbs.
Speed (″/s)	0.3 inches
Gear ratio	30:1
Screw	Acme Screw
Thread Diameter	12 mm
Input	12V Dc
Max Draw	5A
Feedback	10K ohm 3-wire potentiometer Linearity +/- 0.23% 10 Turn potentiometer Power rating 1 – 1.5 W

3.5.2 Joints

Universal joints are usually the most suitable for applications where it is difficult to avoid large angular misalignment. Universal joints can also handle parallel misalignment by connecting in series two joints, and axial misalignment by introducing a spline or sliding shaft to the assembled joint (Lazarevic, 1997). The actuators and platform should be connected using universal joints since they provide a greater range of rotational motion around the joints than the ball-and-socket joints.

For this study, we used a prototype heavy duty inline booted ball joint linkage (female shank with stud). It has a stud and shank thread size of 5/16"-24, length (A) of 1 3/16", Stud length (B) of 5/8", Length (C) of 1 3/16", and thread depth (F) of 9/16" (Mcmaster-carr, 2016).

Table 3. Specifications for Joints

Inch/Metric	Inch
Stud and Shank Thread Size	5/16"-24
Length (A)	1 3/16"
Stud Length (B)	5/8"
Length (C)	1 3/16"
Thread Depth (F)	9/16"
Max Draw	5A

3.6 Methodology

Kinematic analysis is important in manipulators as they are useful in determining how the manipulator moves with respect to the actuator input. The reason why the kinematic analysis of the modified Stewart platform is carried out is to create methods for analyzing the basic kinematic feature of the mechanism and also to develop a computer-aided procedure capable of carrying out such analyses (Gong, 1992). Some of these kinematic characteristics include position and velocity of the links, workspace management, motion range of the mechanism and to identify its physical constraints, hence, helping to acquire both design and device application recommendation for this mechanism (Gong, 1992). The type of inverse kinematics used in the article by (Bingul & Karahan, 2012) will be followed.

Figure 16 shows the adaptive control system to adjust the misalignment. It consists of the input signal, linear actuators, system dynamic model, moving plate, the output signal, feedback

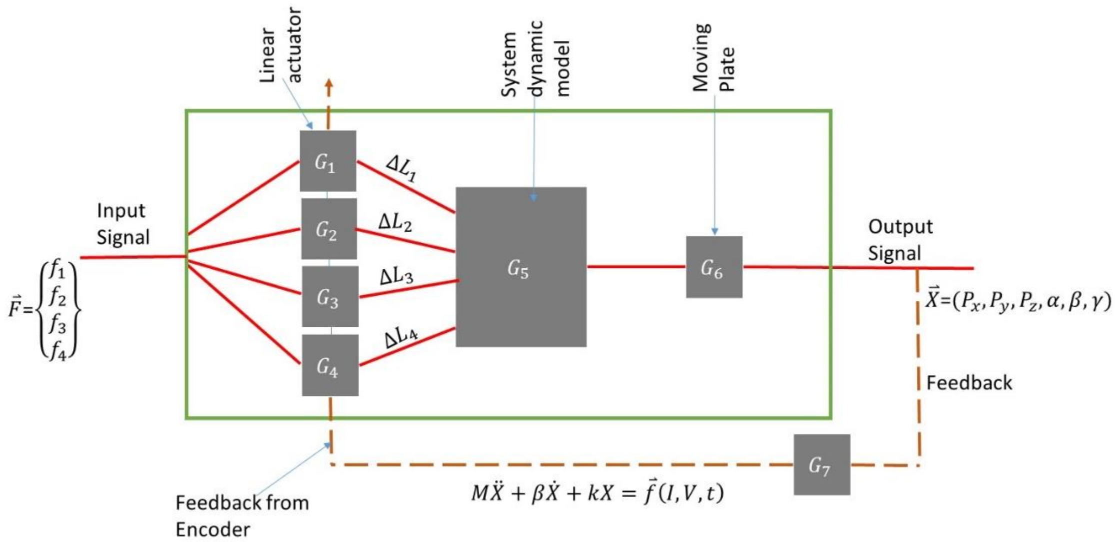

Figure 16: Adaptive control system to adjust the misalignment.

and the feedback from the encoder. The signal $\vec{F}$ is inputted into the four linear actuators G_1, G_2, G_3, G_4 with the change in length of the four actuator $(\Delta l_1, \Delta l_2, \Delta l_3, \Delta l_4)$ connected to the system dynamic model G_5. The signal from the system dynamic model is transferred into the moving plate G_6 to cause rotation and produces an output signal $\vec{X}$. The feedback runs through the encoder G_7 and back through the four actuators.

The Jacobian matrix which is necessary for accurate simulation model was derived. Finally, MATLAB was used to simulate the dynamic equations including the rigid body and actuator dynamics.

For this modified Stewart platform manipulator, first, the inverse algorithm in MATLAB environment or 20 sims will be used. Secondly, the structural mechanical analysis using ANSYS workbench to determine the static and dynamic characteristics and the contact between the clamp and grasped object will be done. Lastly, an analysis on the optimization of the structure to a predefined structure. The Lagrangian method and Jacobian matrix was used to develop the kinematic analysis on the model with the position and orientation of the top plate defined (Gong, 1992).

3.7 Back of the Envelop Modeling

Stewart platform used in correcting misalignment was designed to solve problems of structures of small misalignment. The kind of deformation to expect on the structures are very small. Taking the simple example below of a fixed and free-end cantilever with small misalignment, we will determine the forces that will adjust the misalignment such that this adjustment will not cause large deformation. Therefore, we will use the theory of small deflection.

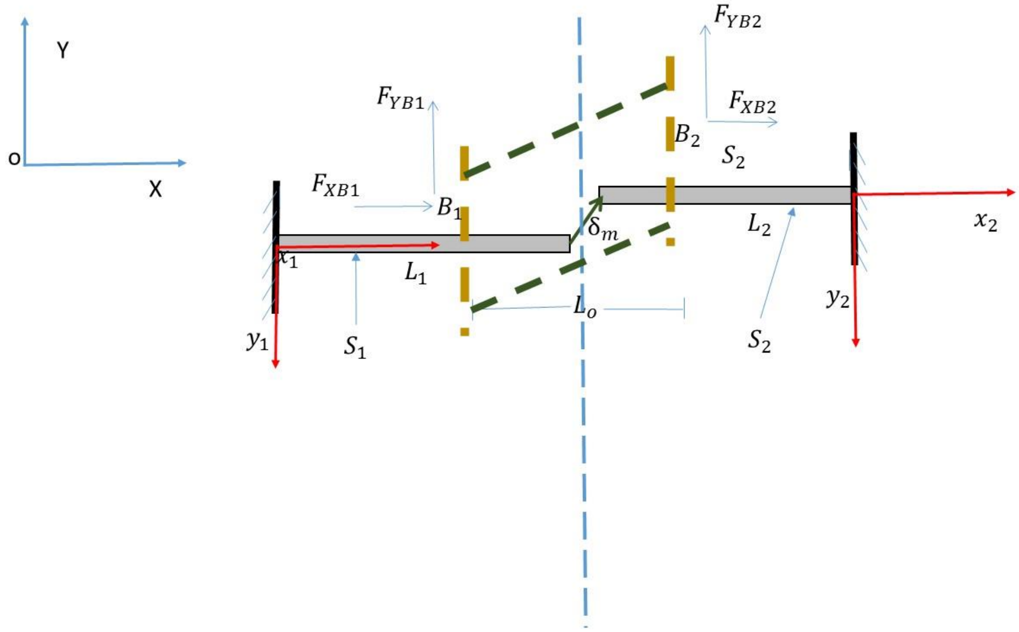

Figure 17: 2D Simple Misalignment Problem with Stewart platform.

Assuming two fixed and two free ends cantilever are misaligned by δ_m, the goal is to find $F_{YB1}, F_{XB1}, F_{YB2}, F_{XB2}$ such that $\delta_m = 0$

For small deflection due to vertical loading at the free end, the deflection profile of the structure S_1 follows:

$$y = F_{YB1} \quad (1)$$

With maximum deflection measured at free end $x = l \Rightarrow$

From (Beam deflection formulas, 2016)

$$\delta_m = \frac{Pa^2}{6EI}(3l - a) \quad (2)$$

$$\theta = \frac{Pa^2}{2EI} \quad (3)$$

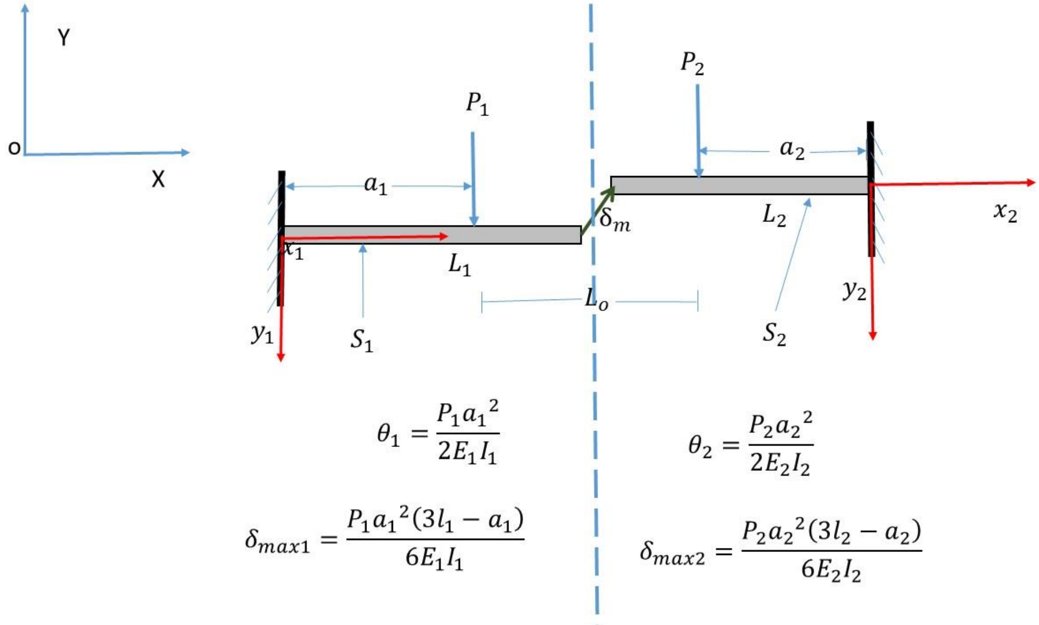

Figure 18: Misalignment Problem showing the max deflection and bending angle.

Where δ_m is the maximum deflection, θ is the bending angle, E is the young modulus and I is the area moment of inertia.

For structure 1, $\theta_1 = \frac{P_1 a_1^2}{2E_1 I_1}$ (4)

and $\delta_{max1} = \frac{P_1 a_1^2(3l_1 - a_1)}{6E_1 I_1}$ (5)

Likewise for structure 2,

$\theta_2 = \frac{P_2 a_2^2}{2E_2 I_2}$ (6)

and $\delta_{max2} = \frac{P_2 a_2^2(3l_2 - a_2)}{6E_2 I_2}$ (7)

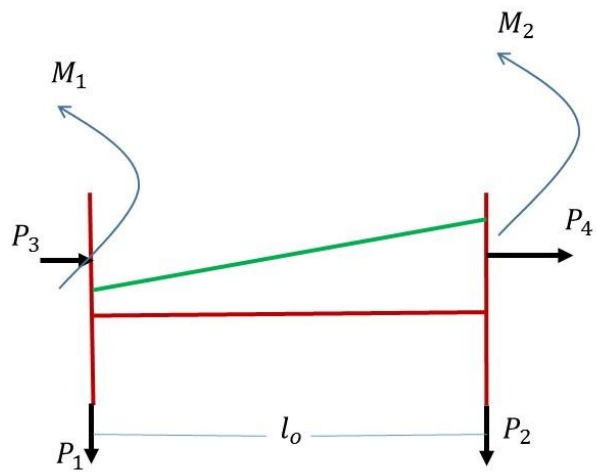

Figure 19: Free-body diagram of Stewart platform.

Where l_o is the length of the Stewart platform, P_1, P_2, P_3, P_4 are the force vectors and M_1, M_2 are the bending moment.

Under quasi-static balance, $\sum F_y = 0$ we obtain

$P_1 = -P_2$. Let, $P_1 = P_2 = P$

Assume that the problem being tried to solve is simply broken and there is no gap between the structures,

$l_o, l_1, l_2, E_1, E_2, I_1, I_2$ are the fixed characteristics of Stewart platform that cannot be changed.

a_1, a_2, P_1, P_2 are the characteristics of Stewart platform that can vary depending on how the MSP is installed, and on the amount of static force applied to the structure.

From, $l_1 + l_2 = a_1 + a_2 + l_o$

$$a_2 = l_1 + l_2 - l_0 - a_1 \quad (8)$$

$$\delta_{max1} = \frac{Pa_1{}^2(3l_1 - a_1)}{6E_1I_1} \tag{9}$$

$$\delta_{max2} = \frac{-P(l_1 + l_2 - l_o - a_1)^2(3l_2 - l_1 - l_2 + l_o + a_1)}{6E_2I_2} \tag{10}$$

The total displacement required aligning the two free is

$$|\delta_{total}| = |\delta_{max1}| + |\delta_{max2}|$$

Rewrite,

$$|\delta_{total}| = \left|\frac{Pa_1{}^2(3l_1 - a_1)}{6E_1I_1}\right| + \left|\frac{-P(l_1 + l_2 - l_o - a_1)^2(3l_2 - l_1 - l_2 + l_o + a_1)}{6E_2I_2}\right| \tag{11}$$

because δ_{total} is a positive number and all lengths are positive, we simplify above equation into

$$\frac{6\delta_{total}}{P} = \frac{a_1{}^2(3l_1 - a_1)}{E_1I_1} + \frac{(l_1 + l_2 - l_o - a_1)^2(3l_2 - l_1 - l_2 + l_o + a_1)}{E_2I_2} \tag{12}$$

To solve this problem, a_1 and P can be any number depending on the constraints and the static balance. Where $0 \leq a_1 \leq l_1$ and $0 \leq P \leq Pmax$. The relationship between a_1 and load P are numerically solved. The exist set of solutions, allowing different possible method of clamping depending on range of allowed a_1 and P.

3.8 Inverse Kinematics

3.8.1 Position Model

The coordinate system illustrated in **Figure 20** describes the motion of the moving platform. The fixed base has a coordinate system (B_{XYZ}) and another coordinate system (T_{xyz}) which is located at the center of mass of the moving platform. The fixed base and moving platforms have connecting points (B_i and T_i) respectively. These points are placed on fixed and moving platforms (**Figure 20.a.)** Also, (T_2 and T_3, T_1 and T_4) are the separation angles between points which are denoted by θ_p as shown in **Figure 20**.**b**. below. Similarly, the separation angles between points (B_1 and B_4, B_2 and B_3) are denoted by θ_b.

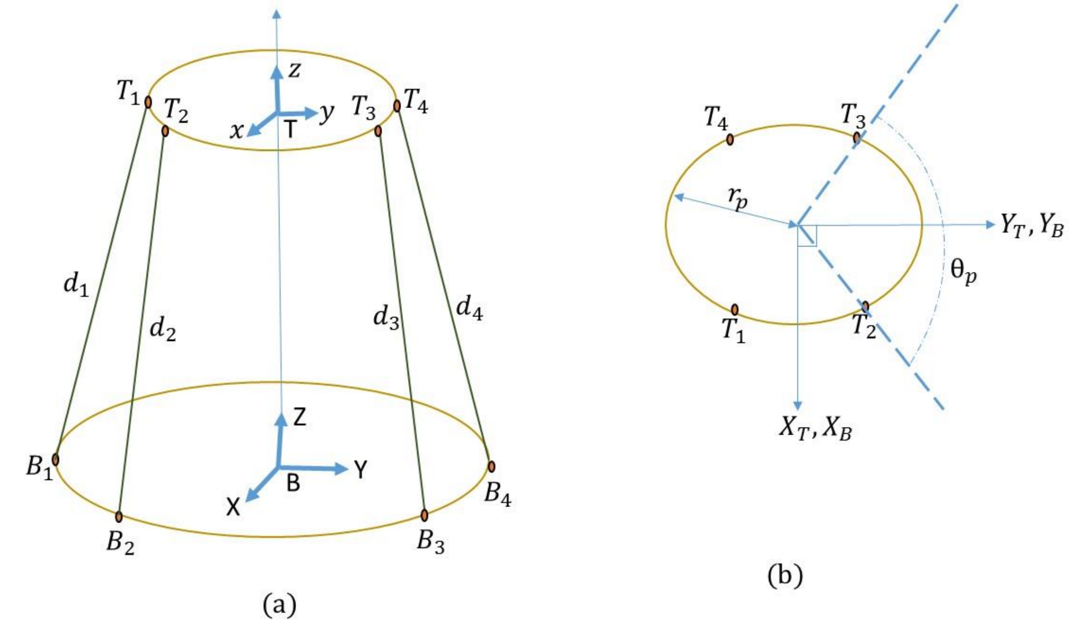

Figure 20: Schematic diagram of the modified SP manipulator.

From Figure 20.b, the location of the i^{th} attachment point (T_i) on the moving platform can be found (Equation 15). The radii of the moving platform and fixed base are r_p and r_{base} respectively. Similarly, the location of the i^{th} attachment point (B_i) on the base platform can be also obtained from Equation 16.

$$GT_i = \begin{bmatrix} GT_{xi} \\ GT_{yi} \\ GT_{zi} \end{bmatrix} = \begin{bmatrix} r_p \cos(\lambda_i) \\ r_p \sin(\lambda_i) \\ 0 \end{bmatrix}, \quad \begin{matrix} \lambda_i = \frac{i\pi}{3} - \frac{\theta_p}{2} & i = 1,3 \\ \lambda_i = \lambda_{i-1} + \theta_p & i = 2,4 \end{matrix} \tag{13}$$

$$B_i = \begin{bmatrix} B_{xi} \\ B_{yi} \\ B_{zi} \end{bmatrix} = \begin{bmatrix} r_{base} \cos(\upsilon_i) \\ r_{base} \sin(\upsilon_i) \\ 0 \end{bmatrix}, \quad \begin{matrix} \upsilon_i = \frac{i\pi}{3} - \frac{\theta_b}{2} & i = 1,3 \\ \upsilon_i = \upsilon_{i-1} + \theta_b & i = 2,4 \end{matrix} \tag{14}$$

The position vector P describes the pose of the moving platform and a rotation matrix B_{R_T}. $R_X(\alpha)$ is the rotation of α about the fixed x-axis, $R_Y(\beta)$ is the rotation of β about the fixed y-axis and $R_z(\gamma)$ is the rotation of γ about the fixed z-axis which are defined by the rotation matrix roll, pitch and yaw respectively. This allows for derivation of the rotation matrix about the base platform coordinate system. The position vector p denotes the translation vector of the origin of the moving platform about the base platform. Based on (Bingul & Karahan, 2012), the rotation matrix and the position vector is given as follows.

$$B_{R_T} = R_z(\gamma)R_Y(\beta)R_X(\alpha) = \begin{bmatrix} r_{11} & r_{12} & r_{13} \\ r_{21} & r_{22} & r_{23} \\ r_{31} & r_{32} & r_{33} \end{bmatrix}$$

$$= \begin{bmatrix} \cos\beta\cos\gamma & \cos\gamma\sin\alpha\sin\beta - \cos\alpha\sin\gamma & \sin\alpha\sin\gamma + \cos\alpha\cos\gamma\sin\beta \\ \cos\beta\sin\gamma & \cos\alpha\cos\gamma + \sin\alpha\sin\beta\sin\gamma & \cos\alpha\sin\beta\sin\gamma - \cos\gamma\sin\alpha \\ -\sin\beta & \cos\beta\sin\alpha & \cos\alpha\cos\beta \end{bmatrix} \quad (15)$$

$$P = \left[P_x\ P_y\ P_z\right]^T \quad (16)$$

The position vector is defined by GT_i and B_i as shown in **Figure 20**. The vector L_i of the link I is obtained as

$$L_i = R_{XYZ}GT_i + P - B_i \qquad i = 1,2, \dots 4. \quad (17)$$

With the position and orientation of the moving platform given as $X_{p-o} = \left[P_x\ P_y\ P_z\ \alpha\ \beta\ \gamma\right]^T$

$$l^2{}_i = \left(P_x - B_{xi} + GT_{xi}r_{11} + GT_{yi}r_{12}\right)^2 + \left(P_y - B_{yi} + GT_{xi}r_{21} + GT_{yi}r_{22}\right)^2 + \left(P_z + GT_{xi}r_{31} + GT_{yi}r_{32}\right)^2 \quad (18)$$

The length of the actuator is $l_i = \|L_i\|$.

3.8.2 Vector Model

The Jacobian matrix relates the actuators velocities to the general platform velocity as given below (Bingul & Karahan, 2012),

$$\dot{L} = J\dot{X} \tag{19}$$

Where $\dot{L}$ and $\dot{X}$ are the velocities of the leg and the moving platform respectively.

The relationship between the actuator velocities and the generalized velocity of the moving platform ($\dot{X}_{p-o}$) is rewritten as

$$\dot{L} = J_A X_{p-o} = J_{IA} \vec{V}_{T_j} \tag{20}$$

Hence, the generalized velocity of the moving platform is

$$\vec{V}_{T_J} = J_{IIA}\, \dot{X}_{p-o} \tag{21}$$

Where $\vec{V}_{T_J}$is the velocity of the platform connection point of the leg.

Based on (Bingul and Karahan 2012) derivation,

The first Jacobian matrix is

$$J_{IB} = \begin{bmatrix} u_{x1} & u_{y1} & u_{z1} & \left(B_{R_T} GT_i \; x\vec{u}_1\right)^T \\ \vdots & \vdots & \vdots & \vdots \\ u_{x6} & u_{y6} & u_{z6} & \left(B_{R_T} GT_6 \; x\vec{u}_6\right)^T \end{bmatrix}_{6x6} \tag{22}$$

The second Jacobian matrix is $J_{IIB} = \begin{bmatrix} 1 & 0 & 0 & 0 & 0 & 0 \\ 0 & 1 & 0 & 0 & 0 & 0 \\ 0 & 0 & 1 & 0 & 0 & 0 \\ 0 & 0 & 0 & \cos\beta & 0 & 0 \\ 0 & 0 & 0 & 0 & 1 & -\sin\alpha \\ 0 & 0 & 0 & -\sin\beta & 0 & \cos\alpha \end{bmatrix}_{6x6}$ (23)

Where $GT_i = \left[GT_{xi}\; GT_{yi}\; GT_{zi}\right]^T$

$$T_j = \left[P_x\; P_y\; P_Z\right]^T + B_{R_T} GT_i = x + B_{R_T} GT_i$$

$\omega = (\omega_x, \omega_y, \omega_z)$ is the angular velocity of the moving platform with reference to the base

u_i is the unit vector along the axis of the prismatic joint of link i.

$$\vec{u}_i = \frac{B_i T_j}{|L_i|} = \frac{L_i}{l_i}, \begin{cases} j = \frac{i+1}{2} & if\ i\ is\ odd \\ j = \frac{i}{2} & if\ i\ is\ even \end{cases}$$

3.9 Finite Element Modelling

Finite element analysis (FEM) is the tool that was used to study the stresses in the structure. The finite element model is built and simulated using ANSYS finite element software. This model is dependent on the use of element technique, retaining the most important degrees of freedom (DOF) of each component to reduce the total number of DOF of the system (Hanieh, 2003). The method for evaluating the performance of the Stewart platform in the alignment of structures was to construct a structure and build a Stewart platform and apply loading or optimize in such a way that the misaligned structure was corrected. The optimization tools in ANSYS will be used to study the right force that is required to align the structure. This also told us how much each actuator moved. FEM predicted that the developed mechanism can be used in close structures.

3.10 Experiment

The experiment for this study was done in the next chapter. A test bed was constructed and used to describe the experimental research of the new product development. It serves as a platform for conducting a test on the modified Stewart platform manipulator. The bed will consist of a top platform and a fixed base. Two misaligned structures were used to test the modified Stewart platform manipulator. One of them was attached to the fixed base and the other attached to the top platform. Unlike the traditional Stewart platform, the modified Stewart platform was carried out on these misaligned structures in a closed loop environment which required the two symmetrical parts separated and then attached to the misaligned beams before joining them back. The top platform has several holes, which allow for changing the position of the misaligned structure attached to it. The position of the misaligned structure can be changed depending on the level of misalignment. The modified Stewart platform is then connected to the two structures to correct the misalignment. The purpose of building the testbed includes:

- Building a structure that represents realistic problems. This structure is closed and has two ends.
- To test the test bed platform for its ability to correct the misalignment. This platform should have different capabilities including the ability to exchange beams with different cross section so that we can see how the modified Stewart platform will adjust for different platforms. Also, to test its ability to change the location of the misalignment with the predetermined offsets so as to see the maximum capacity of the modified Stewart platform manipulator to bend things.
- To compare analytical results that are obtained with the numerical simulations.

To build the testbed, we purchased standard beams which were be connected by welding. The frame of the beam will be a rigid structure. The bottom and top of the test bed was modular with a stud coming from the bottom where the beam is screwed. The cross-section of the top of the bed was modular but adjustable. This was achieved by different idea preliminary by inserting different holes on the top of the bed but this time the stud is on the beam itself so that there is room to screw.

To fabricate the modified Stewart platform, some components that were purchased were used. We used the standard linear actuators and the standard ball joints to create the first symmetrical part all fitted together which were machined in the school’s laboratory and with the school’s machines. For the control, the four linear actuators came with an encoder each to measure their distance and that gave an idea of how much the base moved by using the inverse kinematics obtained to tell in an open loop how it is expected to move. With this in place, the movement angle was measured. Also, an experiment to test the relationship between the linear displacement and the base.

In the future work, sensors will be added to the test bed to measure the distance and to make it automatic adjustments. This bed will have proximity sensors that will measure how much of offset is required. This will be used to feed information to the modified Stewart platform, which makes this mechanism take correction automatically.

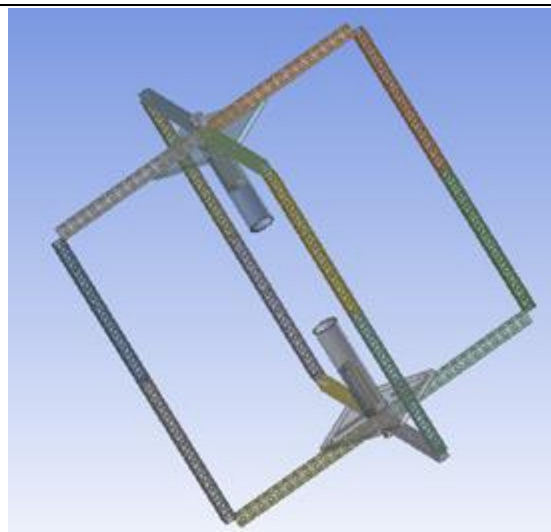

Figure 21: Test Bed showing two misaligned structures.

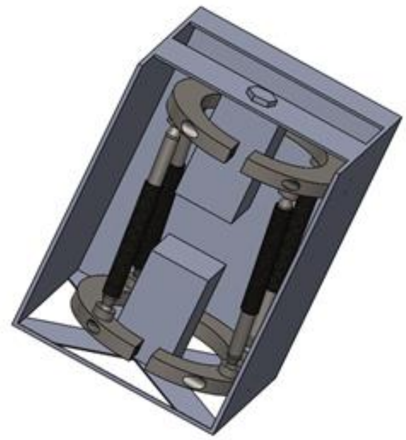

Figure 22: The MSP used to align two misaligned structures in a test bed.

3.12 Chapter Summary

This chapter provided a detailed description of the procedure used to achieve the objectives of the study. The restatement of the problem was followed by design specification requirement. The innovation, merits, impacts of the modified Stewart platform were described. Finally, the chapter also addressed the structure description, methodology, back of the envelope modeling, inverse kinematics and the finite element modeling of the proposed study.

CHAPTER FOUR: FINDINGS

This chapter provides the results of simulation and experiment according to the procedure developed in chapter three. The first section discusses the simulation of the modified Stewart platform by performing the analysis of 3D model while the other section discusses the experimental aspect of the analyzed 3D model. The structural mechanical analysis using ANSYS workbench to determine the static and dynamic characteristics and the contact between the clamp and grasped object is done. An analysis on the optimization of the structure of a predefined structure is also carried out.

4.1 Kinematic Analysis Based on Mathematical Model

In chapter three, a mathematical model was obtained to relate the relationship between external forces applied by Stewart platform and the displacement of the bent-structure. A back of the envelop study is conducted to understand the relationship for several sets of selected material and dimensions. MATLAB was used to simulate the dynamic equations including the rigid body and actuator dynamics. For this modified Stewart platform manipulator, the inverse algorithm in MATLAB environment is used to simulate the math's for the parameters.

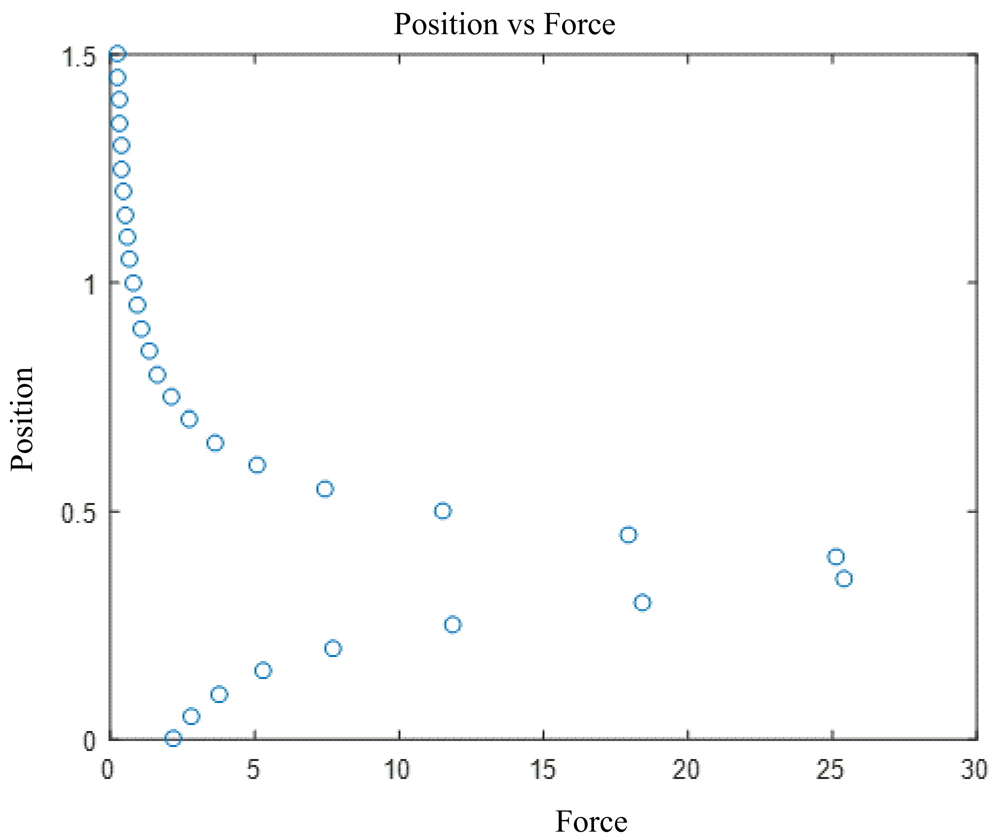

Figure 23: Relationship between the Position of the actuator and the force applied

4.2 Finite Element Modeling of Alignment Problem

This section consists of the results of the structural mechanical analysis. To study the stresses in the structure, the Finite element analysis tool is used. The finite element model is built and simulated using ANSYS finite element software. ANSYS is the software that implements the finite element simulations on structures, solid mechanics, and fluid. This model is dependent on the use of element technique, retaining the most important degrees of freedom (DOF) of each component to reduce the total number of DOF of the system (Hanieh, 2003). The method for evaluating the performance of the Stewart platform in the alignment of structures was to construct a structure, build a Stewart platform, and apply loading in such a way that the misaligned structure is corrected.

The reason for using this tool is to (1) simulate the structural displacement of the assembly under load, which shows the ability of the Stewart Platform to correct misalignment and (2) simulate the stress distribution to predict whether or not the structure will fail. This will also tell how much each actuator should move. The misaligned structure is an anchored pipe broken into two pieces.

Table 4.

Table 4. Material properties for PVC plastic

Physical Properties	Value	Unit (SI)
Young Modulus E	2.3*10e9	Pa
Poisson ratio	0.35	
Bulk Modulus	2.5556e+09	Pa
Shear Modulus	8.5185e+08	Pa

4.3 Failure Study

The failure study is carried out on two PVC material beam and two stainless steel material beams, which is attached to two fixed aluminum plate to compare their structural analysis. The purpose of this study is to simulate and visualize the behavior of the misaligned beams when actuation load is applied and to evaluate the safest maximum load. The directional deformation along the x, y and z-axes and the maximum stress output is obtained in this analysis. The study is carried out by considering five input displacements throughout the analyses and applying loads of 100N, 500N, 1000N, 2000N and 3000N on the misaligned beam to determine its deformation and its equivalent stress. These displacements are chosen based on the size of the beams to be aligned and the length of actuators. The resulting stresses are examined based on the load inputted to determine if it does not exceed the ultimate tensile strength of the material taking note that exceeding this property number shows that the device will fail under the given load. In addition, the actuation load is taken from the previous chapter, which are the specifications of the actuators and ball joints given by the manufacturer.

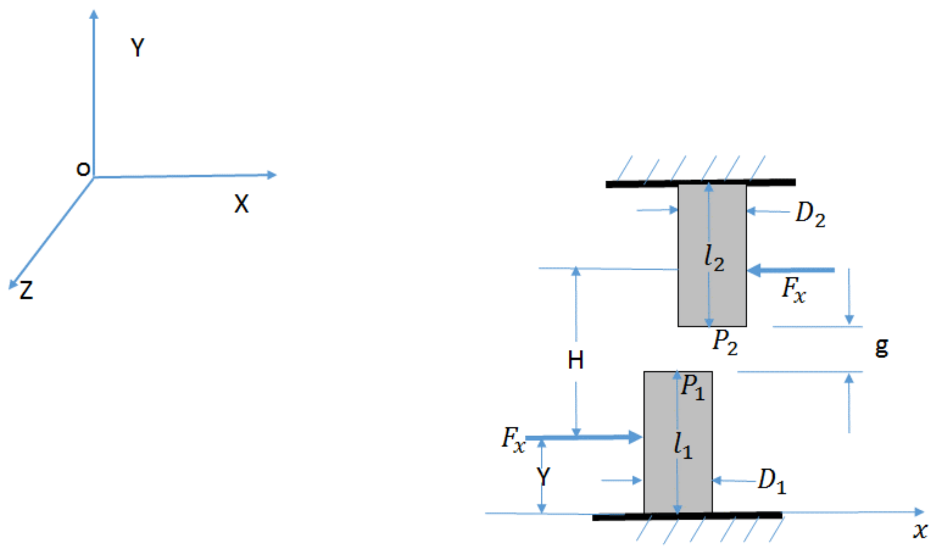

Figure 24: Illustration showing the location of the load with respect to the assembly

Figure 24 above is an illustration showing the location of the load with respect to the assembly that matches the finite element model simulation. Two PVC pipes are attached to two fixed plates. H is the length of the modified Stewart platform. D_1D_2 are the diameters of pipes one and two, l_1l_2 are the lengths of pipes of pipes one and two. Y is the displacement between the load applied on pipe one and the fixed plate. F_x is the load applied on the two pipes with that acting on pipe two in the opposite direction. The point of loading is the position of the top and bottom base. P_1P_2 is the center to center distance of the pipes which is the misalignment $\left|\left(\overrightarrow{P_1p_2}\right)_x\right|$and $g = 1\ mm$ is the distance between the two pipes. The initial misalignment before applying load was 1mm and the gap was 1 mm.

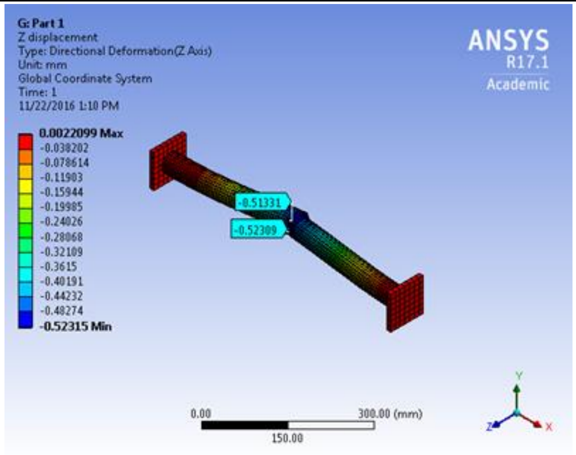

Figure 25: Output result along Z-axis of two misaligned beams

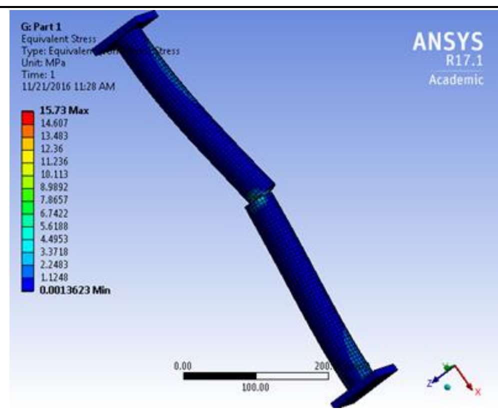

Figure 26: Output result of maximum equivalent stress of two misaligned beams

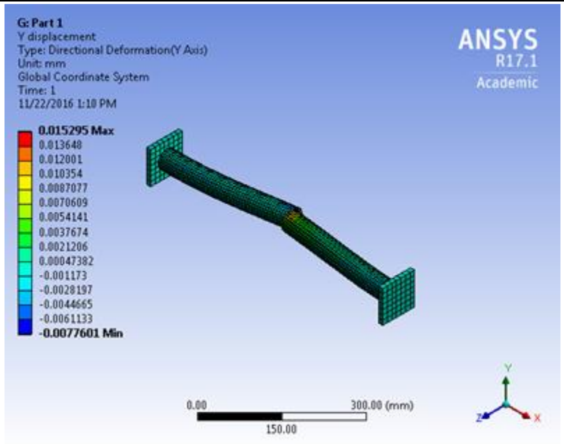

Figure 27: Output result along X-axis of two misaligned beams

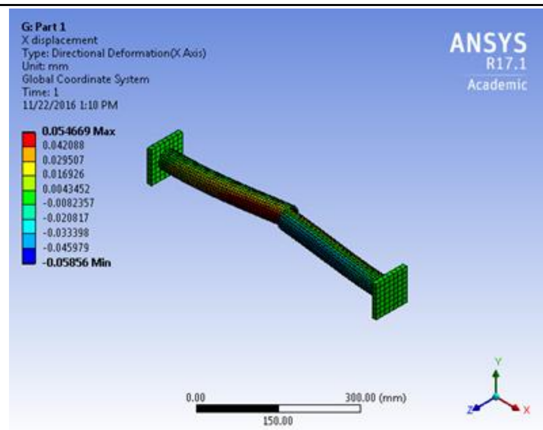

Figure 28: Output result along Y-axis of two misaligned beams

Figures 25, 26, 27, and 28 are the output results of a 100N load applied to the two PVC beams in opposite directions at the initial position of y= 0. It is observed that the directional deformation is at the tip of the beams along the Z-axis. The deformation of beam 1 is obtained as -0.51986mm while that of beam 2 is -0.52309mm. The equivalent stress is obtained as 15.73Mpa. Also, the directional deformation along x-axis and z-axis are -0.05856mm and -0.0077601mm respectively.

The output results for x and y directional deformation are -0.00077 mm and -0.05856 mm. These values of deformation are very small and as such are not significant. The stress distribution is observed at the tip of the two pipes. A graph is plotted for the results of loads 100N, 500N, 1000N, 2000N and 3000N for y= 0. The result of the above case for the five applied loads is tabulated in **Table 5** given below. The output results of loads 500N, 1000N, 2000N and 3000N when applied to PVC material and that of stainless steel material is shown in the appendix.

Table 5. Static Structural analysis results for two misaligned PVC beams for y= 0

Force	(P1)x	(P2)x	Max Stress	1-[(P1)x – (P2)x}
0	0	0	0	1
100	-0.51986	-0.52309	15.73	0.4249
500	-2.7529	-2.7674	82.954	-4.5203
1000	-5.5053	-5.5347	165.91	-10.04
2000	-11.011	-11.069	331.82	-21.08
3000	-16.517	-16.604	497.72	-32.121

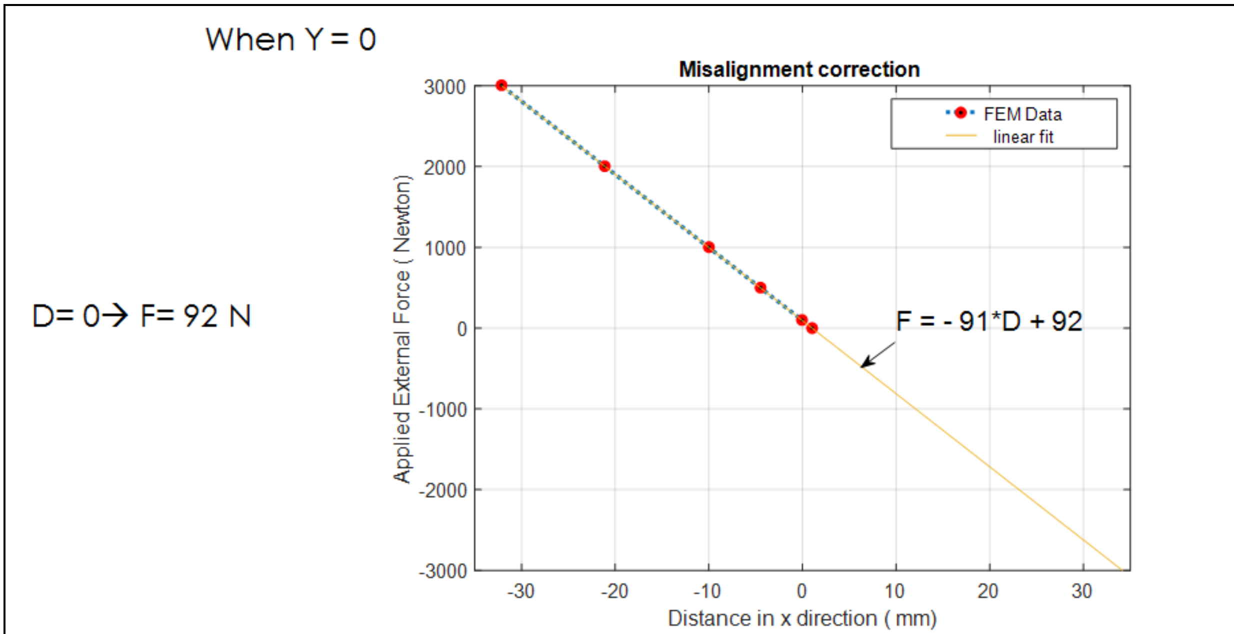

Figure 29: Relationship between loads applied to the beams and distance

Figure 29 is a graph showing the relationship between various loads and the displacement of the two pipes. This result is for when y = 0 for several loads applied to the two plastic pipes where g is 1 mm and $(\overrightarrow{P_1 p_2})_x$ is 1 mm. It is observed that as the load decreases, the more the misalignment is been corrected. This results shows that it is better to fix the modified Stewart platform at a location close to the base so it does not move or not hanging up on the misaligned structure. Since the load applied does not exceed this maximum stress, then we can say the structure safely passed. When the mechanism is placed at a zero position, a 92N force is required to correct a 1 mm misalignment.

4.3.1 Mechanism provide force that resists the structure stiffness

One of the critical parts of the modified Stewart platform is the actuator assembly and as such, we will be analyzing this part. The actuators were purchased from Firgelli Automations company (Firgelli Automations, 2016) and McMaster-Carr commercial company (Mcmaster-carr, 2016) respectively. The reason for analysis on this assembly is because it is the part that ensures the required precision control as it affects the relative positions of the misaligned structure that needs correction. As this assembly moves, the misalignment is corrected. The hypothesis is tested to determine that the actuator assembly can provide the force required to resist the structure stiffness. The approach was to use the linear actuators capable of resisting stiffness, which enables the platform to manipulate loads of up to 20kN. In **Figure 30** below, the maximum total deformation of 1.2635e-5 m is observed at the bottom of the sliding cylinder due to the positive force that is applied at the bottom of the sliding cylinder. The force is 889.64 N. The equivalent stress is observed at the bottom of the ball attached to the top joint with the equivalent stress been 5.4426e-7 Pa. The stress is located at that point because the negative force is located at the base which causes the actuator to be pulled down.

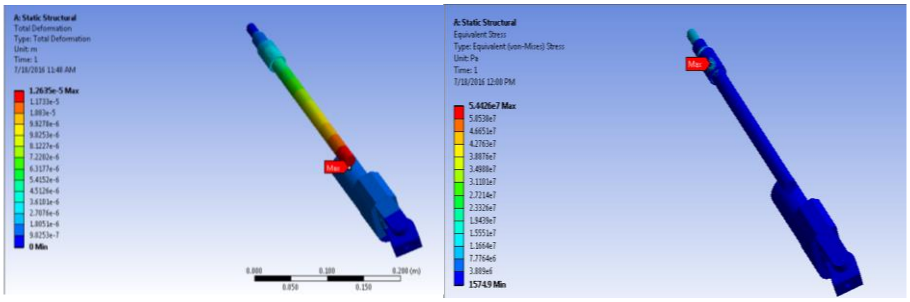

Figure 30: Output results for overall actuator and ball joint model with combined design

In **Figure 31** below, the total deformation is pointing down at the bottom due to the force that the sliding cylinder is acting on. The total deformation is observed at 2.6189e-6 m. Also, the equivalent stress is observed right under the ball as 2.6039e-7 Pa due to the force pulling the actuator downwards.

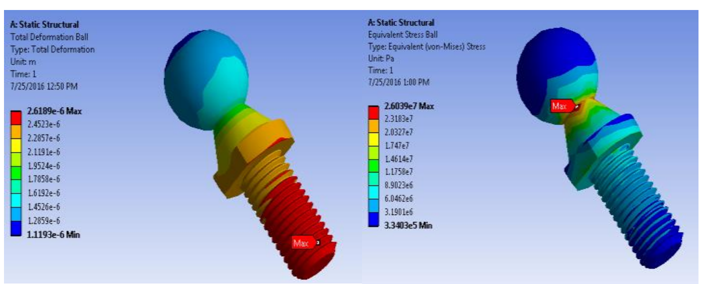

Figure 31: Output results for ball joint model

In **Figure 32** below, for the bottom joint designed, the maximum deformation, 4.7057e-7 m is observed at the side of the joint. This is because the joint moves in different directions and is not stable. For the equivalent stress, the middle of the hole of the bottom joint is observed to be the stress location. The stress, which is 8.6098e-6, is observed in this position because the joint is carrying the whole actuator and is being directed downwards.

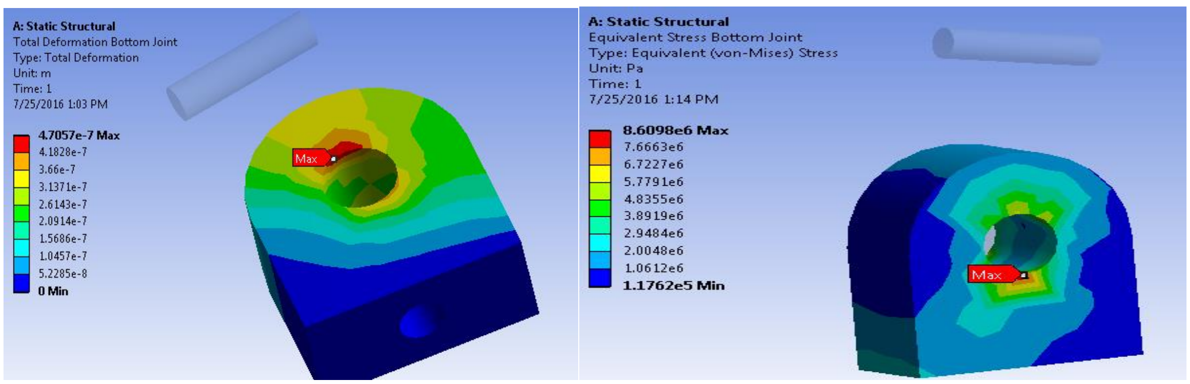

Figure 32: Output results for bottom joint design

Figure 33 below shows the output results for the top, middle and bottom pin. The top pin has a maximum deformation of 4.4423e-6 m is observed at the center of the top pin because as the sliding cylinder is moving vertically, it pulls it down which allows all the stress to go to the center. The middle pin has a maximum total deformation observed at 1.0706e-6 m which is pointing to the middle right of the pin. The pin is under pressure as a result of the sliding cylinder and the movement of the whole actuator. The bottom pin has a maximum deformation of 8.8318e-7 m. This is observed at the center of the left pin due to the force that the whole actuator is applying on.

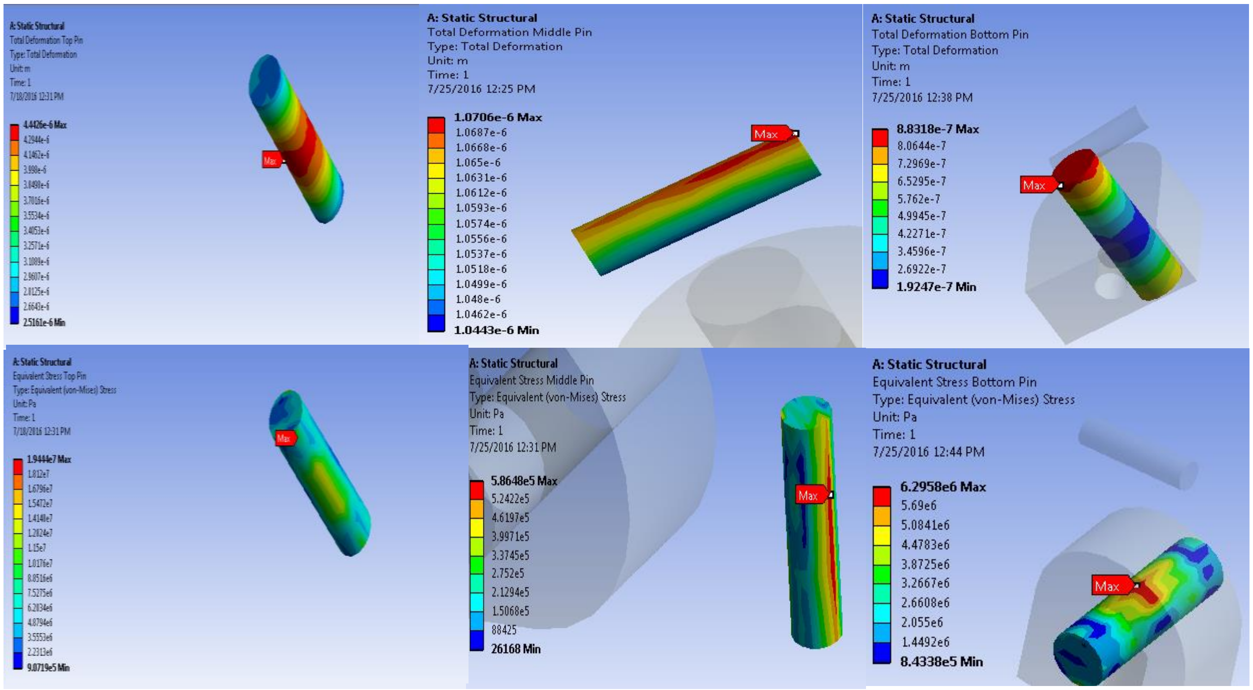

Figure 33: Output results for bottom joint pin model

As shown in **Figure 33** above, the stress acting on the top pin is located on top of the pin with the maximum equivalent stress at 1.94467 Pa. Also, the equivalent stress is exactly in the middle of the pin due to the force acting downwards. This equivalent stress is 5.8642e5 Pa. For the bottom pin, the force is located exactly in the middle of the pin. This is because the force acting down is 889.64 N and the equivalent stress 6.2958e6 Pa.

4.3.2 Mechanism used in closed and open structures

FEM predicts that the developed mechanism can be used in closed structures; two symmetrical parts were developed with the two parts mounted on structures. In addition, finite element model is built and simulated using ANSYS finite element software. **Figure 34** shows the two symmetrical parts with the adjustable clamps.

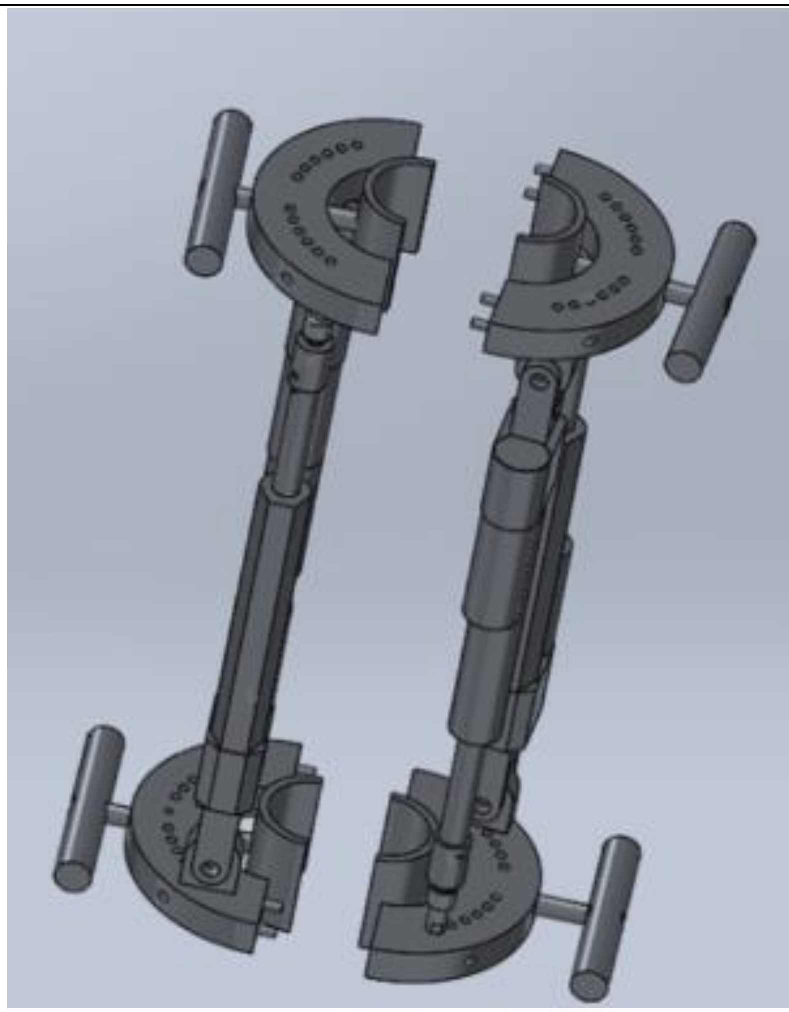

Figure 34: Two symmetrical parts

4.3.3 Mechanism can hold beam of cross sectional shape mainly Pipe

The future work for this research work will include grasping problem. The hypothesis is tested to determine that the base when flipped upside down and connected symmetrically can hold various beams especially circle. The design is in such a way that the lead screw is attached to the base and a grasping clamp attached to the end of the screw for proper grasping of the beam. One advantage of this is that, the lead screw expands and contracts to accommodate the required cross-section. This will also improve or increase the stiffness. The adjustable clamp also offers the advantage of been mounted around a range of cross-sectional area so as not to lose grip while adjusting the relative position between two ends of the platform. Another advantage is that the adjustable clamp will be easy to use. One disadvantage is that the grasping clamp has to be changed for different shapes of misaligned parts that needs to be corrected. A spring-loaded adjustable clamp shown in **Figure 35** below is designed to help achieve this aim.

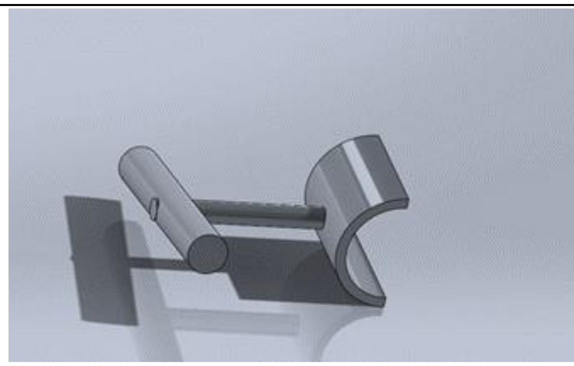

Figure 235: Spring loaded adjustable clamp

4.4 Manufacturing of Stewart Platform

For the modified Stewart platform, four prototyped feedback rod linear actuators are used with a built-in potentiometer for each of them, which helps to determine the actuator position at any time. **Figure 36** gives the initial drawing of one of the actuators and ball joint with combined design taken for analysis. Actuation load is taken from the previous chapter, which are the specifications of the actuators given by the manufacturing industries as shown in **Table 2**.

4.4.1 CAD Design

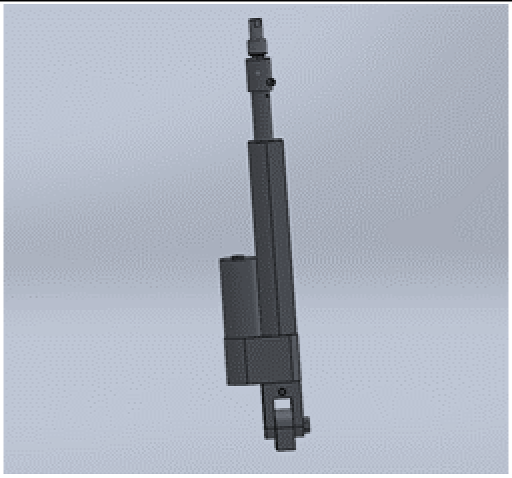

Figure 36: CAD drawing of actuator connected to a ball joint with a combined design

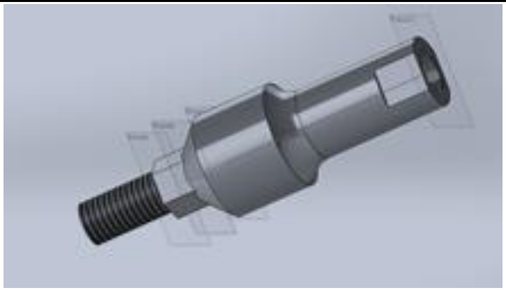

Figure 37: CAD drawing of ball joint

The ball joint is connected at the top of the actuator and is responsible for limiting only translation at the joint, and allowing for rotation about all three axes (Hartt, Gilchrist, & Truman, 2012). These joints will help align the actuators.

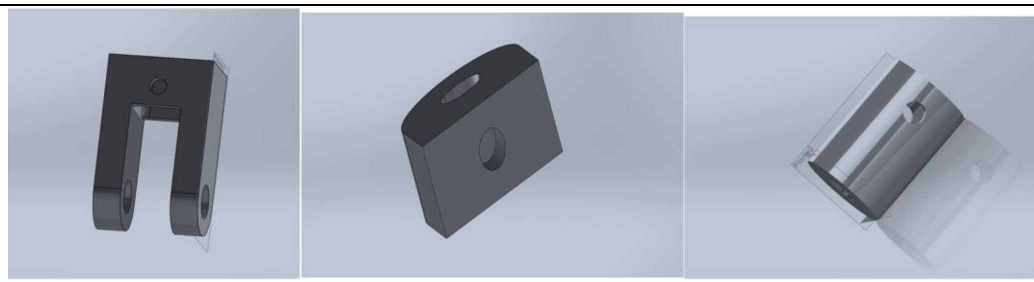

Figure 38: Combined design parts

The combined design shown in **Figure 38** consists of three parts, one, two and three. Part two is designed to fit into part one. Part three is designed in such a way that the actuator can be connected to it. These parts are designed to help control the movement of the actuator and the ball joint and to better correct the misalignment.

4.4.2 Material and Specification

This mechanism consists of parts made from aluminum, Zinc and steel materials. The housing of the ball joint and stud joint is made of Zinc-plated steel. The actuators purchased from the manufacturer consists of an aluminum inner and an outer tube paired with a zinc alloy housing Also, the fabricated parts are made from aluminum materials. Below are the engineering specifications for the materials used to develop the mechanism. The linkages of the ball joint compensate for the misalignment by making pivoting connections.

The actuators and ball joints whose engineering specifications have been listed in **Table 6** above were purchased from Firgelli Automations company (Firgelli Automations, 2016) and McMaster-Carr commercial company (Mcmaster-carr, 2016) respectively.

Table 6. Engineering Specification

Spec #	**Parameter Description**	**Requirements**
1	**Cost/Actuator**	$139.99 per actuator
2	**Ball Joint linkages**	$11.08 each
3	**Actuator force**	889.6 N
4	**Actuator Input**	12V DC
5	**Actuator Stroke**	12"
6	**Actuator Speed (**"/S**)**	0.3"
7	**Actuator Operational Temperature**	65°C
8	**Retracted length**	17.9"
9	**Extended length**	29.9"
10	**Ball joint length**	2 3/8"
11	**Ball joint stud and thread size**	5/16"-24
12	**Thread depth**	9/16"
13	**Ball Joint Temperature**	Up to 80°C

4.4.3 Machining Procedures

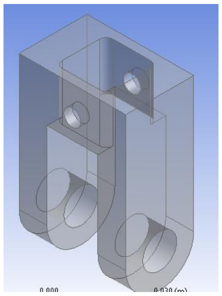


Figure 39: Designed Part 1

Combined Design:

a. Designed Part 1

   i. Aluminum bar is cut and machined into the correct size as shown in **Figure 39**

   ii. Drill top hole for mounting of the bottom of the actuator, as well as holes at the bottom for connecting part 2 shown in **Figure 40** below**.**

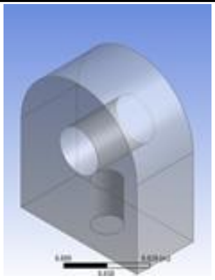


Figure 2440 Designed Part 2

b. Designed Part 2

   i. Aluminum bar is cut and machined into the correct size shown in **Figure 40** above

ii. Drill hole on the side for attaching part 1 and another at the bottom for attaching the base.

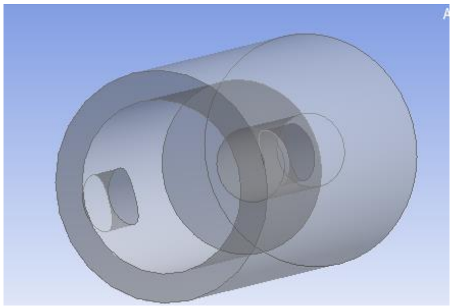

Figure 4125: Designed Part 3

c. Designed Part 3

i. Aluminum bar is cut and machined into the correct size as shown in **Figure 41** above.

ii. Drill holes on the side and bottom for attaching both actuator and ball joint respectively.

Figure 4226: Aluminum ring for Base

Actuator Mount:

i. Cut rings shown in **Figure 42** above into two equal parts to make two bases.

ii. Step one above is repeated to get the remaining two base.

iii. Drill holes on the base in **Figure 43** below for mounting of the ball joint, actuator, and designed part 3, as well as holes for mounting the adjustable clamp and holes for the two-top base and two-bottom base.

Figure 4327: Base

4.4.4 Assembly Procedures

The design of the mechanism is an improvement and modification on the existing system. This section, however, presents the results of human design assembled together to solve problems and to reduce assembly errors. It is important to note that the chances of a product are termed perfectly reduces the number of parts assembled together rises. Mistake-proof product assembly also known as Poka-yoke was implemented in the assembly so that the mechanism can be assembled in one way. The step-by-step assembly procedure is presented below. First, a part-by-part assembly analysis was done to determine if the parts can be combined, how they can be combined, and if some parts can be eliminated. Consideration was also given to the material properties, the reason why all the assembly parts are aluminum. The prototype of the modified Stewart platform is initially produced by assembling the scaled 3D model of the parts in order to test the mechanism under real conditions before progressing into full production. Each step of the assembly procedure is started and completed after the previous step has been completed. The unnecessary part was avoided since they will involve extra efforts and the assembly proceeded vertically with parts added on top of the other. **Figure 44** below shows the two symmetrical parts, which is first assembled, before been joined together as shown in **Figure 45**.

Figure 4428: Assembled symmetrical parts

Figure 45: Assembled mechanism

4.5 Product/Preliminary Test

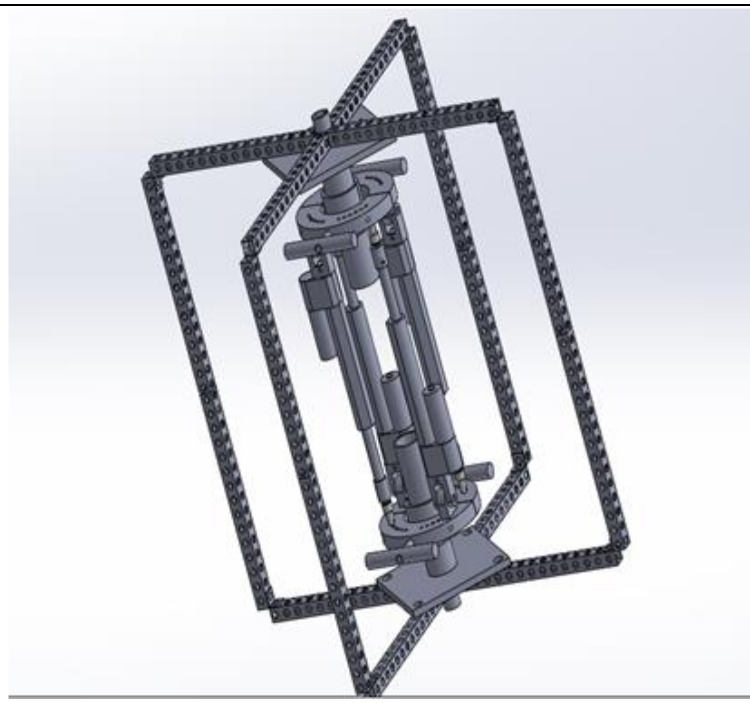

Figure 46: CAD model of the assembly and test bed

In order to ensure that the mechanism designed meets all the geometrical requirements, a test bed, and several small-scale models are initially designed in 3D shown in **Figure 46** above. A scale model is then constructed to achieve the necessary stroke and performance. Testing was done by constructing a test bed shown in **Figure 47** below which was used to describe the experimental research of the new product development. It is a platform for conducting a test on the modified Stewart platform. Two misaligned beams are used to test the modified Stewart platform and are attached to the test bed. The assembly mechanism is then attached to the misaligned beams. Testing is initialized with four actuators and is verified that it meets performance requirements with tests designed specifically for the four actuators. The assembly is clamped to the two misaligned beams and load is applied to correct the misalignment. The load and range of motion is then verified with the manufacturer's specifications for the ball joints and actuators. To test the motion of the symmetrical parts, we placed the symmetrical parts on the floor and moved around to see the directions of motion as shown in **Figure 44** above.

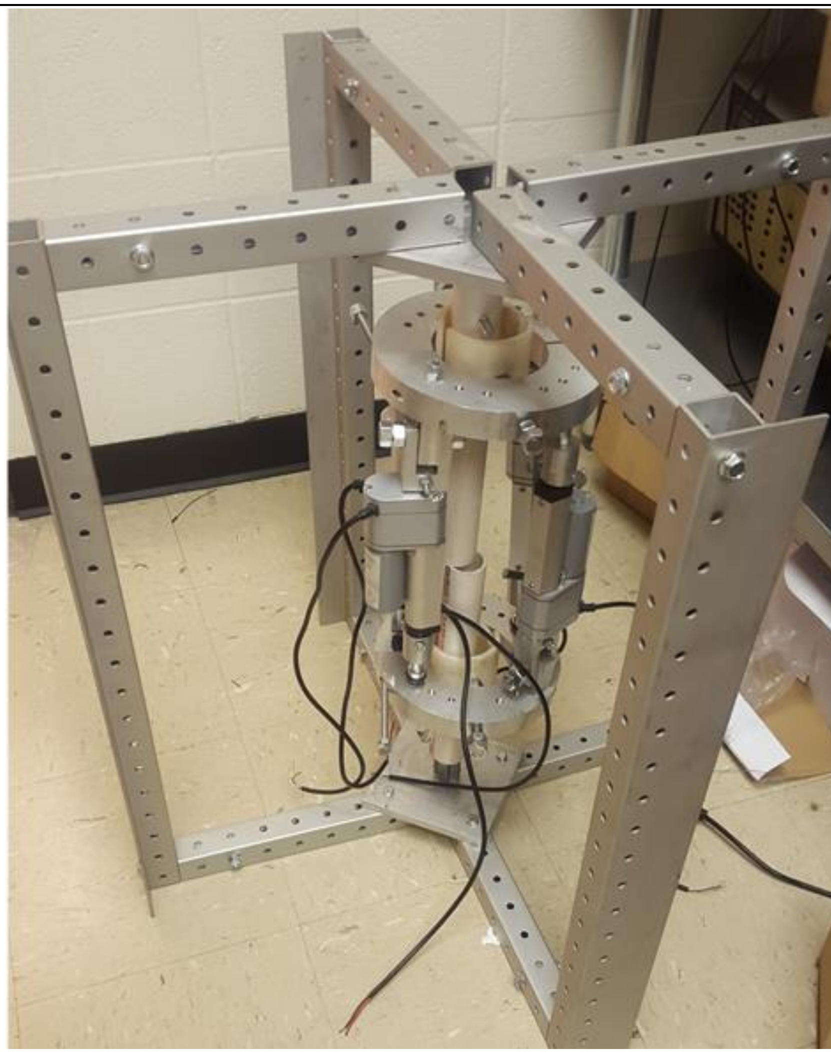

Figure 47: Assembled mechanism attached to test bed

4.6 Quality of Machining

This study examines the surface quality of machined parts to determine if they meet technical requirement. The most efficient process is used in the machining so that each of the parts meets all specifications and ensured that inspections are done after each machining to justify the accuracy of each dimension. The data for each machined part is collected and recorded in **Tables 7, 8, 9** and **10** below for comparison. Variables A, B, C, D, E, F, G, H, I, J, K, L, M, N represents the side hole, bottom hole, width of top hole, width, length, length of top hole, external diameter of part 3, internal diameter of part 3, internal diameter of base, external diameter of base, clamping hole, actuator hole and base connector hole respectively.

Table 7. Dimensions for Designed part 1

Sample	Length (Inch) E	Width D (Inch)	Thickness F (Inch)	Bottom hole Diameter B (Inch)	Side hole diameter A (Inch)	Width of Top hole C (Inch)	Length of Top hole G (Inch)
1	2.65	1.50	0.80	0.49	0.27	0.73	0.70
2	2.60	1.56	0.90	0.5	0.27	0.73	0.71
3	2.60	1.56	0.90	0.5	0.27	0.73	0.71
4	2.50	1.56	0.90	0.49	0.27	0.73	0.71
Mean	2.59	1.55	0.875	0.495	0.27	0.73	0.708
Standard Deviation	0.00025	0.001	0	0	0	0	0.00000025

Table 8. Dimensions for Designed part 2

Sample	Length E (Inch)	Width D (Inch)	Thickness F (Inch)	Bottom hole Diameter B (Inch)	Side hole diameter A(Inch)
1	1.74	1.50	0.74	0.27	0.48
2	1.75	1.52	0.72	0.27	0.48
3	1.76	1.52	0.72	0.27	0.49
4	1.75	1.52	0.72	0.27	0.48
Mean	1.75	1.515	0.725	0.27	0.483
Standard Deviation	0	0	0	0	0

Table 9. Dimensions for Designed part 3

Sample	External Diameter H (Inch)	Internal Diameter I (Inch)	Bottom hole Diameter B (Inch)	Side hole diameter A (Inch)
1	1.253	0.793	2.50	0.27
2	1.251	0.793	2.51	0.27
3	1.251	0.793	2.50	0.27
4	1.251	0.793	2.50	0.27
Mean	1.252	0.793	2.502	0.27
Standard Deviation	0.000001	0	0	0

Table 10. Dimensions for Base

Sample	External Diameter K (Inch)	Internal Diameter J (Inch)	Thickness F (Inch)	Clamping hole L (Inch)	Actuator hole M (Inch)	Base Connector hole N (Inch)
1	8	4	1	0.49	0.27	0.27
2	8	4	1	0.48	0.27	0.27
3	8	4	1	0.49	0.27	0.27
4	8	4	1	0.49	0.27	0.27
Mean	8	4	1	0.483	0.27	0.27
Standard Deviation	0	0	0	0.000081	0	0

For all the machined part, the maximum tolerance is 0.001 inches. This tolerance proves that the quality of the machining process is good. The tolerance caters for both human and machine error. The results confirm that the dimensions of the parts are good enough to perform the functions it was designed for and thus, is of good quality. It is not surprising to know that the machining of the parts took more time than anticipated. Averagely, a set (four samples) of each designed part took as much as ten hours which gave a total of thirty hours to machine all the parts. This time justifies while the tolerance is as minimal as possible.

4.7 Summary

To answer project objective one, section 4.3 presented the analysis carried out to confirm that the mechanism can correct misalignment of a small millimeter scale misalignment. This was achieved by attaching two misaligned PVC beam to the testbed with the modified Stewart platform attached and load applied. It is observed that as the load decreases, the more the misalignment is been corrected. This result showed that it is better to fix the modified Stewart platform at a location close to the base so it does not move and that to achieve a zero misalignment for an initial 1 mm misalignment; 92N load is applied on the beams.

The actuator assembly was analyzed as described in Section 4.3.1 to answer project objective two. This analysis was carried out on this assembly since it is a critical part of the modified Stewart platform due to serious contact problem that could be from the sliding actuator cylinder, various joints from the designed parts in order to determine where the stresses lie. The deformation and maximum equivalent stresses of the actuator assembly were observed to be lower than the structure stiffness, which proves that the pipes can resist structure stiffness of actuator.

Section 4.3.2 presented the answer to project objective three. The method used was develop the modified Stewart platform in such a way that it has two symmetrical parts which can be connected to misaligned structures and also disconnected from them. The symmetrical parts can be connected using a connect-disconnect mechanism by flipping the other part. The symmetrical parts allows for misalignment corrections of bigger structures that cannot be done using the original Stewart platform, which mostly is used for predefined specific sizes.

The adjustable clamp is important for grasping in the two symmetrical parts that allow for different shapes and different cross-sectional area. As such, a 3D printed clamp was attached to the base, which could be expanded and contracted to hold the pipes. These adjustments confirms that the adjustable clamp can hold smaller and larger plastics of various sizes. This clamp was designed especially for circular pipes because of the material of the clamp, which is made of ABS plastic. The future work for this study will be to design adjustable clamps using different materials and different shapes.

CHAPTER FIVE: RESULTS, DISCUSSION, AND CONCLUSION

This chapter records the result of the project, covers the discussion and addresses the conclusion.

5.1 Results and Discussion

The major objective of this study was to design a modified Stewart platform manipulator that can be firmly mounted around a cross-sectional area without losing the grip while adjusting the relative position of the two ends of the Stewart platform. Other objectives were to understand the usage of the mechanism for closed-end and open-end structure applications, understand the characteristics of the mechanism for misalignment problems, apply the concept of Stewart platform manipulator to the modified version, study the performance of the proposed mechanism and finally understanding the significance and importance of the development of analytical tools such as mechanical manipulator. ANSYS workbench is used to simulate the device performance to achieve the specified objectives. The specification for the actuators and ball joints is taken from its manufacturing website. A SOLIDWORKS model is made initially to assemble the parts for the best design resulting in maximum load range. The functionality of the mechanism is tested by performing static structural analysis on the actuators, ball joints and design components of the mechanism.

5.2 Conclusion

The finite element analysis was done in this study using ANSYS workbench to simulate the performance of the modified Stewart Platform to achieve the stated objectives. The assembled actuator when a load of 889.64N has a total deformation of 1.2635e-5m. This is found at the bottom of the sliding cylinder due to positive force been applied at the bottom of the sliding cylinder. With the same load applied, the maximum equivalent stress is 5.4426e-7 Pa. The stress distribution is seen at the bottom of the ball joint, which causes the actuator to be pulled down. Based on the finite element analysis results, the assembled actuator, which is one of the critical part of the modified Stewart platform, is able to provide force required to resist the structure stiffness. Also, for the two misaligned pipes, at a load of 100 N and 3000 N, the directional deformation along the z-axis is -0.51986 and -0.43211. With these same loads applied, the maximum equivalent stress is 15.73 MPa and 90.723 MPa. The stress distribution for all the various loads applied was seen at the tips of the pipes. Similar to the FEM results, the modified Stewart platform experiment carried out on an anchored PVC pipe broken into two pieces attached to the test bed showed that as the actuator positions changed, the pipes moved closer to each other.

Few challenges were encountered in the machining process, and the ones that did come up were detected early enough. One vital issue was pertaining to the machining of the smaller design parts and the base. I believe I had addressed this issue by reducing the number of parts to be machined by humans, but there was still a lot more human errors detected. This could be addressed by using a CNC milling machine, which would eliminate most or all of the human error.

5.3 Future Work

This chapter introduces the recommendation for future work. First, it is important to carry out more research to avoid the failures as seen in the modified Stewart platform and its construction. The recommendation for future work is stated below:

- Fabrication can be done by 3-D printing to obtain a compliant structure. Also, a control system can be integrated into the mechanism to control the movement of the actuator. The kinematic model of the actuator should be studied along with the sensitivity of the actuator.
- For the test bed, it is suggested that sensors be added to the test bed to measure the distance and to make it automatic adjustments. This bed can have proximity sensors that will

measure how much of offset is required. This will be used to feed information to the Stewart platform which makes the Stewart platform take correction automatically.

- To a large extent, parts were all designed well but lacked little manufacturing skills. For instance, some of the fabricated parts could not hold the tight tolerances needed for smooth operation. Extra care should be taken when machining these pieces, as a result, I would recommend more practice time be taken and more time allowed for finishing the machining process. To improve on machining these parts in the future, a CNC milling machine should be used to achieve tight tolerances to ensure much more useful results, also keeping in mind that parts made with a CNC milling machine would certainly speed up the manufacturing process, as many parts took longer to complete. In the Bowling Green State University workshop, there is a high number of usage for the traditional mills, but since CNC milling machines require a very high level of certification in order to use, they usually just sit idle.

Appendix A

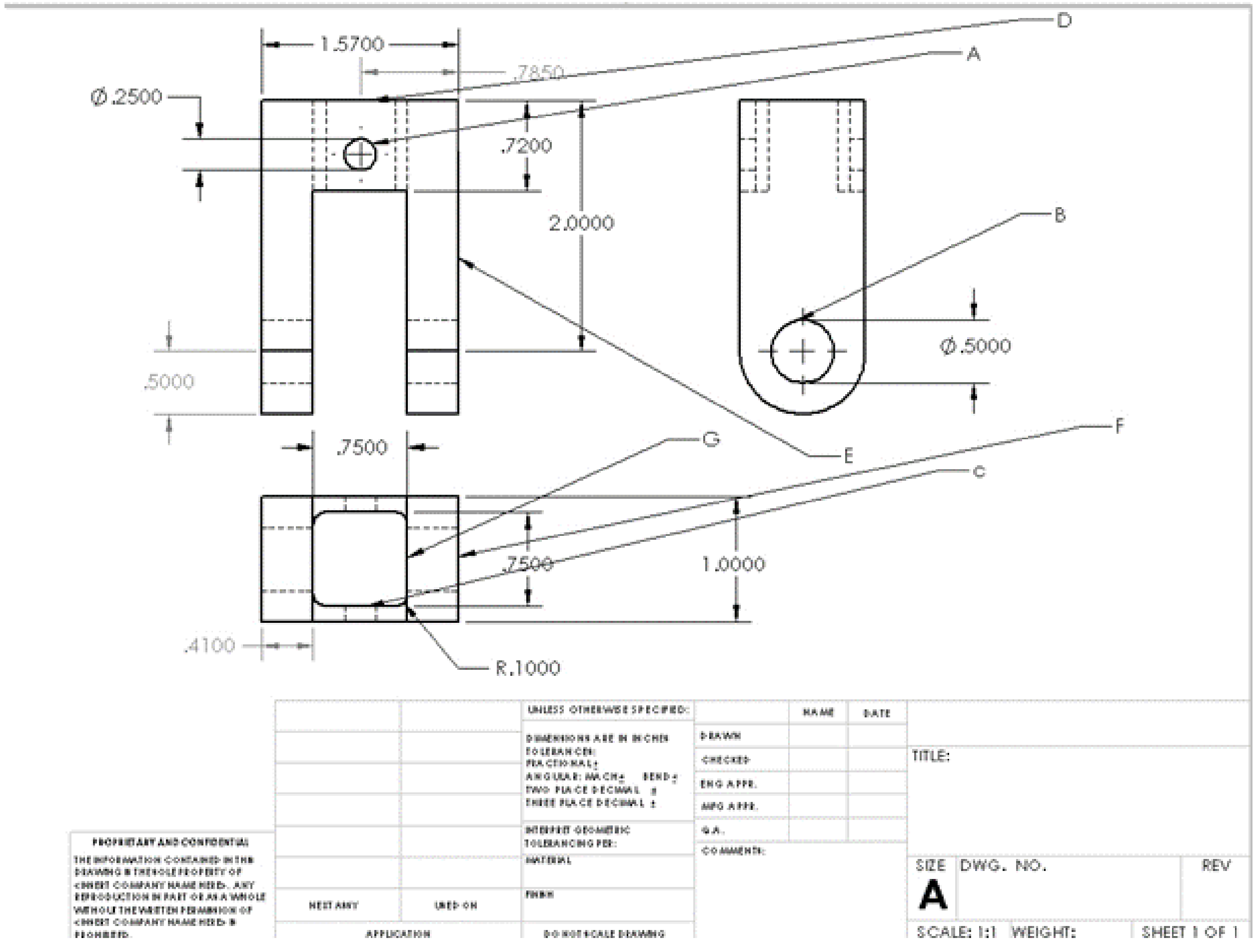

CAD drawing of designed part 1 showing critical dimensions labelled with variables

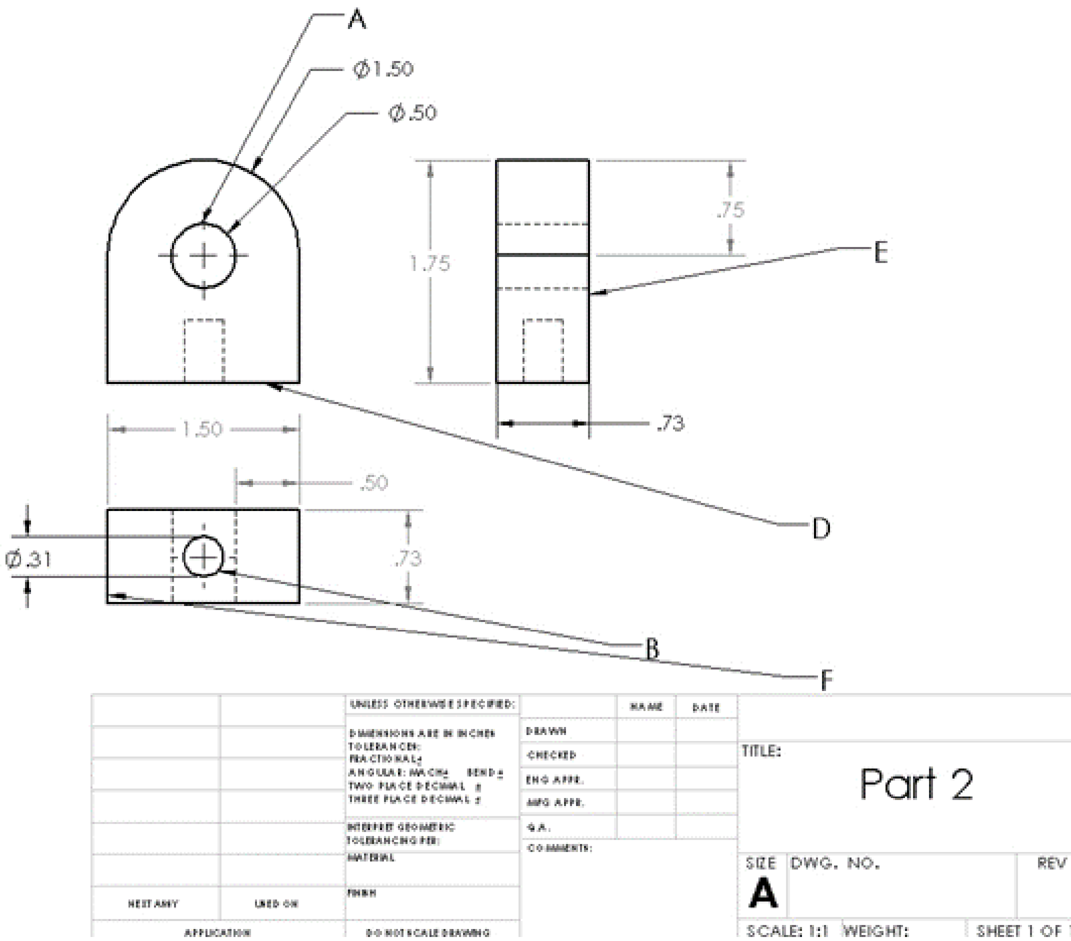

CAD drawing of designed part 2 showing critical dimensions labelled with variables

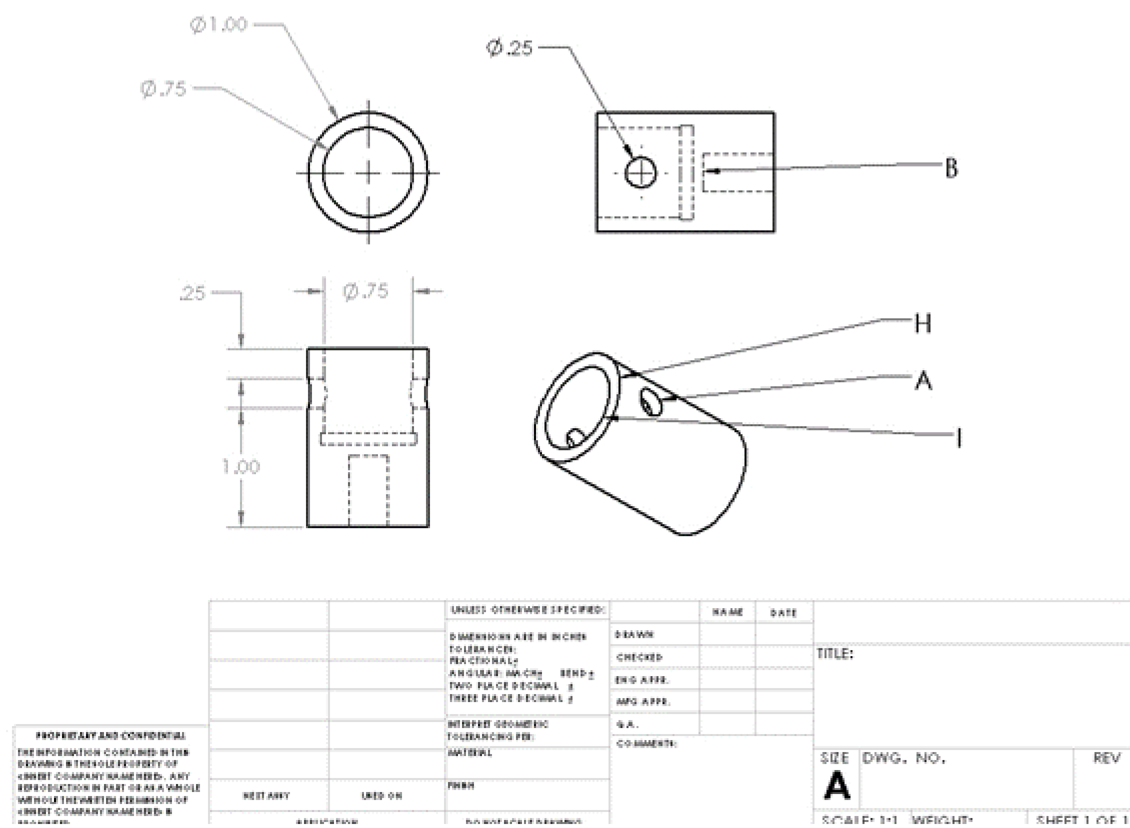

CAD drawing of designed part 3 showing critical dimensions labelled with variables

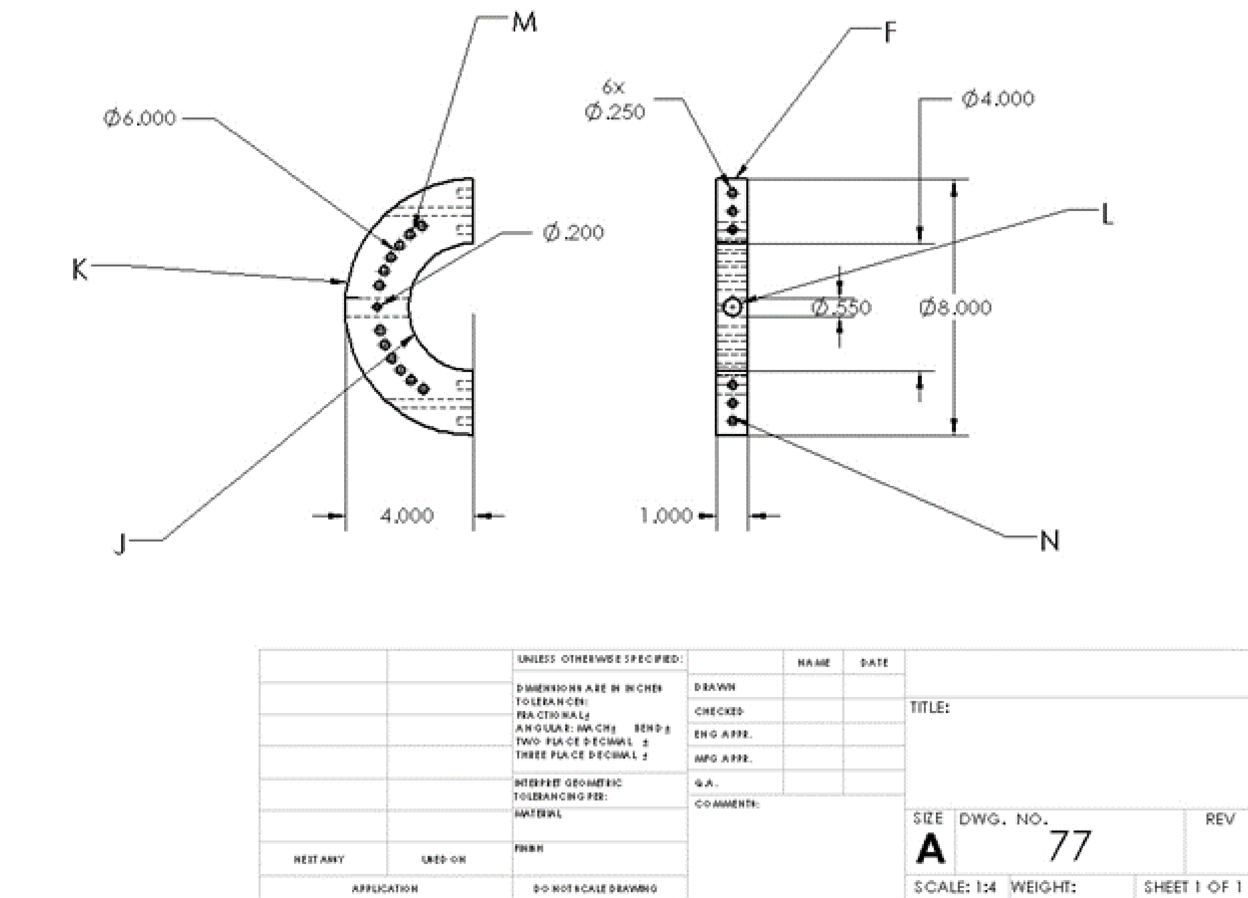

CAD drawing of base showing critical dimensions labelled with variables

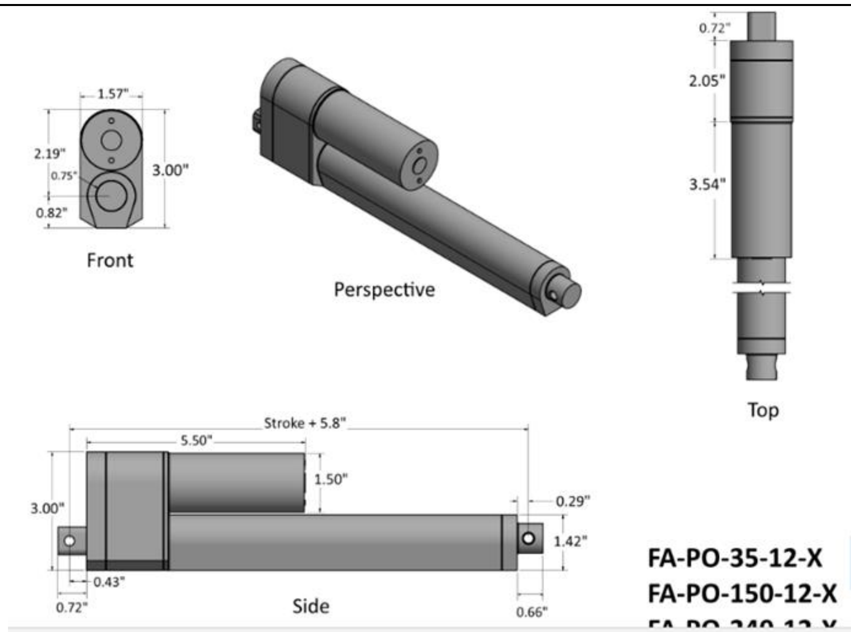

CAD drawing of actuator

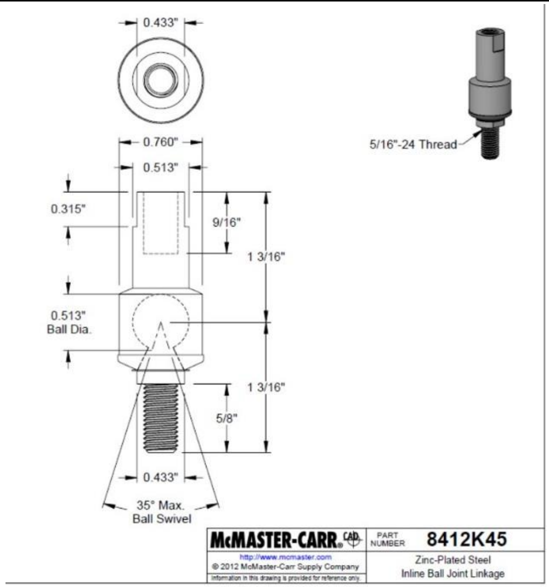

CAD drawing of ball joint

Appendix B

Matlab Code

```
clear all;
close all;
del=3e-3; % missalignment in Meter
R1=5e-2 % radius of the first beam
l1=.5;  % length of the first beam
I1=1/4*pi*R1^4; % assume the beams are circular
R2=1e-2 % radius of the first beam
l2=2; % length of the second beam
I2=1/4*pi*R1^4; % assume the beams are circular
lo=2.1; % total length between the two bases.
E1=50e6; % modulus of elasticity for steel in PSI unit system
E2=30e6; % modulus of elasticity for steel in PSI unit system

% assume that the force P is given

% solve('6*del/P=a1^2*(3*l1-a1)/(E1*I1)+(l1+l2-lo-a1)^2*(3*l2-
l1+lo+a1)/(E2*I2)','a1');
% So=[];
% for P=0:10:1000; % force in Newton
%
% a1= ((E1*I1*P*l2 - 3*E1*I1*P*l1 + 3*E2*I2*P*l1 +
3*E1*I1*P*lo)^2/(9*(E1*I1*P - E2*I2*P)^2) - (3*E1*I1*P*l1^2 - 2*E1*I1*P*l1*l2
- 6*E1*I1*P*l1*lo - 5*E1*I1*P*l2^2 + 2*E1*I1*P*l2*lo +
3*E1*I1*P*lo^2)/(3*(E1*I1*P - E2*I2*P)))/((((E1*I1*P*l2 - 3*E1*I1*P*l1 +
3*E2*I2*P*l1 + 3*E1*I1*P*lo)^3/(27*(E1*I1*P - E2*I2*P)^3) + (- E1*I1*P*l1^3 +
E1*I1*P*l1^2*l2 + 3*E1*I1*P*l1^2*lo + 5*E1*I1*P*l1*l2^2 - 2*E1*I1*P*l1*l2*lo
- 3*E1*I1*P*l1*lo^2 + 3*E1*I1*P*l2^3 - 5*E1*I1*P*l2^2*lo + E1*I1*P*l2*lo^2 +
E1*I1*P*lo^3 - 6*E1*E2*I1*I2*del)/(2*(E1*I1*P - E2*I2*P)) - ((E1*I1*P*l2 -
3*E1*I1*P*l1 + 3*E2*I2*P*l1 + 3*E1*I1*P*lo)*(3*E1*I1*P*l1^2 - 2*E1*I1*P*l1*l2
- 6*E1*I1*P*l1*lo - 5*E1*I1*P*l2^2 + 2*E1*I1*P*l2*lo +
3*E1*I1*P*lo^2))/(6*(E1*I1*P - E2*I2*P)^2))^2 - ((E1*I1*P*l2 - 3*E1*I1*P*l1 +
3*E2*I2*P*l1 + 3*E1*I1*P*lo)^2/(9*(E1*I1*P - E2*I2*P)^2) - (3*E1*I1*P*l1^2 -
2*E1*I1*P*l1*l2 - 6*E1*I1*P*l1*lo - 5*E1*I1*P*l2^2 + 2*E1*I1*P*l2*lo +
3*E1*I1*P*lo^2)/(3*(E1*I1*P - E2*I2*P)))^3)^(1/2) - (- E1*I1*P*l1^3 +
E1*I1*P*l1^2*l2 + 3*E1*I1*P*l1^2*lo + 5*E1*I1*P*l1*l2^2 - 2*E1*I1*P*l1*l2*lo
- 3*E1*I1*P*l1*lo^2 + 3*E1*I1*P*l2^3 - 5*E1*I1*P*l2^2*lo + E1*I1*P*l2*lo^2 +
E1*I1*P*lo^3 - 6*E1*E2*I1*I2*del)/(2*(E1*I1*P - E2*I2*P)) - (E1*I1*P*l2 -
3*E1*I1*P*l1 + 3*E2*I2*P*l1 + 3*E1*I1*P*lo)^3/(27*(E1*I1*P - E2*I2*P)^3) +
((E1*I1*P*l2 - 3*E1*I1*P*l1 + 3*E2*I2*P*l1 + 3*E1*I1*P*lo)*(3*E1*I1*P*l1^2 -
2*E1*I1*P*l1*l2 - 6*E1*I1*P*l1*lo - 5*E1*I1*P*l2^2 + 2*E1*I1*P*l2*lo +
3*E1*I1*P*lo^2))/(6*(E1*I1*P - E2*I2*P)^2))^(1/3) - (E1*I1*P*l2 -
3*E1*I1*P*l1 + 3*E2*I2*P*l1 + 3*E1*I1*P*lo)/(3*(E1*I1*P - E2*I2*P)) +
((((E1*I1*P*l2 - 3*E1*I1*P*l1 + 3*E2*I2*P*l1 + 3*E1*I1*P*lo)^3/(27*(E1*I1*P -
E2*I2*P)^3) + (- E1*I1*P*l1^3 + E1*I1*P*l1^2*l2 + 3*E1*I1*P*l1^2*lo +
5*E1*I1*P*l1*l2^2 - 2*E1*I1*P*l1*l2*lo - 3*E1*I1*P*l1*lo^2 + 3*E1*I1*P*l2^3 -
5*E1*I1*P*l2^2*lo + E1*I1*P*l2*lo^2 + E1*I1*P*lo^3 -
6*E1*E2*I1*I2*del)/(2*(E1*I1*P - E2*I2*P)) - ((E1*I1*P*l2 - 3*E1*I1*P*l1 +
3*E2*I2*P*l1 + 3*E1*I1*P*lo)*(3*E1*I1*P*l1^2 - 2*E1*I1*P*l1*l2 -
6*E1*I1*P*l1*lo - 5*E1*I1*P*l2^2 + 2*E1*I1*P*l2*lo +
3*E1*I1*P*lo^2))/(6*(E1*I1*P - E2*I2*P)^2))^2 - ((E1*I1*P*l2 - 3*E1*I1*P*l1 +
```

```
3*E2*I2*P*l1 + 3*E1*I1*P*lo)^2/(9*(E1*I1*P - E2*I2*P)^2) - (3*E1*I1*P*l1^2 -
2*E1*I1*P*l1*l2 - 6*E1*I1*P*l1*lo - 5*E1*I1*P*l2^2 + 2*E1*I1*P*l2*lo +
3*E1*I1*P*lo^2)/(3*(E1*I1*P - E2*I2*P)))^3)^(1/2) - (- E1*I1*P*l1^3 +
E1*I1*P*l1^2*l2 + 3*E1*I1*P*l1^2*lo + 5*E1*I1*P*l1*l2^2 - 2*E1*I1*P*l1*l2*lo
- 3*E1*I1*P*l1*lo^2 + 3*E1*I1*P*l2^3 - 5*E1*I1*P*l2^2*lo + E1*I1*P*l2*lo^2 +
E1*I1*P*lo^3 - 6*E1*E2*I1*I2*del)/(2*(E1*I1*P - E2*I2*P)) - (E1*I1*P*l2 -
3*E1*I1*P*l1 + 3*E2*I2*P*l1 + 3*E1*I1*P*lo)^3/(27*(E1*I1*P - E2*I2*P)^3) +
((E1*I1*P*l2 - 3*E1*I1*P*l1 + 3*E2*I2*P*l1 + 3*E1*I1*P*lo)*(3*E1*I1*P*l1^2 -
2*E1*I1*P*l1*l2 - 6*E1*I1*P*l1*lo - 5*E1*I1*P*l2^2 + 2*E1*I1*P*l2*lo +
3*E1*I1*P*lo^2))/(6*(E1*I1*P - E2*I2*P)^2))^(1/3)
%  So=[So;P,a1];
% end
% plot(So(:,1),So(:,2),'o');
%
%
% solve('6*del/P=a1^2*(3*l1-a1)/(E1*I1)+(l1+l2-lo-a1)^2*(3*l2-
l1+lo+a1)/(E2*I2)','P');
% solve('6*del/P=a1^2*(3*l1-a1)/(E1*I1)+(l1+l2-lo-a1)^2*(3*l2-
l1+lo+a1)/(E2*I2)','a1');
So=[];
for a1=0:.05:1.5; % force in Newton

P=(6*del)/(((a1 - l1 - l2 + lo)^2*(a1 - l1 + 3*l2 + lo))/(E2*I2) - (a1^2*(a1
- 3*l1))/(E1*I1))
 So=[So;P,a1];
end
plot(So(:,1),So(:,2),'o');
```

Appendix C

Tables and Graph for first simulation when PVC beam is misaligned by 1mm for forces 500N, 1000N, 2000N and 3000N when y = 0, 2.5, 4, 5.5, and 7.

Y= 2.5	(P1)x	(P2)x	Max Stress	(P1)x – (P2)x
0	0	0	0	1
100	-0.39476	-0.39815	12.084	0.20709
500	-1.9739	-1.9907	60.409	-2.9646
1000	-3.9478	-3.9814	120.82	-6.9292
2000	-7.8954	-7.9627	241.64	-14.8581
3000	-11.843	-11.944	362.45	-22.787

When Y = 2.5

D= 0→ F= 1.7e+002 N

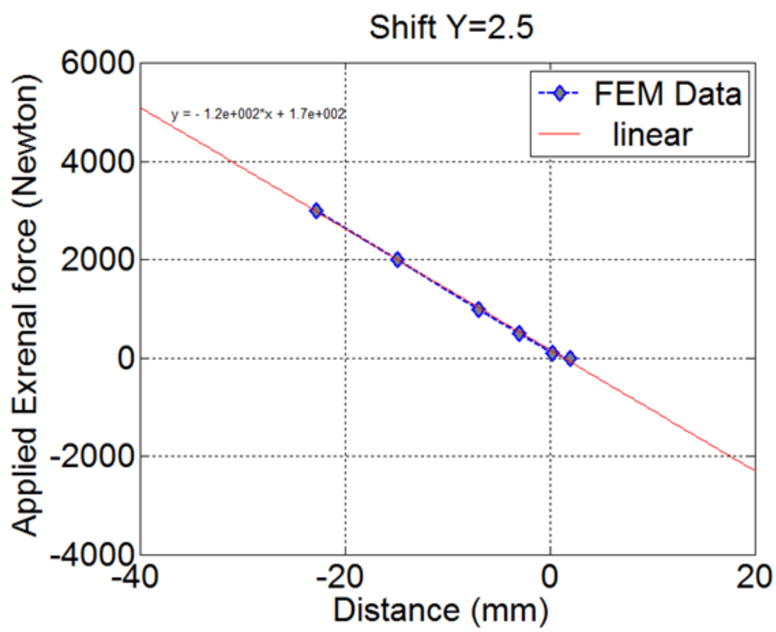

Relationship between force and displacement of beams for y = 2.5

Y= 4	(P1)x	(P2)x	Max Stress	(P1)x – (P2)x
0	0	0	0	1
100	-0.27578	-0.27924	8.6143	0.44498
500	-1.3788	-1.3962	43.071	-1.775
1000	-2.7578	-2.7924	86.143	-4.5502
2000	-5.5157	-5.5849	172.29	-10.1006
3000	-8.2736	-8.3773	258.43	-15.6509

When Y = 4

D= 0→ F= 2.4e+002 N

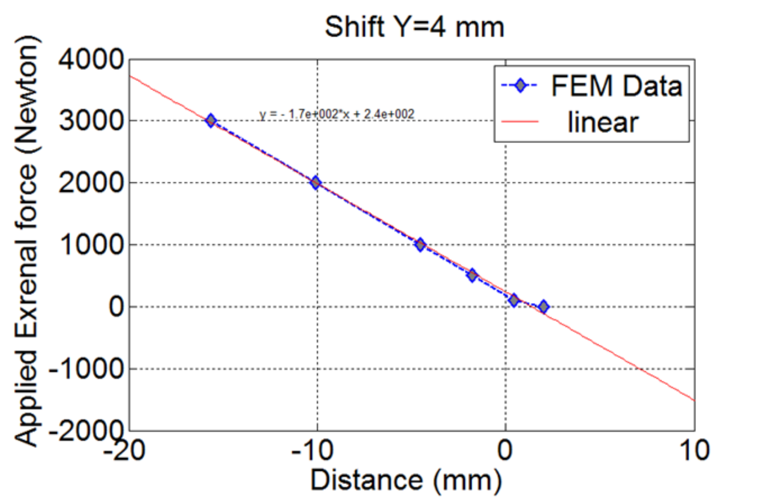

Fig. 27: Relationship between loads applied to beams and displacement for y= 4

Relationship between force and displacement of beams for y = 4 mm

Y= 5.5	(P1)x	(P2)x	Max Stress	1- (P1)x – (P2)x
0	0	0	0	1
100	-0.021171	-0.21521	6.7498	0.763619
500	-1.0585	-1.076	33.749	-1.1345
1000	-2.1171	-2.152	67.498	-3.2691
2000	-4.2341	-4.3041	135	-7.5382
3000	-6.3512	-6.4566	202.49	-11.8078

When Y = 5.5

D= 0→ F= 3.2e+002 N

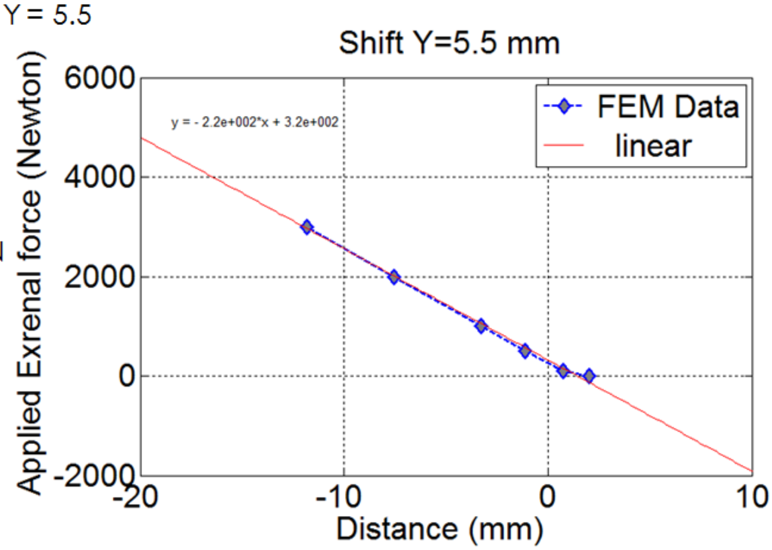

Relationship between force and displacement of beams for y = 5.5

Y= 7	(P1)x	(P2)x	Max Stress	1-(P1)x – (P2)x
0	0	0	0	1
100	-0.092771	-0.09632	3.3053	0.810909
500	-0.46387	-0.48156	16.526	0.05457
1000	-0.92775	-0.9631	33.053	-0.89085
2000	-1.8555	-1.9262	66.105	-2.7817
3000	-2.7831	-2.8893	99.158	-4.6724

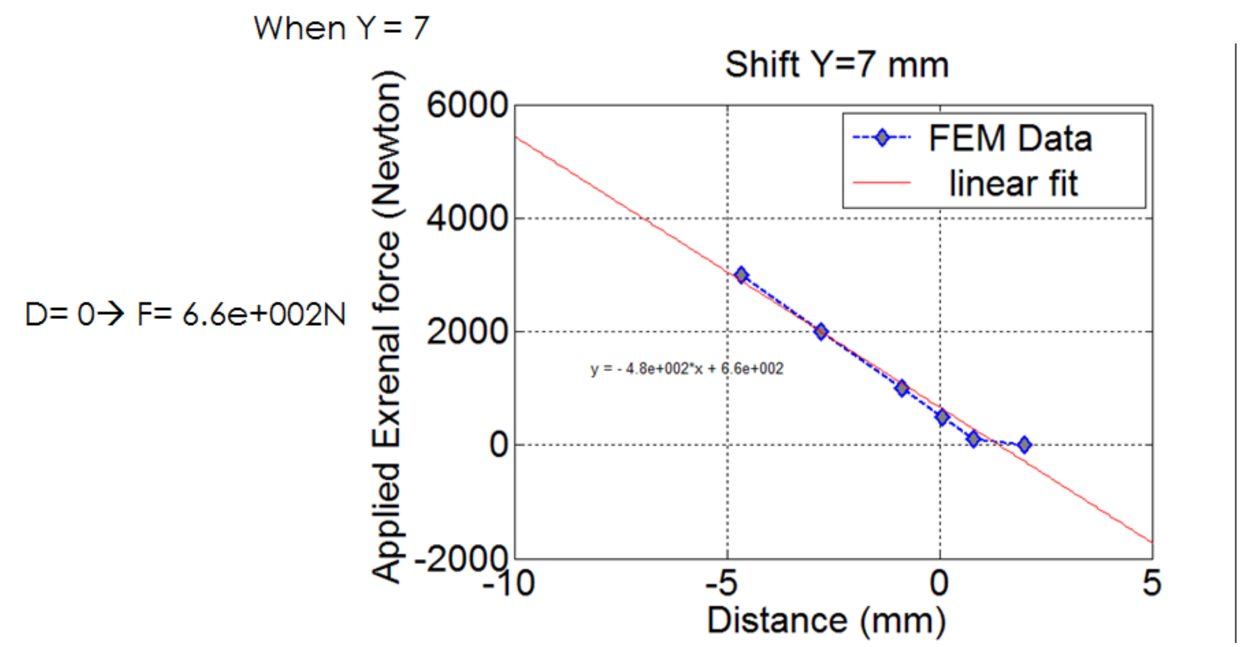

Relationship between force and displacement of beams for y = 7 mm

Appendix D

Output Result for first simulation when PVC beam is misaligned by 1mm for forces 100N, 500N, 1000N, 2000N and 3000N

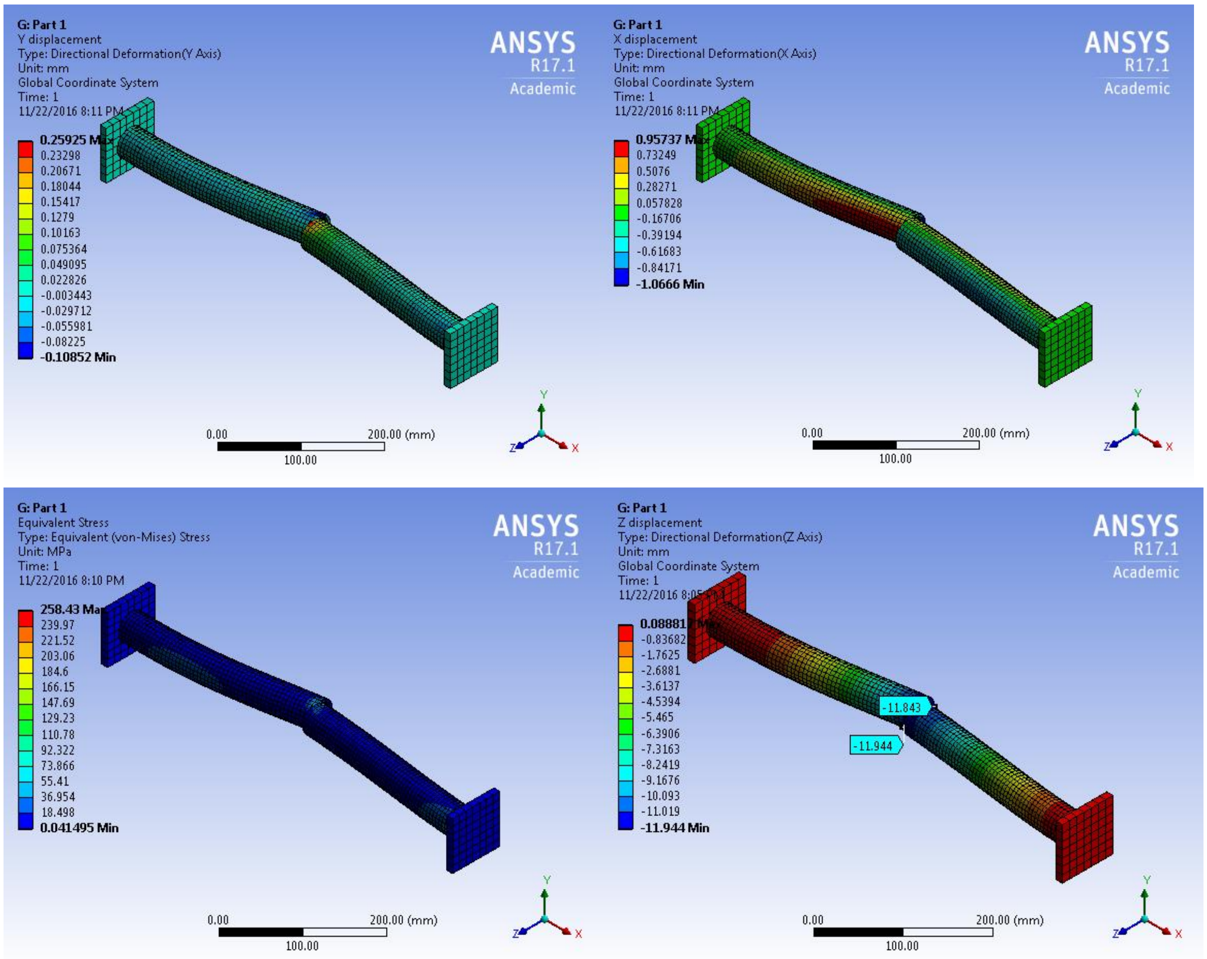

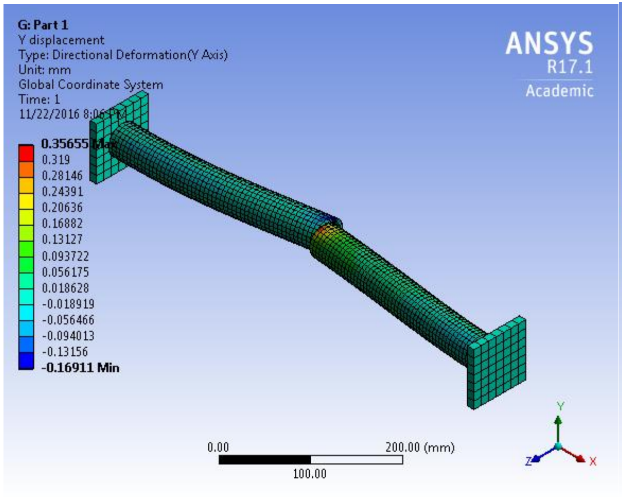
G: Part 1
Y displacement
Type: Directional Deformation(Y Axis)
Unit: mm
Global Coordinate System
Time: 1
0.35655 Max
0.319
0.28146
0.24391
0.20636
0.16882
0.13127
0.093722
0.056175
0.018628
-0.018919
-0.056466
-0.094013
-0.13156
-0.16911 Min
ANSYS
R17.1
Academic
0.00
200.00 (mm)
100.00

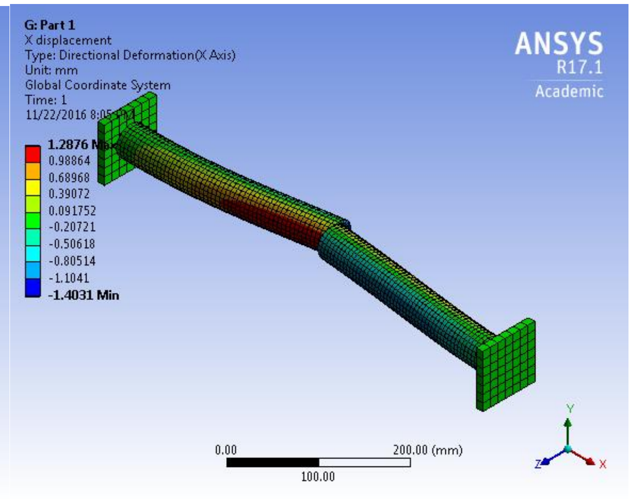
G: Part 1
X displacement
Type: Directional Deformation(X Axis)
Unit: mm
Global Coordinate System
Time: 1
1.2876 Max
0.98864
0.68968
0.39072
0.091752
-0.20721
-0.50618
-0.80514
-1.1041
-1.4031 Min
ANSYS
R17.1
Academic
0.00
200.00 (mm)
100.00

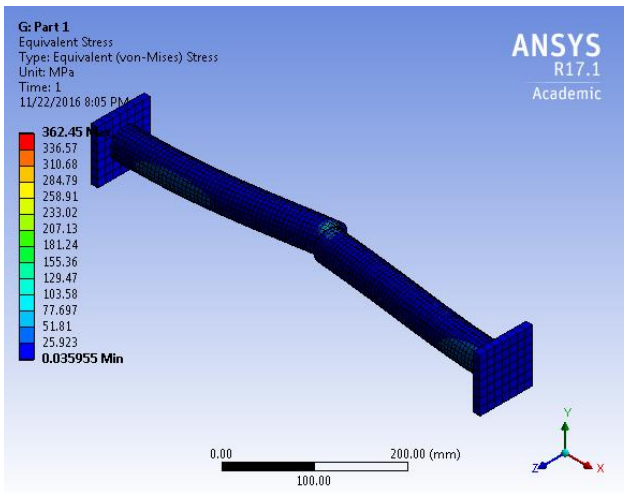
G: Part 1
Equivalent Stress
Type: Equivalent (von-Mises) Stress
Unit: MPa
Time: 1
11/22/2016 8:05 PM
362.45 Max
336.57
310.68
284.79
258.91
233.02
207.13
181.24
155.36
129.47
103.58
77.697
51.81
25.923
0.035955 Min
ANSYS
R17.1
Academic
0.00
200.00 (mm)
100.00

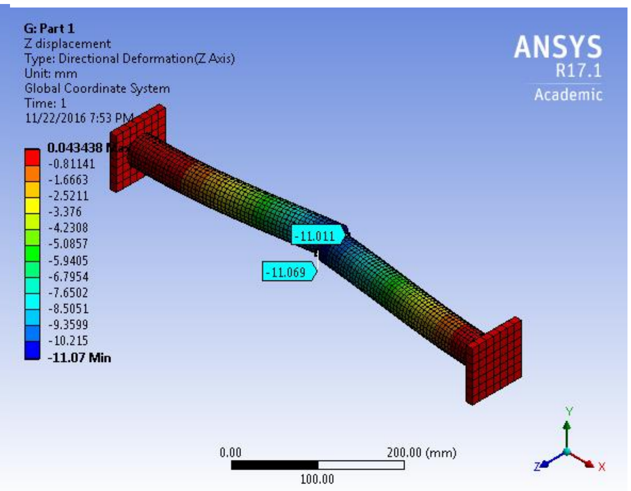
G: Part 1
Z displacement
Type: Directional Deformation(Z Axis)
Unit: mm
Global Coordinate System
Time: 1
11/22/2016 7:53 PM
0.043438 Max
-0.81141
-1.6663
-2.5211
-3.376
-4.2308
-5.0857
-5.9405
-6.7954
-7.6502
-8.5051
-9.3599
-10.215
-11.07 Min
-11.011
-11.069
ANSYS
R17.1
Academic
0.00
200.00 (mm)
100.00

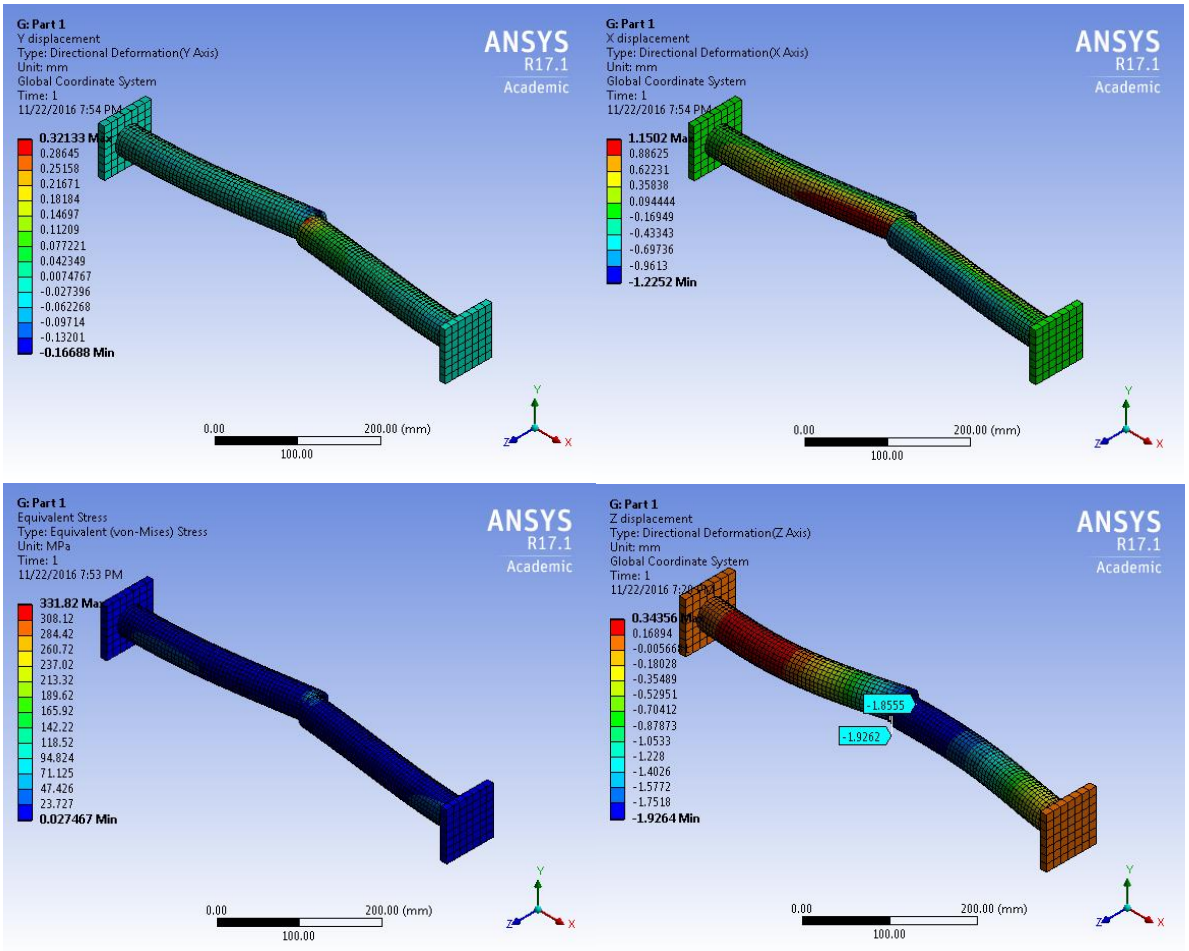
G: Part 1
Y displacement
Type: Directional Deformation(Y Axis)
Unit: mm
Global Coordinate System
Time: 1
11/22/2016 7:54 PM
0.32133 M
0.28645
0.25158
0.21671
0.18184
0.14697
0.11209
0.077221
0.042349
0.0074767
-0.027396
-0.062268
-0.09714
-0.13201
-0.16688 Min
ANSYS
R17.1
Academic
0.00
100.00
200.00 (mm)
G: Part 1
X displacement
Type: Directional Deformation(X Axis)
Unit: mm
Global Coordinate System
Time: 1
11/22/2016 7:54 PM
1.1502 Ma
0.88625
0.62231
0.35838
0.094444
-0.16949
-0.43343
-0.69736
-0.9613
-1.2252 Min
ANSYS
R17.1
Academic
0.00
100.00
200.00 (mm)
G: Part 1
Equivalent Stress
Type: Equivalent (von-Mises) Stress
Unit: MPa
Time: 1
11/22/2016 7:53 PM
331.82 Ma
308.12
284.42
260.72
237.02
213.32
189.62
165.92
142.22
118.52
94.824
71.125
47.426
23.727
0.027467 Min
ANSYS
R17.1
Academic
0.00
100.00
200.00 (mm)
G: Part 1
Z displacement
Type: Directional Deformation(Z Axis)
Unit: mm
Global Coordinate System
Time: 1
0.34356
0.16894
-0.18028
-0.35489
-0.52951
-0.70412
-0.87873
-1.0533
-1.228
-1.4026
-1.5772
-1.7518
-1.9264 Min
-1.8555
-1.9262
ANSYS
R17.1
Academic
0.00
100.00
200.00 (mm)

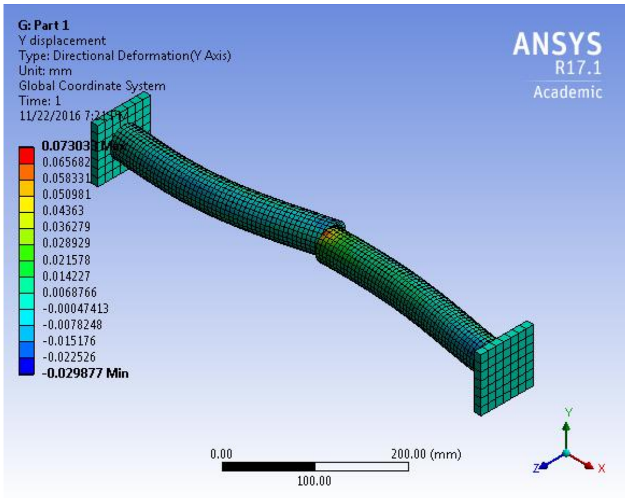
G: Part 1
Y displacement
Type: Directional Deformation(Y Axis)
Unit: mm
Global Coordinate System
Time: 1
0.065682
0.058331
0.050981
0.04363
0.036279
0.028929
0.021578
0.014227
0.0068766
-0.00047413
-0.0078248
-0.015176
-0.022526
-0.029877 Min
ANSYS
R17.1
Academic
0.00
200.00 (mm)
100.00
Y
Z
X

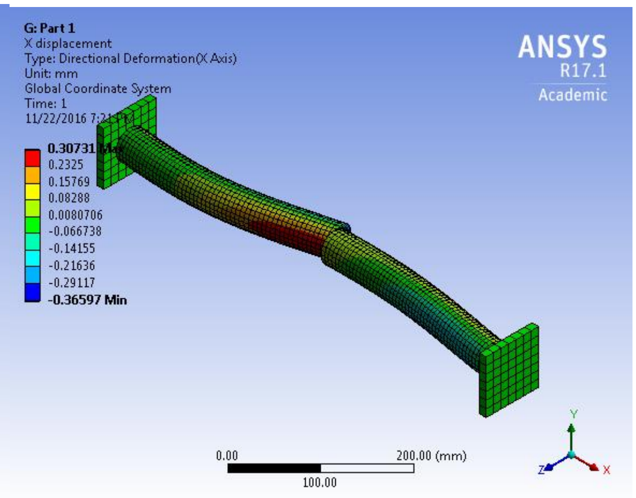
G: Part 1
X displacement
Type: Directional Deformation(X Axis)
Unit: mm
Global Coordinate System
Time: 1
0.2325
0.15769
0.08288
0.0080706
-0.066738
-0.14155
-0.21636
-0.29117
-0.36597 Min
ANSYS
R17.1
Academic
0.00
200.00 (mm)
100.00
Y
Z
X

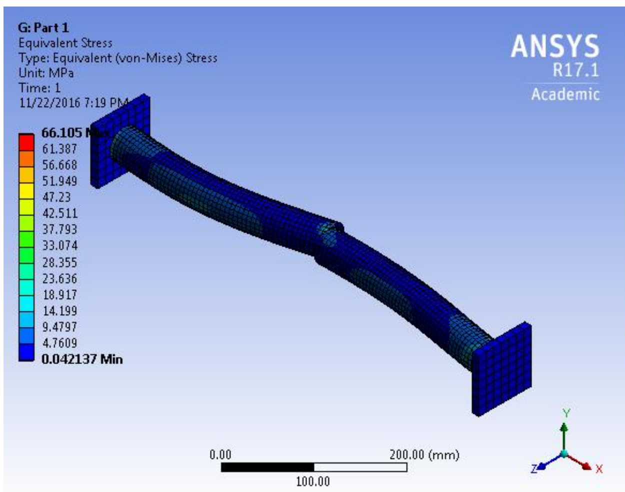
G: Part 1
Equivalent Stress
Type: Equivalent (von-Mises) Stress
Unit: MPa
Time: 1
11/22/2016 7:19 PM
66.105
61.387
56.668
51.949
47.23
42.511
37.793
33.074
28.355
23.636
18.917
14.199
9.4797
4.7609
0.042137 Min
ANSYS
R17.1
Academic
0.00
200.00 (mm)
100.00
Y
Z
X

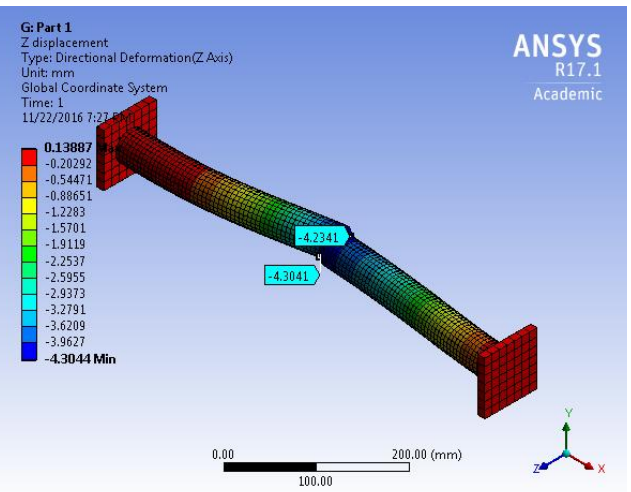
G: Part 1
Z displacement
Type: Directional Deformation(Z Axis)
Unit: mm
Global Coordinate System
Time: 1
0.13887
-0.20292
-0.54471
-0.88651
-1.2283
-1.5701
-1.9119
-2.2537
-2.5955
-2.9373
-3.2791
-3.6209
-3.9627
-4.3044 Min
-4.2341
-4.3041
ANSYS
R17.1
Academic
0.00
200.00 (mm)
100.00
Y
Z
X

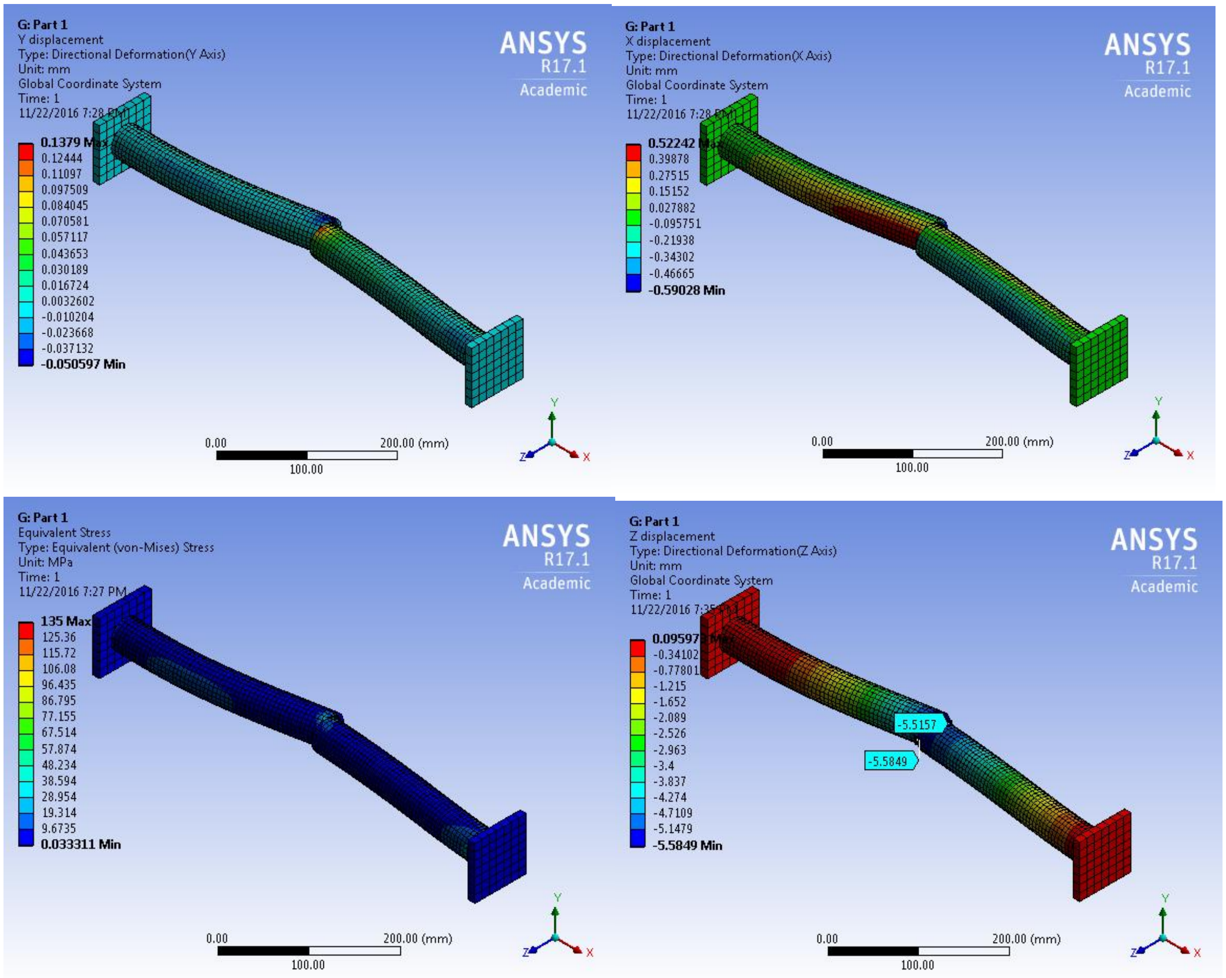
G: Part 1
Y displacement
Type: Directional Deformation(Y Axis)
Unit: mm
Global Coordinate System
Time: 1
0.1379 Max
0.12444
0.11097
0.097509
0.084045
0.070581
0.057117
0.043653
0.030189
0.016724
0.0032602
-0.010204
-0.023668
-0.037132
-0.050597 Min
ANSYS
R17.1
Academic
0.00
100.00
200.00 (mm)
G: Part 1
X displacement
Type: Directional Deformation(X Axis)
Unit: mm
Global Coordinate System
Time: 1
0.39878
0.27515
0.15152
0.027882
-0.095751
-0.21938
-0.34302
-0.46665
-0.59028 Min
ANSYS
R17.1
Academic
G: Part 1
Equivalent Stress
Type: Equivalent (von-Mises) Stress
Unit: MPa
Time: 1
11/22/2016 7:27 PM
135 Max
125.36
115.72
106.08
96.435
86.795
77.155
67.514
57.874
48.234
38.594
28.954
19.314
9.6735
0.033311 Min
ANSYS
R17.1
Academic
G: Part 1
Z displacement
Type: Directional Deformation(Z Axis)
Unit: mm
Global Coordinate System
Time: 1
-1.215
-1.652
-2.089
-2.526
-2.963
-3.4
-3.837
-4.274
-4.7109
-5.1479
-5.5849 Min
-5.5157
-5.5849
ANSYS
R17.1
Academic

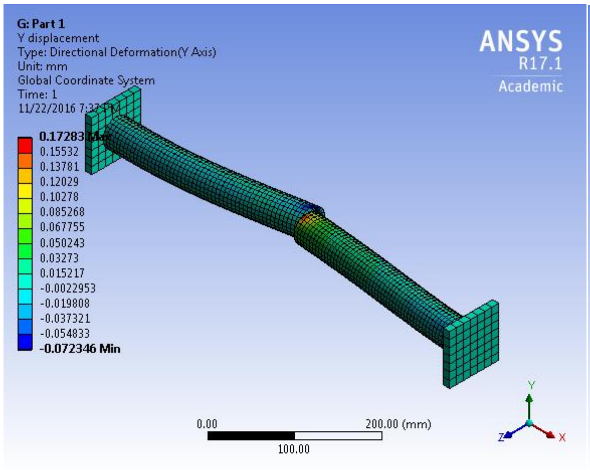
G: Part 1
Y displacement
Type: Directional Deformation(Y Axis)
Unit: mm
Global Coordinate System
Time: 1
ANSYS
R17.1
Academic
0.17283
0.15532
0.13781
0.12029
0.10278
0.085268
0.067755
0.050243
0.03273
0.015217
-0.0022953
-0.019808
-0.037321
-0.054833
-0.072346 Min
0.00
200.00 (mm)
100.00

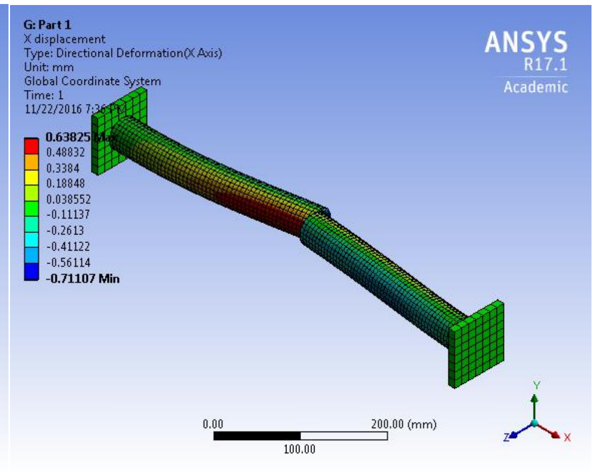
G: Part 1
X displacement
Type: Directional Deformation(X Axis)
Unit: mm
Global Coordinate System
Time: 1
ANSYS
R17.1
Academic
0.63825
0.48832
0.3384
0.18848
0.038552
-0.11137
-0.2613
-0.41122
-0.56114
-0.71107 Min
0.00
200.00 (mm)
100.00

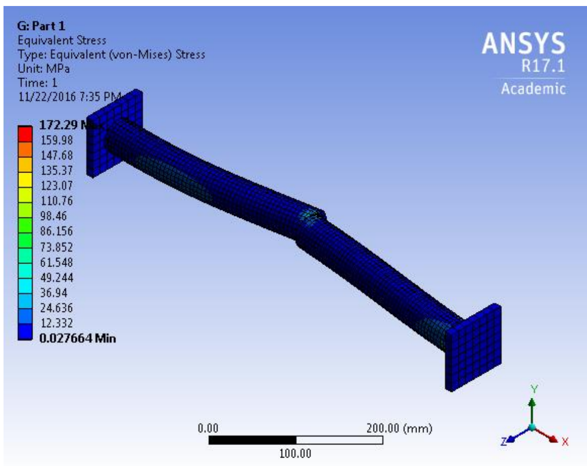
G: Part 1
Equivalent Stress
Type: Equivalent (von-Mises) Stress
Unit: MPa
Time: 1
ANSYS
R17.1
Academic
172.29
159.98
147.68
135.37
123.07
110.76
98.46
86.156
73.852
61.548
49.244
36.94
24.636
12.332
0.027664 Min
0.00
200.00 (mm)
100.00

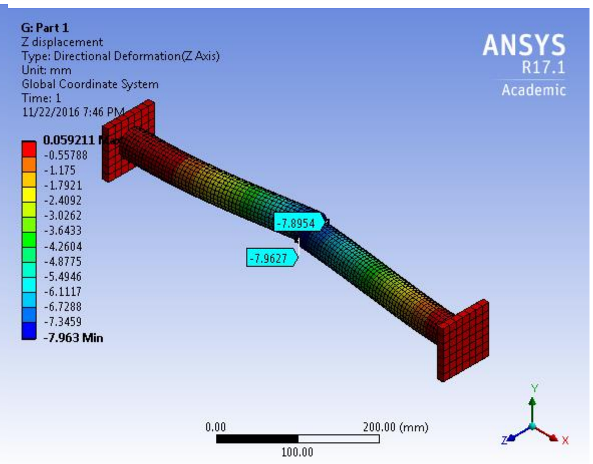
G: Part 1
Z displacement
Type: Directional Deformation(Z Axis)
Unit: mm
Global Coordinate System
Time: 1
11/22/2016 7:46 PM
ANSYS
R17.1
Academic
0.059211
-0.55788
-1.175
-1.7921
-2.4092
-3.0262
-3.6433
-4.2604
-4.8775
-5.4946
-6.1117
-6.7288
-7.3459
-7.963 Min
-7.8954
-7.9627
0.00
200.00 (mm)
100.00

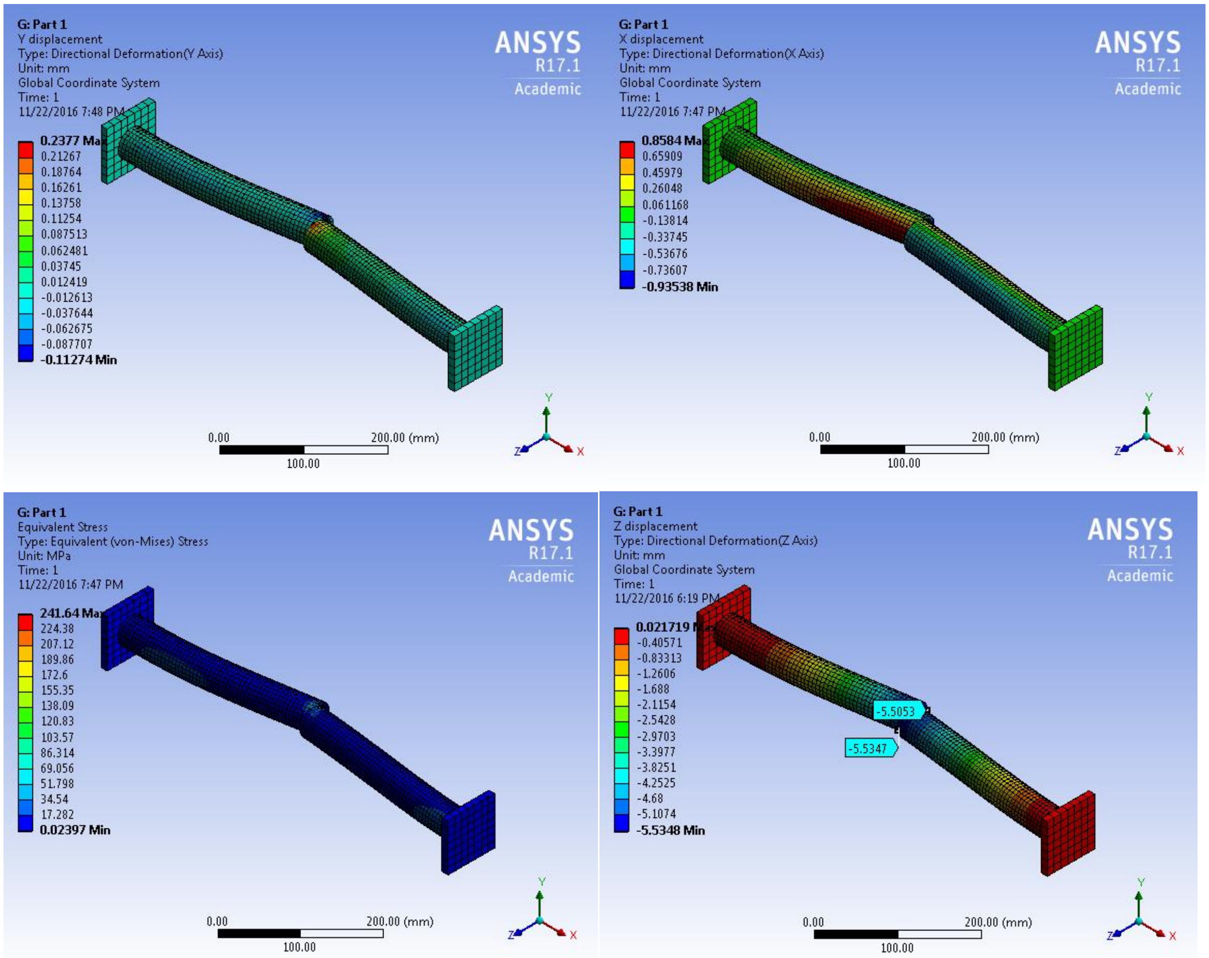
G: Part 1
Y displacement
Type: Directional Deformation(Y Axis)
Unit: mm
Global Coordinate System
Time: 1
11/22/2016 7:48 PM
ANSYS
R17.1
Academic
0.2377 Max
0.21267
0.18764
0.16261
0.13758
0.11254
0.087513
0.062481
0.03745
0.012419
-0.012613
-0.037644
-0.062675
-0.087707
-0.11274 Min
G: Part 1
X displacement
Type: Directional Deformation(X Axis)
Unit: mm
Global Coordinate System
Time: 1
11/22/2016 7:47 PM
0.8584 Max
0.65909
0.45979
0.26048
0.061168
-0.13814
-0.33745
-0.53676
-0.73607
-0.93538 Min
G: Part 1
Equivalent Stress
Type: Equivalent (von-Mises) Stress
Unit: MPa
Time: 1
11/22/2016 7:47 PM
241.64 Max
224.38
207.12
189.86
172.6
155.35
138.09
120.83
103.57
86.314
69.056
51.798
34.54
17.282
0.02397 Min
G: Part 1
Z displacement
Type: Directional Deformation(Z Axis)
Unit: mm
Global Coordinate System
Time: 1
11/22/2016 6:19 PM
0.021719 Max
-0.40571
-0.83313
-1.2606
-1.688
-2.1154
-2.5428
-2.9703
-3.3977
-3.8251
-4.2525
-4.68
-5.1074
-5.5348 Min
-5.5053
-5.5347
0.00
100.00
200.00 (mm)
Y
X
Z

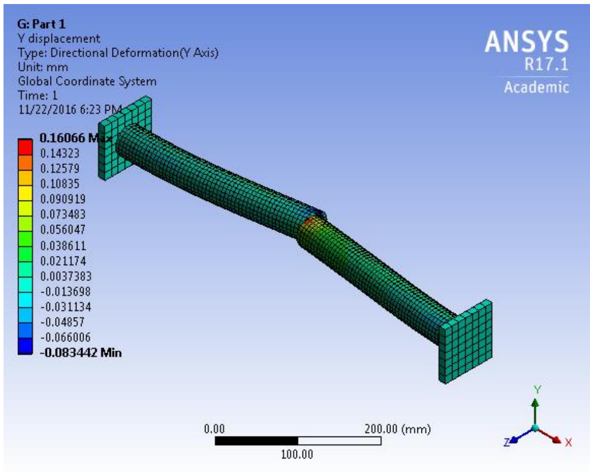
G: Part 1
Y displacement
Type: Directional Deformation(Y Axis)
Unit: mm
Global Coordinate System
Time: 1
11/22/2016 6:23 PM
0.16066 Max
0.14323
0.12579
0.10835
0.090919
0.073483
0.056047
0.038611
0.021174
0.0037383
-0.013698
-0.031134
-0.04857
-0.066006
-0.083442 Min
ANSYS
R17.1
Academic
0.00
200.00 (mm)
100.00
Y
Z
X

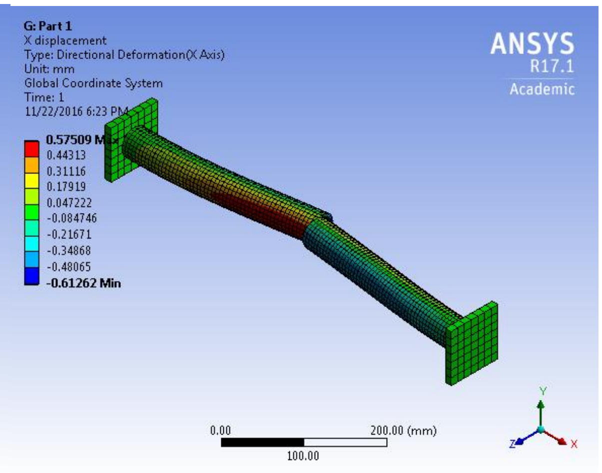
G: Part 1
X displacement
Type: Directional Deformation(X Axis)
Unit: mm
Global Coordinate System
Time: 1
11/22/2016 6:23 PM
0.57509 Max
0.44313
0.31116
0.17919
0.047222
-0.084746
-0.21671
-0.34868
-0.48065
-0.61262 Min
ANSYS
R17.1
Academic
0.00
200.00 (mm)
100.00
Y
Z
X

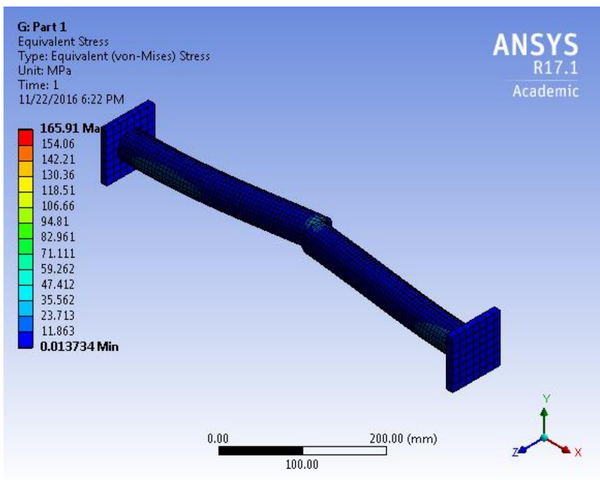
G: Part 1
Equivalent Stress
Type: Equivalent (von-Mises) Stress
Unit: MPa
Time: 1
11/22/2016 6:22 PM
165.91 Max
154.06
142.21
130.36
118.51
106.66
94.81
82.961
71.111
59.262
47.412
35.562
23.713
11.863
0.013734 Min
ANSYS
R17.1
Academic
0.00
200.00 (mm)
100.00
Y
Z
X

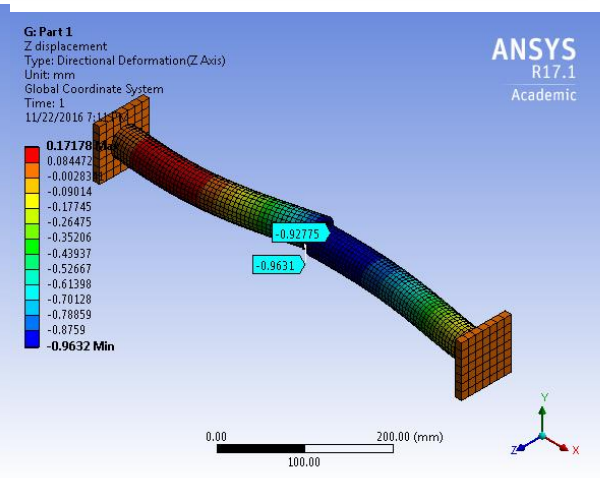
G: Part 1
Z displacement
Type: Directional Deformation(Z Axis)
Unit: mm
Global Coordinate System
Time: 1
0.17178 Max
0.084472
-0.09014
-0.17745
-0.26475
-0.35206
-0.43937
-0.52667
-0.61398
-0.70128
-0.78859
-0.8759
-0.9632 Min
-0.92775
-0.9631
ANSYS
R17.1
Academic
0.00
200.00 (mm)
100.00
Y
Z
X

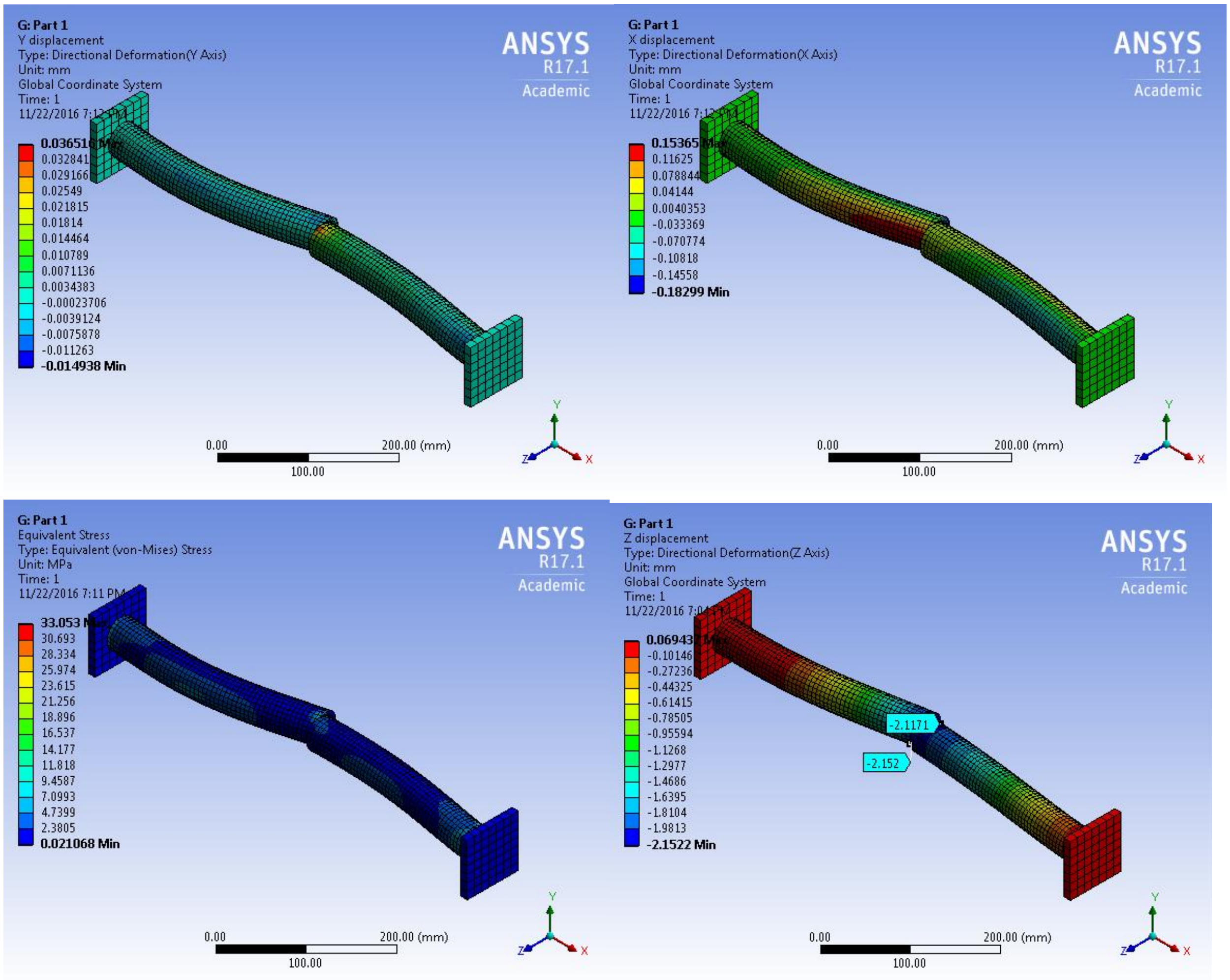
G: Part 1
Y displacement
Type: Directional Deformation(Y Axis)
Unit: mm
Global Coordinate System
Time: 1
0.032841
0.029166
0.02549
0.021815
0.01814
0.014464
0.010789
0.0071136
0.0034383
-0.00023706
-0.0039124
-0.0075878
-0.011263
-0.014938 Min
ANSYS
R17.1
Academic
0.00
200.00 (mm)
100.00
G: Part 1
X displacement
Type: Directional Deformation(X Axis)
Unit: mm
Global Coordinate System
Time: 1
0.11625
0.078844
0.04144
0.0040353
-0.033369
-0.070774
-0.10818
-0.14558
-0.18299 Min
G: Part 1
Equivalent Stress
Type: Equivalent (von-Mises) Stress
Unit: MPa
Time: 1
30.693
28.334
25.974
23.615
21.256
18.896
16.537
14.177
11.818
9.4587
7.0993
4.7399
2.3805
0.021068 Min
G: Part 1
Z displacement
Type: Directional Deformation(Z Axis)
Unit: mm
Global Coordinate System
Time: 1
-0.10146
-0.27236
-0.44325
-0.61415
-0.78505
-0.95594
-1.1268
-1.2977
-1.4686
-1.6395
-1.8104
-1.9813
-2.1522 Min
-2.1171
-2.152

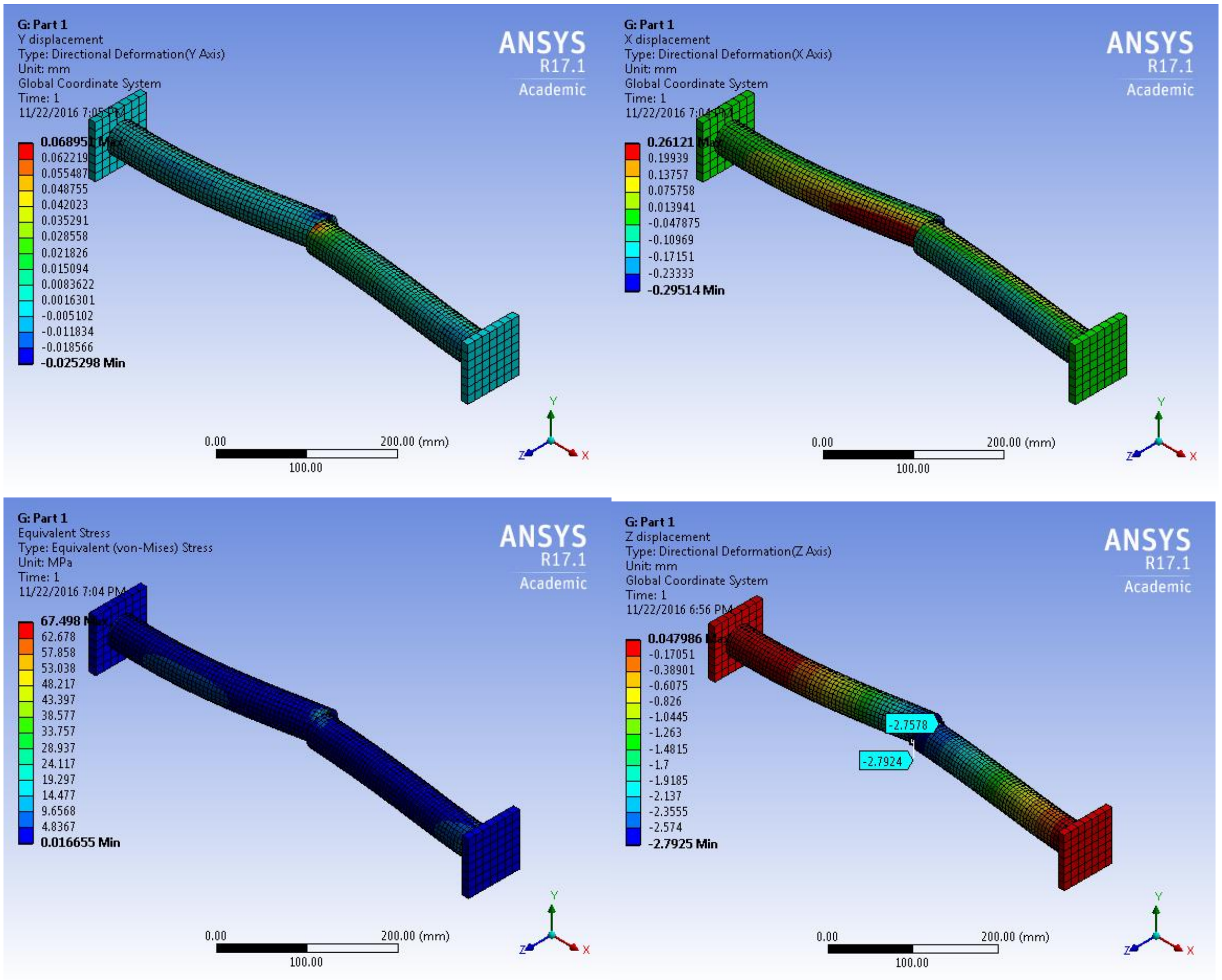
G: Part 1
Y displacement
Type: Directional Deformation(Y Axis)
Unit: mm
Global Coordinate System
Time: 1
0.068951 Max
0.062219
0.055487
0.048755
0.042023
0.035291
0.028558
0.021826
0.015094
0.0083622
0.0016301
-0.005102
-0.011834
-0.018566
-0.025298 Min
ANSYS
R17.1
Academic
0.00
200.00 (mm)
100.00
G: Part 1
X displacement
Type: Directional Deformation(X Axis)
Unit: mm
Global Coordinate System
Time: 1
0.26121 Max
0.19939
0.13757
0.075758
0.013941
-0.047875
-0.10969
-0.17151
-0.23333
-0.29514 Min
ANSYS
R17.1
Academic
0.00
200.00 (mm)
100.00
G: Part 1
Equivalent Stress
Type: Equivalent (von-Mises) Stress
Unit: MPa
Time: 1
11/22/2016 7:04 PM
67.498 Max
62.678
57.858
53.038
48.217
43.397
38.577
33.757
28.937
24.117
19.297
14.477
9.6568
4.8367
0.016655 Min
ANSYS
R17.1
Academic
0.00
200.00 (mm)
100.00
G: Part 1
Z displacement
Type: Directional Deformation(Z Axis)
Unit: mm
Global Coordinate System
Time: 1
11/22/2016 6:56 PM
0.047986 Max
-0.17051
-0.38901
-0.6075
-0.826
-1.0445
-1.263
-1.4815
-1.7
-1.9185
-2.137
-2.3555
-2.574
-2.7925 Min
-2.7578
-2.7924
ANSYS
R17.1
Academic
0.00
200.00 (mm)
100.00

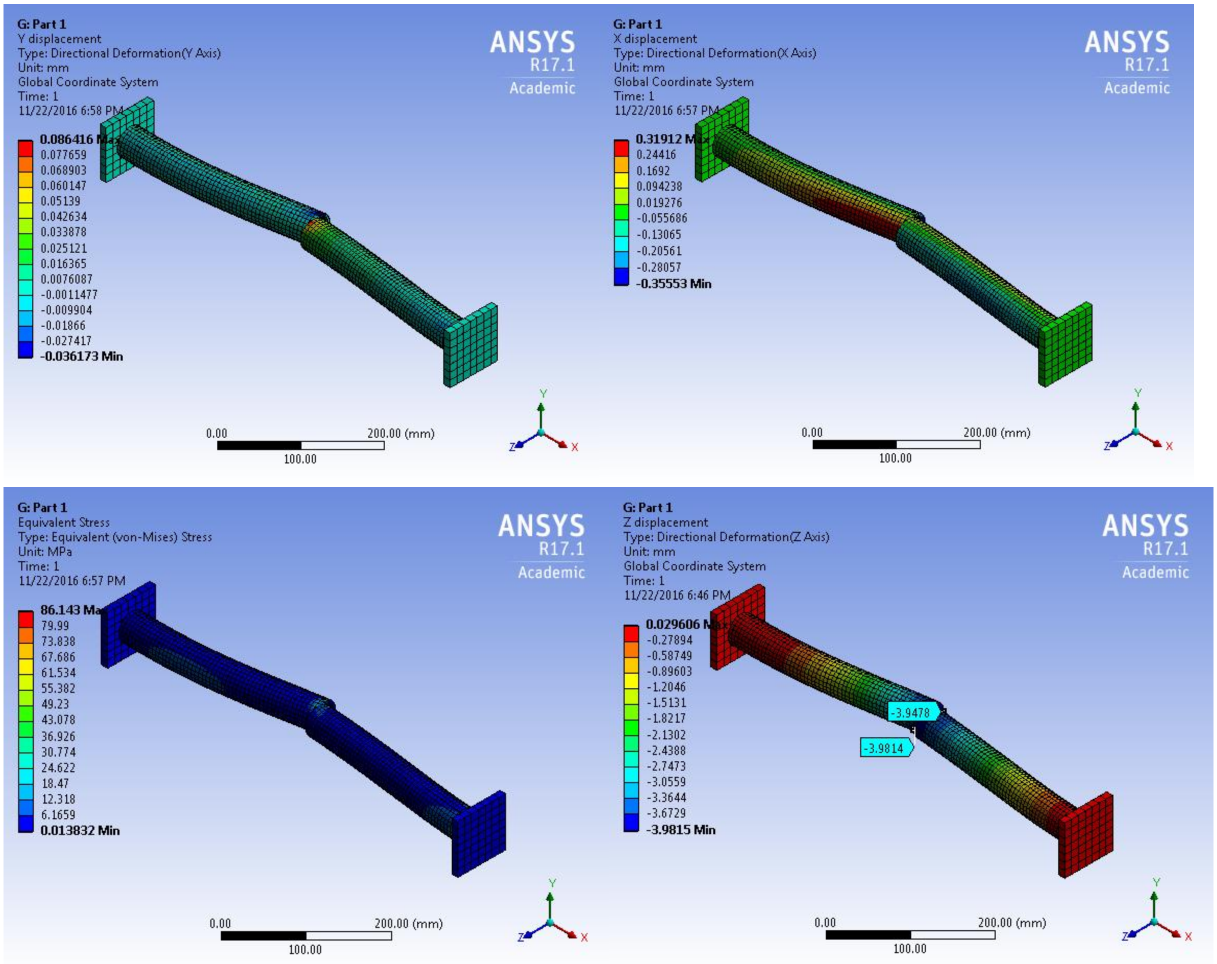
G: Part 1
Y displacement
Type: Directional Deformation(Y Axis)
Unit: mm
Global Coordinate System
Time: 1
11/22/2016 6:58 PM
0.086416 Max
0.077659
0.068903
0.060147
0.05139
0.042634
0.033878
0.025121
0.016365
0.0076087
-0.0011477
-0.009904
-0.01866
-0.027417
-0.036173 Min
ANSYS
R17.1
Academic
0.00
100.00
200.00 (mm)
G: Part 1
X displacement
Type: Directional Deformation(X Axis)
Unit: mm
Global Coordinate System
Time: 1
11/22/2016 6:57 PM
0.31912 Max
0.24416
0.1692
0.094238
0.019276
-0.055686
-0.13065
-0.20561
-0.28057
-0.35553 Min
ANSYS
R17.1
Academic
0.00
100.00
200.00 (mm)
G: Part 1
Equivalent Stress
Type: Equivalent (von-Mises) Stress
Unit: MPa
Time: 1
11/22/2016 6:57 PM
86.143 Max
79.99
73.838
67.686
61.534
55.382
49.23
43.078
36.926
30.774
24.622
18.47
12.318
6.1659
0.013832 Min
ANSYS
R17.1
Academic
0.00
100.00
200.00 (mm)
G: Part 1
Z displacement
Type: Directional Deformation(Z Axis)
Unit: mm
Global Coordinate System
Time: 1
11/22/2016 6:46 PM
0.029606 Max
-0.27894
-0.58749
-0.89603
-1.2046
-1.5131
-1.8217
-2.1302
-2.4388
-2.7473
-3.0559
-3.3644
-3.6729
-3.9815 Min
-3.9478
-3.9814
ANSYS
R17.1
Academic
0.00
100.00
200.00 (mm)

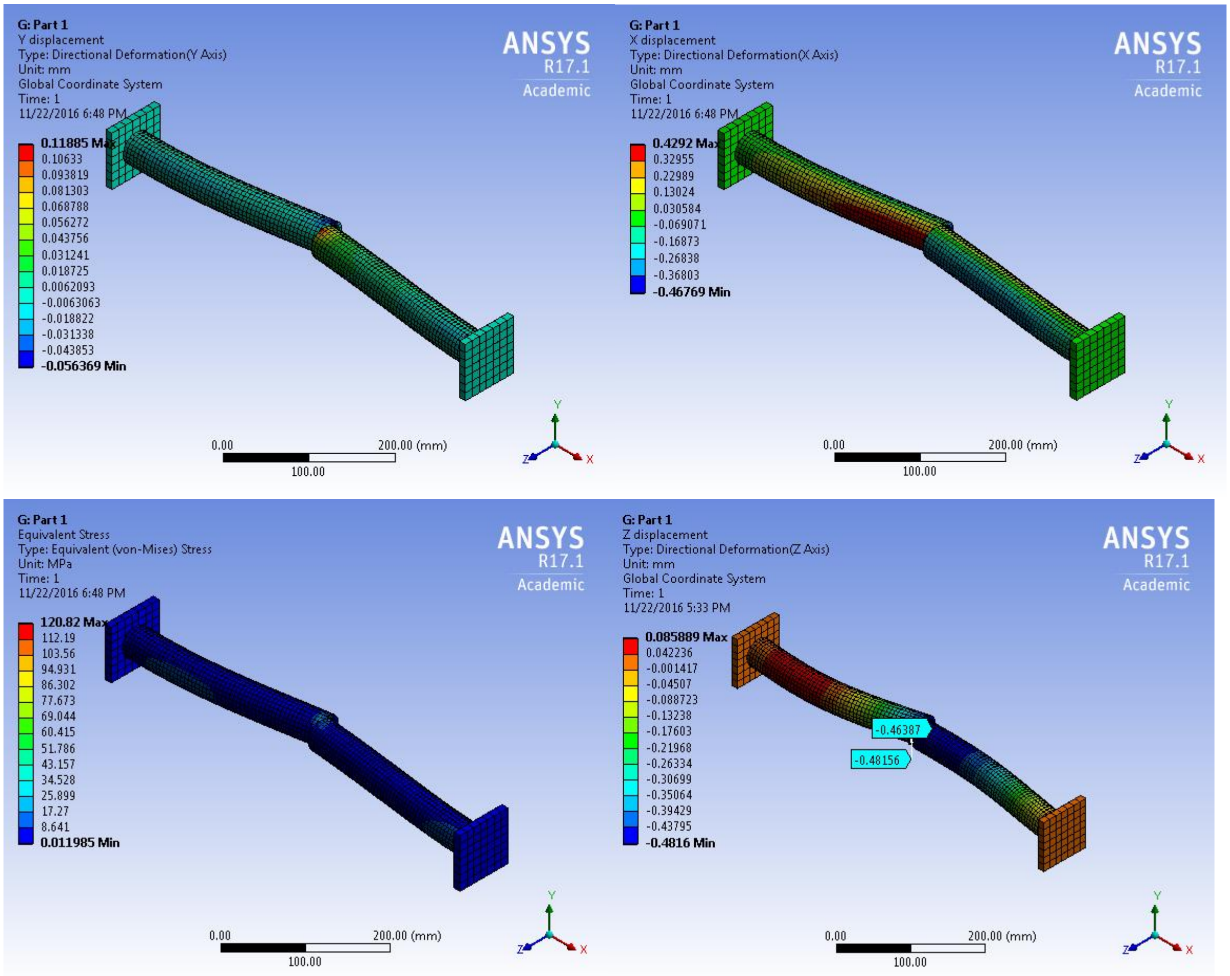
G: Part 1
Y displacement
Type: Directional Deformation(Y Axis)
Unit: mm
Global Coordinate System
Time: 1
11/22/2016 6:48 PM
0.11885 Max
0.10633
0.093819
0.081303
0.068788
0.056272
0.043756
0.031241
0.018725
0.0062093
-0.0063063
-0.018822
-0.031338
-0.043853
-0.056369 Min
ANSYS
R17.1
Academic
0.00
100.00
200.00 (mm)
G: Part 1
X displacement
Type: Directional Deformation(X Axis)
Unit: mm
Global Coordinate System
Time: 1
11/22/2016 6:48 PM
0.4292 Max
0.32955
0.22989
0.13024
0.030584
-0.069071
-0.16873
-0.26838
-0.36803
-0.46769 Min
ANSYS
R17.1
Academic
0.00
100.00
200.00 (mm)
G: Part 1
Equivalent Stress
Type: Equivalent (von-Mises) Stress
Unit: MPa
Time: 1
11/22/2016 6:48 PM
120.82 Max
112.19
103.56
94.931
86.302
77.673
69.044
60.415
51.786
43.157
34.528
25.899
17.27
8.641
0.011985 Min
ANSYS
R17.1
Academic
0.00
100.00
200.00 (mm)
G: Part 1
Z displacement
Type: Directional Deformation(Z Axis)
Unit: mm
Global Coordinate System
Time: 1
11/22/2016 5:33 PM
0.085889 Max
0.042236
-0.001417
-0.04507
-0.088723
-0.13238
-0.17603
-0.21968
-0.26334
-0.30699
-0.35064
-0.39429
-0.43795
-0.4816 Min
-0.46387
-0.48156
ANSYS
R17.1
Academic
0.00
100.00
200.00 (mm)

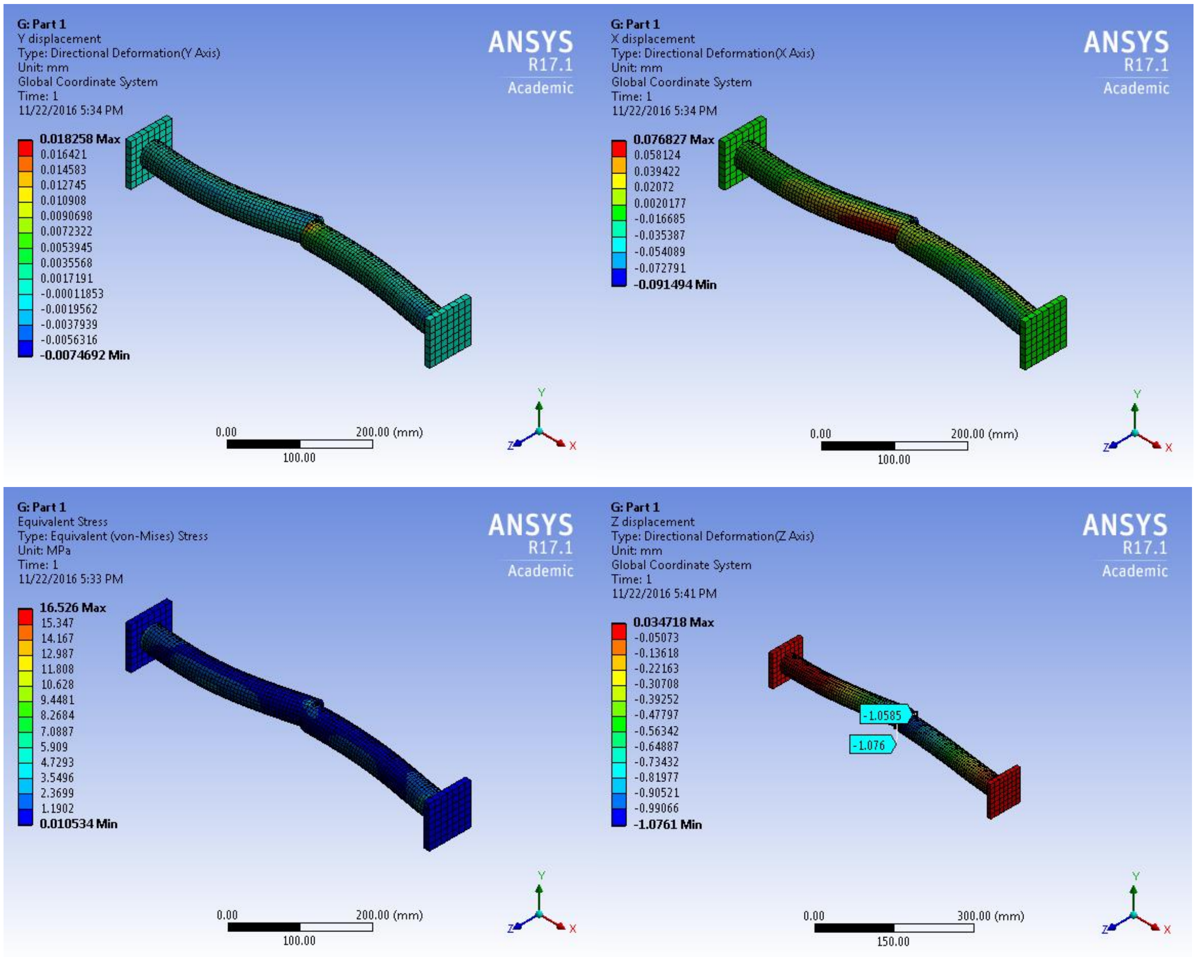
G: Part 1
Y displacement
Type: Directional Deformation(Y Axis)
Unit: mm
Global Coordinate System
Time: 1
11/22/2016 5:34 PM
0.018258 Max
0.016421
0.014583
0.012745
0.010908
0.0090698
0.0072322
0.0053945
0.0035568
0.0017191
-0.00011853
-0.0019562
-0.0037939
-0.0056316
-0.0074692 Min
ANSYS
R17.1
Academic
0.00
200.00 (mm)
100.00
G: Part 1
X displacement
Type: Directional Deformation(X Axis)
Unit: mm
Global Coordinate System
Time: 1
11/22/2016 5:34 PM
0.076827 Max
0.058124
0.039422
0.02072
0.0020177
-0.016685
-0.035387
-0.054089
-0.072791
-0.091494 Min
ANSYS
R17.1
Academic
0.00
200.00 (mm)
100.00
G: Part 1
Equivalent Stress
Type: Equivalent (von-Mises) Stress
Unit: MPa
Time: 1
11/22/2016 5:33 PM
16.526 Max
15.347
14.167
12.987
11.808
10.628
9.4481
8.2684
7.0887
5.909
4.7293
3.5496
2.3699
1.1902
0.010534 Min
ANSYS
R17.1
Academic
0.00
200.00 (mm)
100.00
G: Part 1
Z displacement
Type: Directional Deformation(Z Axis)
Unit: mm
Global Coordinate System
Time: 1
11/22/2016 5:41 PM
0.034718 Max
-0.05073
-0.13618
-0.22163
-0.30708
-0.39252
-0.47797
-0.56342
-0.64887
-0.73432
-0.81977
-0.90521
-0.99066
-1.0761 Min
-1.0585
-1.076
ANSYS
R17.1
Academic
0.00
300.00 (mm)
150.00

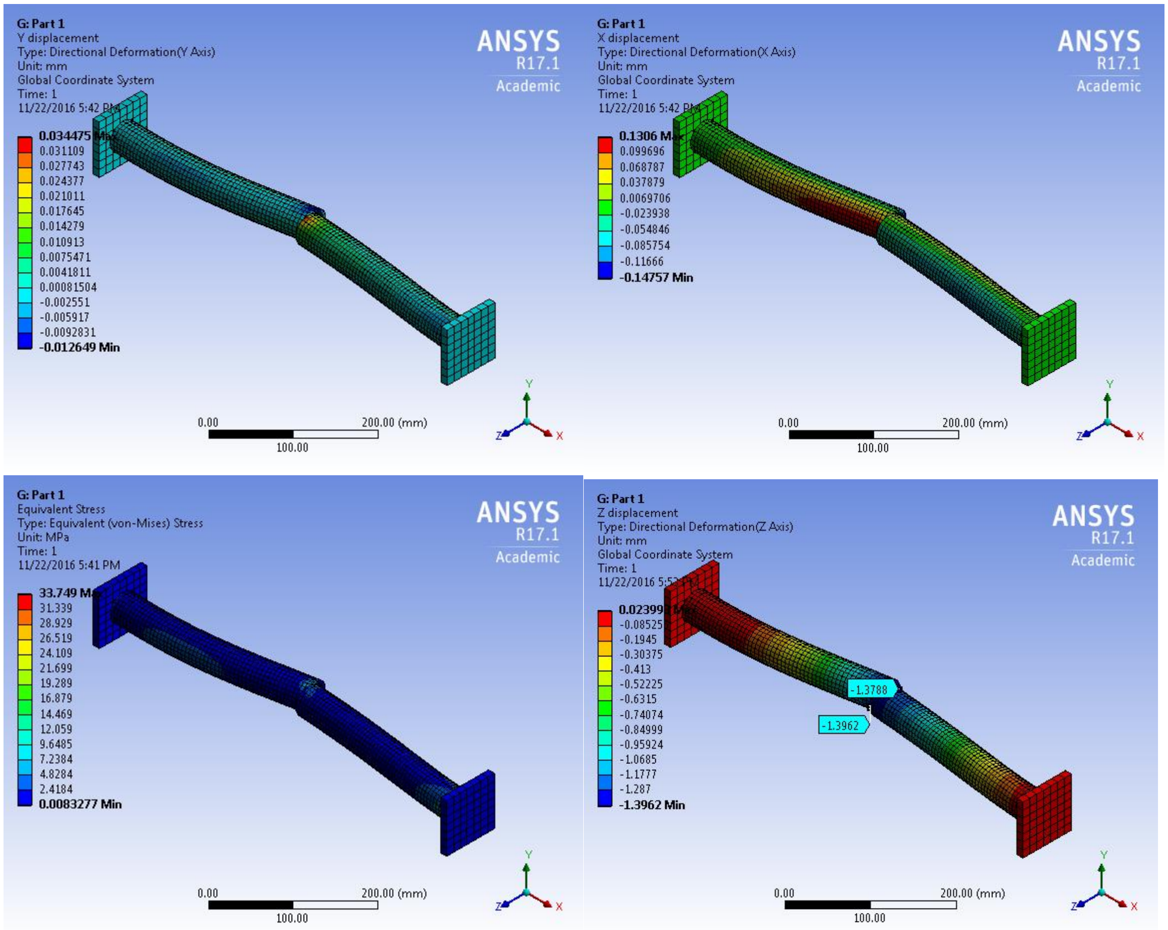
G: Part 1
Y displacement
Type: Directional Deformation(Y Axis)
Unit: mm
Global Coordinate System
Time: 1
0.034475 Max
0.031109
0.027743
0.024377
0.021011
0.017645
0.014279
0.010913
0.0075471
0.0041811
0.00081504
-0.002551
-0.005917
-0.0092831
-0.012649 Min
ANSYS
R17.1
Academic
0.00
200.00 (mm)
100.00
G: Part 1
X displacement
Type: Directional Deformation(X Axis)
Unit: mm
Global Coordinate System
Time: 1
0.1306 Max
0.099696
0.068787
0.037879
0.0069706
-0.023938
-0.054846
-0.085754
-0.11666
-0.14757 Min
ANSYS
R17.1
Academic
0.00
200.00 (mm)
100.00
G: Part 1
Equivalent Stress
Type: Equivalent (von-Mises) Stress
Unit: MPa
Time: 1
11/22/2016 5:41 PM
31.339
28.929
26.519
24.109
21.699
19.289
16.879
14.469
12.059
9.6485
7.2384
4.8284
2.4184
0.0083277 Min
ANSYS
R17.1
Academic
0.00
200.00 (mm)
100.00
G: Part 1
Z displacement
Type: Directional Deformation(Z Axis)
Unit: mm
Global Coordinate System
Time: 1
-0.08525
-0.1945
-0.30375
-0.413
-0.52225
-0.6315
-0.74074
-0.84999
-0.95924
-1.0685
-1.1777
-1.287
-1.3962 Min
-1.3788
-1.3962
ANSYS
R17.1
Academic
0.00
200.00 (mm)
100.00

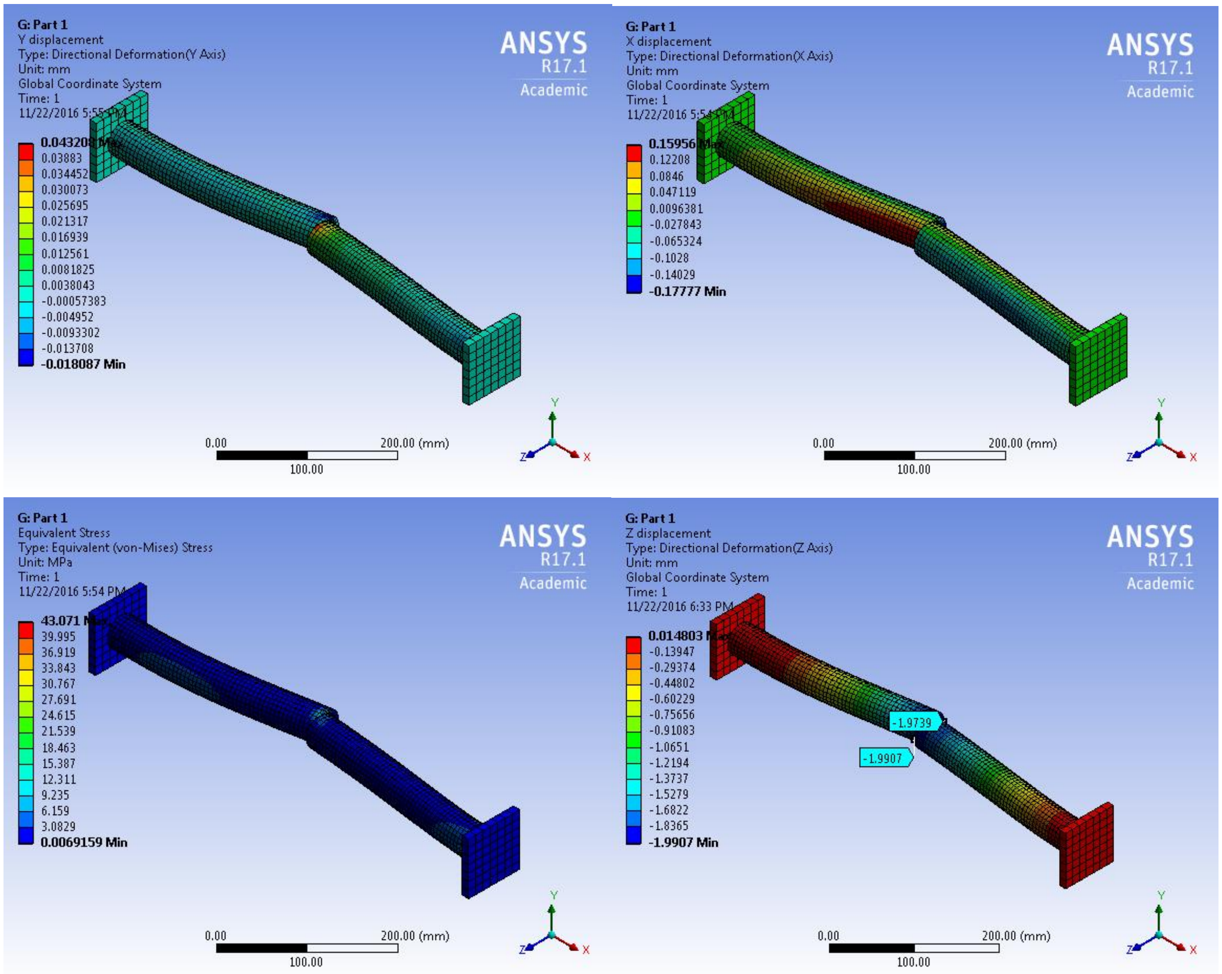
G: Part 1
Y displacement
Type: Directional Deformation(Y Axis)
Unit: mm
Global Coordinate System
Time: 1
0.043208
0.03883
0.034452
0.030073
0.025695
0.021317
0.016939
0.012561
0.0081825
0.0038043
-0.00057383
-0.004952
-0.0093302
-0.013708
-0.018087 Min
ANSYS
R17.1
Academic
0.00
100.00
200.00 (mm)
G: Part 1
X displacement
Type: Directional Deformation(X Axis)
Unit: mm
Global Coordinate System
Time: 1
0.15956
0.12208
0.0846
0.047119
0.0096381
-0.027843
-0.065324
-0.1028
-0.14029
-0.17777 Min
ANSYS
R17.1
Academic
0.00
100.00
200.00 (mm)
G: Part 1
Equivalent Stress
Type: Equivalent (von-Mises) Stress
Unit: MPa
Time: 1
11/22/2016 5:54 PM
43.071
39.995
36.919
33.843
30.767
27.691
24.615
21.539
18.463
15.387
12.311
9.235
6.159
3.0829
0.0069159 Min
ANSYS
R17.1
Academic
0.00
100.00
200.00 (mm)
G: Part 1
Z displacement
Type: Directional Deformation(Z Axis)
Unit: mm
Global Coordinate System
Time: 1
11/22/2016 6:33 PM
0.014803
-0.13947
-0.29374
-0.44802
-0.60229
-0.75656
-0.91083
-1.0651
-1.2194
-1.3737
-1.5279
-1.6822
-1.8365
-1.9907 Min
-1.9739
-1.9907
ANSYS
R17.1
Academic
0.00
100.00
200.00 (mm)

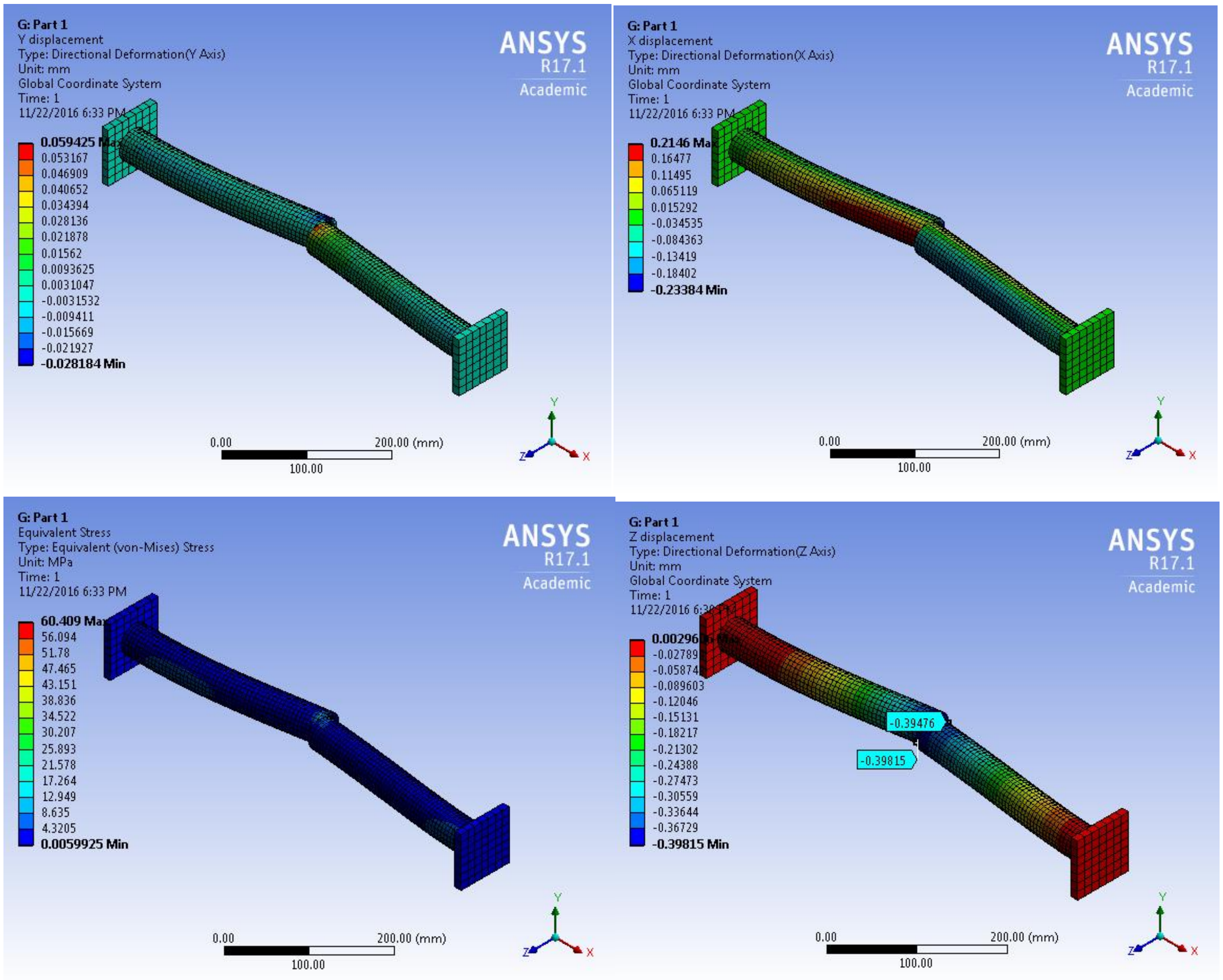
G: Part 1
Y displacement
Type: Directional Deformation(Y Axis)
Unit: mm
Global Coordinate System
Time: 1
11/22/2016 6:33 PM
0.059425 Max
0.053167
0.046909
0.040652
0.034394
0.028136
0.021878
0.01562
0.0093625
0.0031047
-0.0031532
-0.009411
-0.015669
-0.021927
-0.028184 Min
ANSYS
R17.1
Academic
0.00
200.00 (mm)
100.00
G: Part 1
X displacement
Type: Directional Deformation(X Axis)
Unit: mm
Global Coordinate System
Time: 1
11/22/2016 6:33 PM
0.2146 Max
0.16477
0.11495
0.065119
0.015292
-0.034535
-0.084363
-0.13419
-0.18402
-0.23384 Min
ANSYS
R17.1
Academic
0.00
200.00 (mm)
100.00
G: Part 1
Equivalent Stress
Type: Equivalent (von-Mises) Stress
Unit: MPa
Time: 1
11/22/2016 6:33 PM
60.409 Max
56.094
51.78
47.465
43.151
38.836
34.522
30.207
25.893
21.578
17.264
12.949
8.635
4.3205
0.0059925 Min
ANSYS
R17.1
Academic
0.00
200.00 (mm)
100.00
G: Part 1
Z displacement
Type: Directional Deformation(Z Axis)
Unit: mm
Global Coordinate System
Time: 1
-0.02789
-0.05874
-0.089603
-0.12046
-0.15131
-0.18217
-0.21302
-0.24388
-0.27473
-0.30559
-0.33644
-0.36729
-0.39815 Min
-0.39476
-0.39815
ANSYS
R17.1
Academic
0.00
200.00 (mm)
100.00

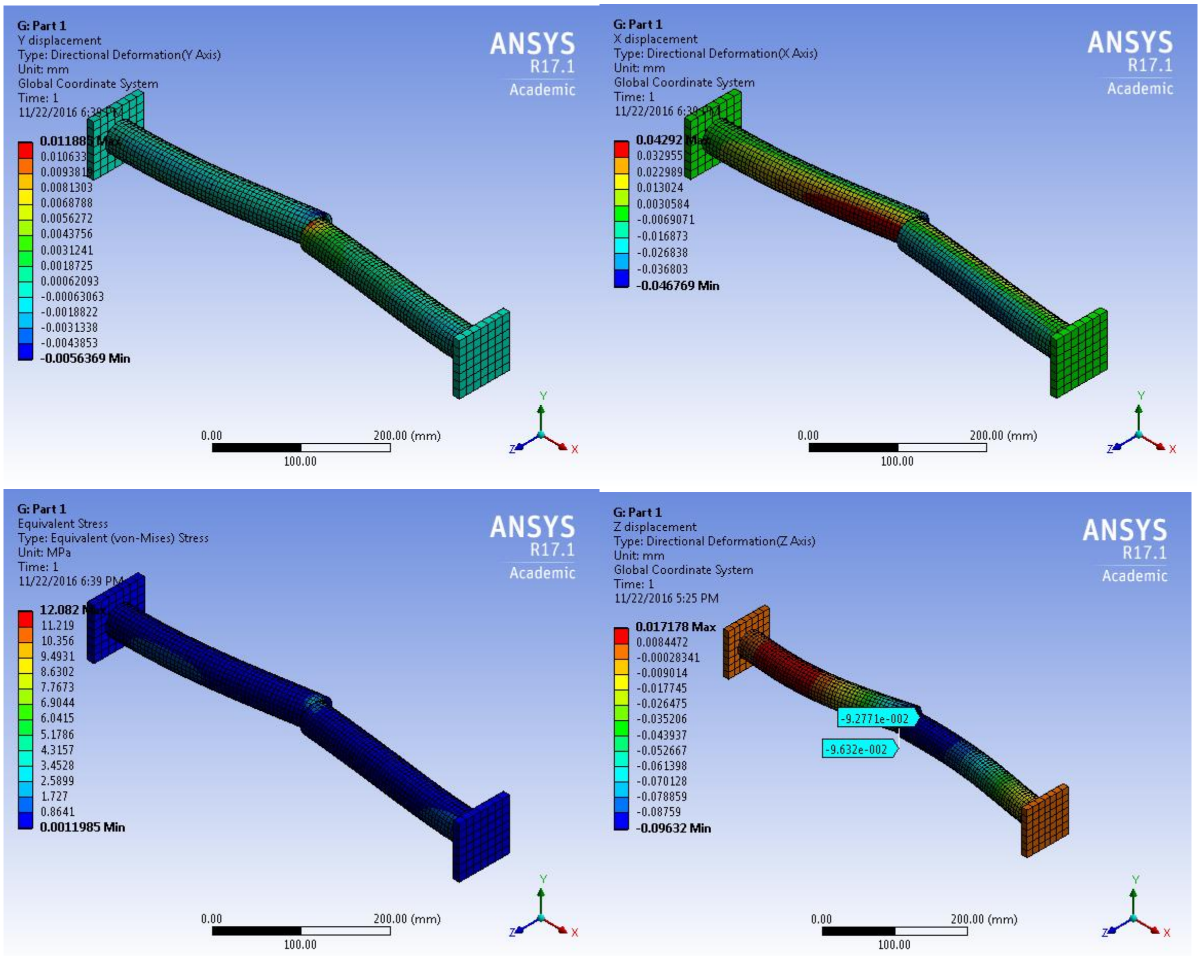
G: Part 1
Y displacement
Type: Directional Deformation(Y Axis)
Unit: mm
Global Coordinate System
Time: 1
ANSYS
R17.1
Academic
0.010633
0.0081303
0.0068788
0.0056272
0.0043756
0.0031241
0.0018725
0.00062093
-0.00063063
-0.0018822
-0.0031338
-0.0043853
-0.0056369 Min
0.00
200.00 (mm)
100.00
G: Part 1
X displacement
Type: Directional Deformation(X Axis)
Unit: mm
Global Coordinate System
Time: 1
ANSYS
R17.1
Academic
0.04292
0.032955
0.022989
0.013024
0.0030584
-0.0069071
-0.016873
-0.026838
-0.036803
-0.046769 Min
0.00
200.00 (mm)
100.00
G: Part 1
Equivalent Stress
Type: Equivalent (von-Mises) Stress
Unit: MPa
Time: 1
ANSYS
R17.1
Academic
12.082
11.219
10.356
9.4931
8.6302
7.7673
6.9044
6.0415
5.1786
4.3157
3.4528
2.5899
1.727
0.8641
0.0011985 Min
0.00
200.00 (mm)
100.00
G: Part 1
Z displacement
Type: Directional Deformation(Z Axis)
Unit: mm
Global Coordinate System
Time: 1
11/22/2016 5:25 PM
ANSYS
R17.1
Academic
0.017178 Max
0.0084472
-0.00028341
-0.009014
-0.017745
-0.026475
-0.035206
-0.043937
-0.052667
-0.061398
-0.070128
-0.078859
-0.08759
-0.09632 Min
-9.2771e-002
-9.632e-002
0.00
200.00 (mm)
100.00

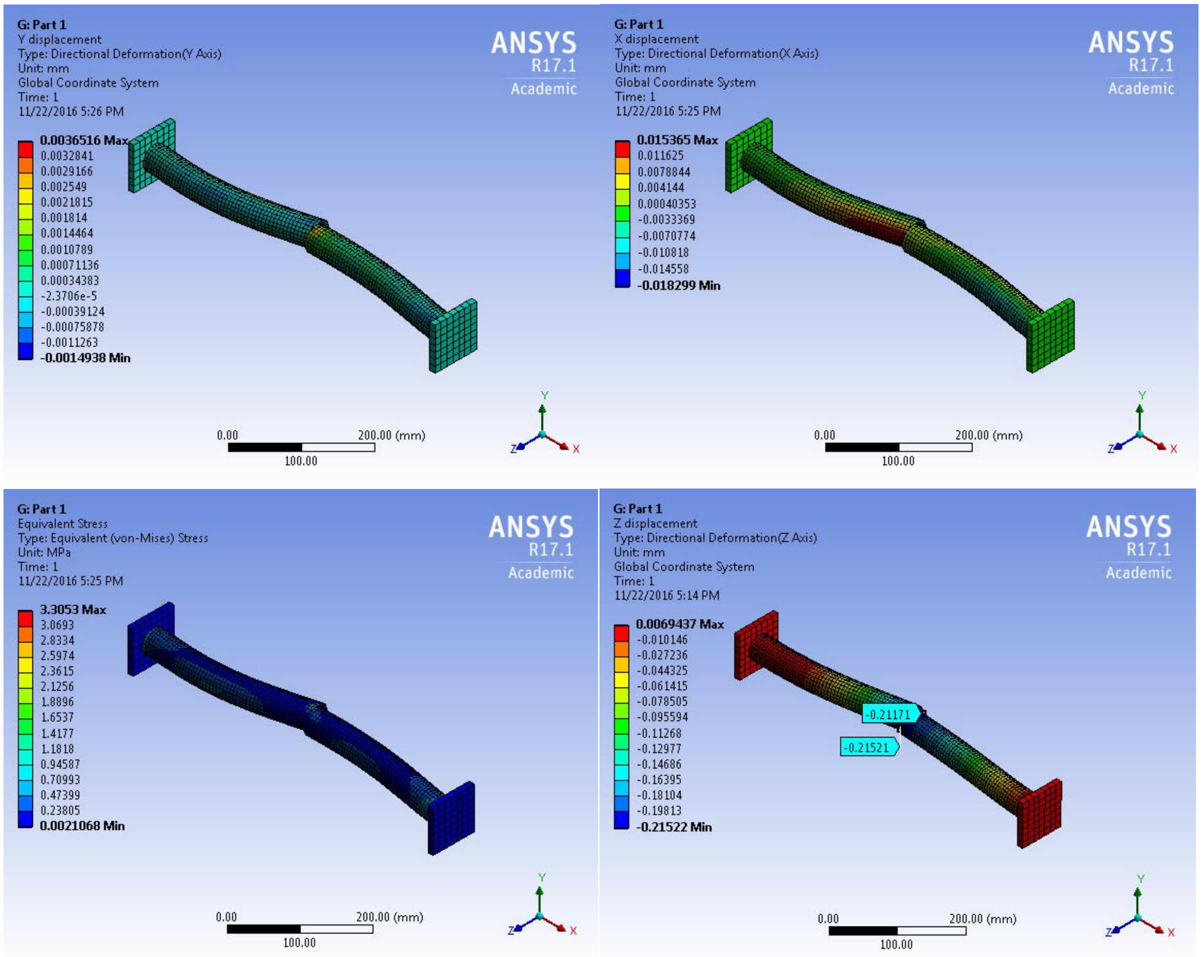
G: Part 1
Y displacement
Type: Directional Deformation(Y Axis)
Unit: mm
Global Coordinate System
Time: 1
11/22/2016 5:26 PM
ANSYS
R17.1
Academic
0.0036516 Max
0.0032841
0.0029166
0.002549
0.0021815
0.001814
0.0014464
0.0010789
0.00071136
0.00034383
-2.3706e-5
-0.00039124
-0.00075878
-0.0011263
-0.0014938 Min
0.00
200.00 (mm)
100.00
G: Part 1
X displacement
Type: Directional Deformation(X Axis)
Unit: mm
Global Coordinate System
Time: 1
11/22/2016 5:25 PM
ANSYS
R17.1
Academic
0.015365 Max
0.011625
0.0078844
0.004144
0.00040353
-0.0033369
-0.0070774
-0.010818
-0.014558
-0.018299 Min
0.00
200.00 (mm)
100.00
G: Part 1
Equivalent Stress
Type: Equivalent (von-Mises) Stress
Unit: MPa
Time: 1
11/22/2016 5:25 PM
ANSYS
R17.1
Academic
3.3053 Max
3.0693
2.8334
2.5974
2.3615
2.1256
1.8896
1.6537
1.4177
1.1818
0.94587
0.70993
0.47399
0.23805
0.0021068 Min
0.00
200.00 (mm)
100.00
G: Part 1
Z displacement
Type: Directional Deformation(Z Axis)
Unit: mm
Global Coordinate System
Time: 1
11/22/2016 5:14 PM
ANSYS
R17.1
Academic
0.0069437 Max
-0.010146
-0.027236
-0.044325
-0.061415
-0.078505
-0.095594
-0.11268
-0.12977
-0.14686
-0.16395
-0.18104
-0.19813
-0.21522 Min
-0.21171
-0.21521
0.00
200.00 (mm)
100.00

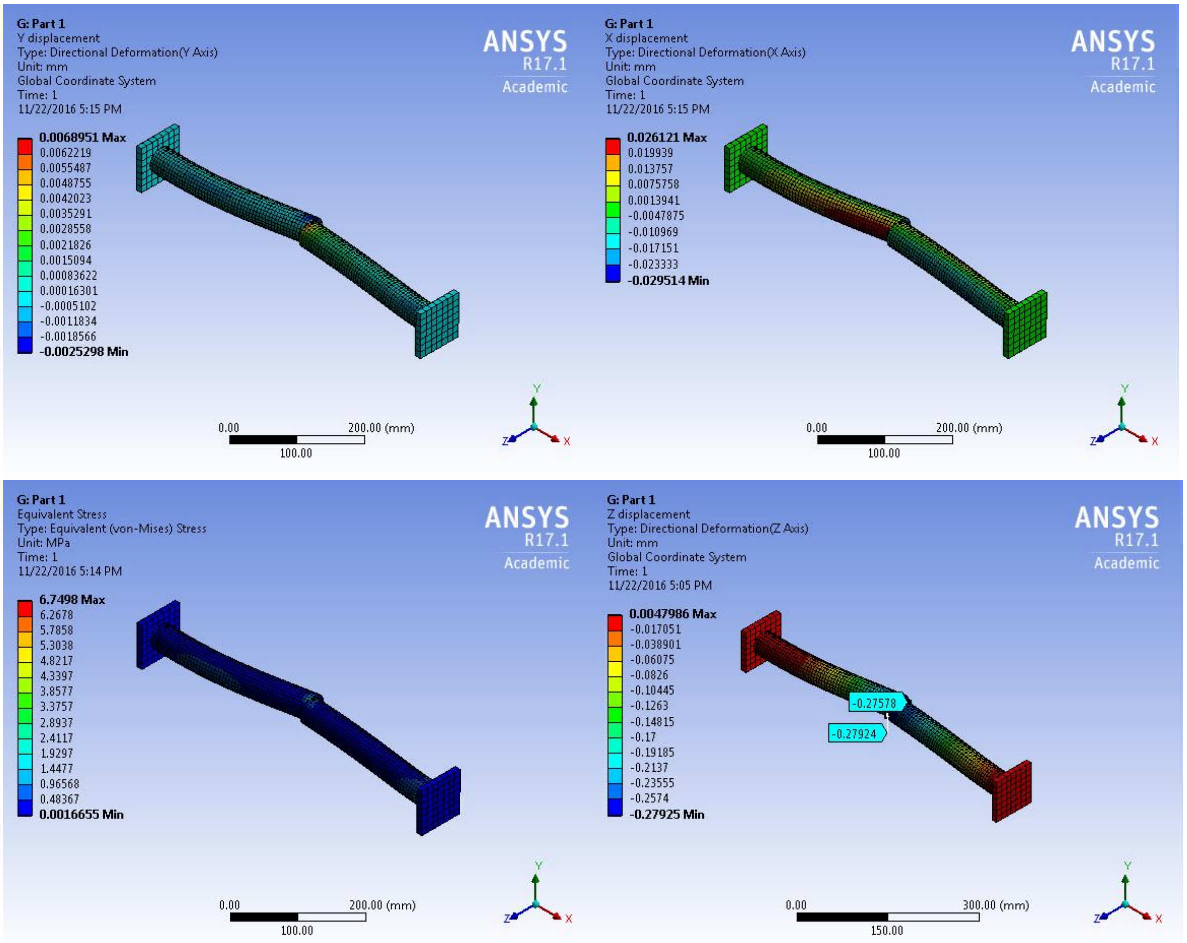
G: Part 1
Y displacement
Type: Directional Deformation(Y Axis)
Unit: mm
Global Coordinate System
Time: 1
11/22/2016 5:15 PM
0.0068951 Max
0.0062219
0.0055487
0.0048755
0.0042023
0.0035291
0.0028558
0.0021826
0.0015094
0.00083622
0.00016301
-0.0005102
-0.0011834
-0.0018566
-0.0025298 Min
ANSYS
R17.1
Academic
0.00
200.00 (mm)
100.00
G: Part 1
X displacement
Type: Directional Deformation(X Axis)
Unit: mm
Global Coordinate System
Time: 1
11/22/2016 5:15 PM
0.026121 Max
0.019939
0.013757
0.0075758
0.0013941
-0.0047875
-0.010969
-0.017151
-0.023333
-0.029514 Min
ANSYS
R17.1
Academic
0.00
200.00 (mm)
100.00
G: Part 1
Equivalent Stress
Type: Equivalent (von-Mises) Stress
Unit: MPa
Time: 1
11/22/2016 5:14 PM
6.7498 Max
6.2678
5.7858
5.3038
4.8217
4.3397
3.8577
3.3757
2.8937
2.4117
1.9297
1.4477
0.96568
0.48367
0.0016655 Min
ANSYS
R17.1
Academic
0.00
200.00 (mm)
100.00
G: Part 1
Z displacement
Type: Directional Deformation(Z Axis)
Unit: mm
Global Coordinate System
Time: 1
11/22/2016 5:05 PM
0.0047986 Max
-0.017051
-0.038901
-0.06075
-0.0826
-0.10445
-0.1263
-0.14815
-0.17
-0.19185
-0.2137
-0.23555
-0.2574
-0.27925 Min
-0.27578
-0.27924
ANSYS
R17.1
Academic
0.00
300.00 (mm)
150.00

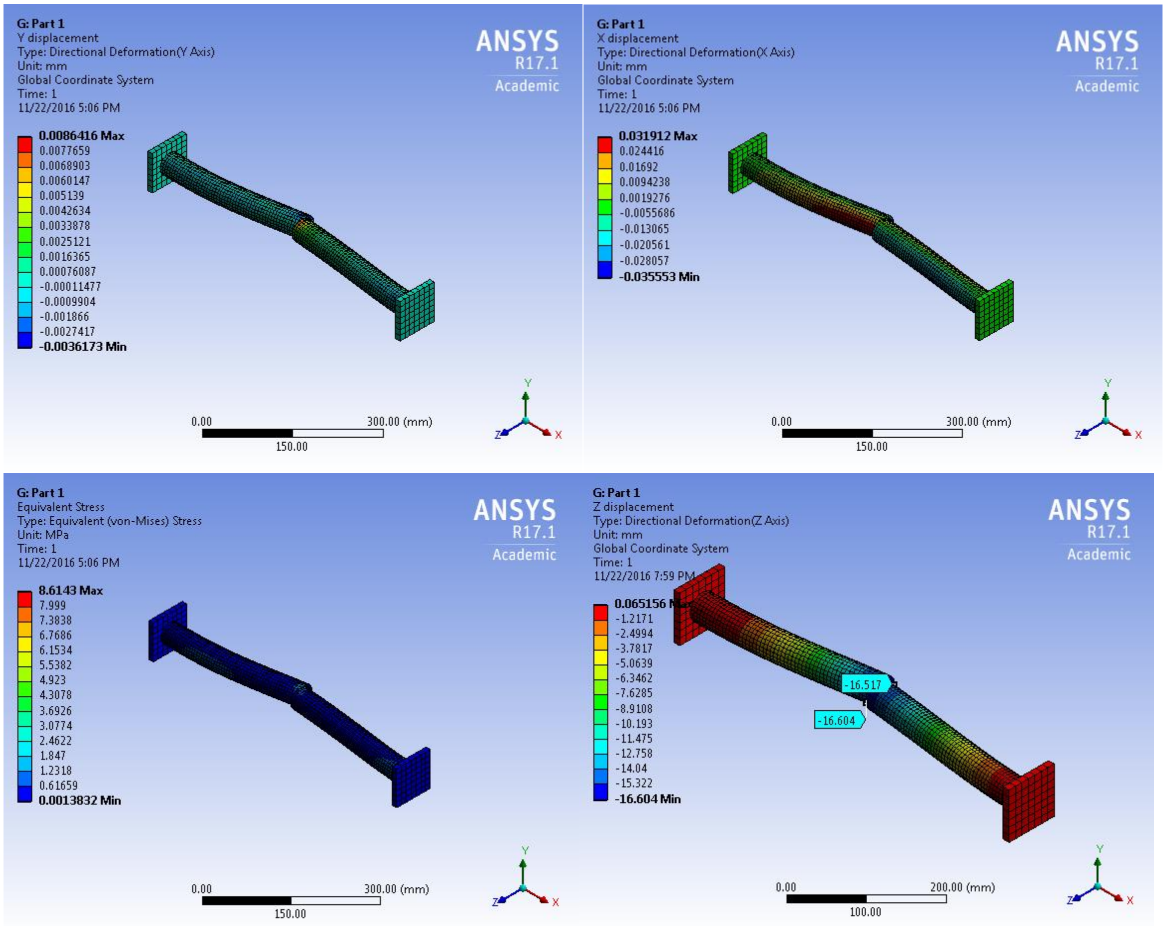
G: Part 1
Y displacement
Type: Directional Deformation(Y Axis)
Unit: mm
Global Coordinate System
Time: 1
11/22/2016 5:06 PM
0.0086416 Max
-0.0036173 Min
ANSYS
R17.1
Academic
G: Part 1
X displacement
Type: Directional Deformation(X Axis)
Unit: mm
Global Coordinate System
Time: 1
11/22/2016 5:06 PM
0.031912 Max
-0.035553 Min
G: Part 1
Equivalent Stress
Type: Equivalent (von-Mises) Stress
Unit: MPa
Time: 1
11/22/2016 5:06 PM
8.6143 Max
0.0013832 Min
G: Part 1
Z displacement
Type: Directional Deformation(Z Axis)
Unit: mm
Global Coordinate System
Time: 1
11/22/2016 7:59 PM
-16.604 Min
-16.517
-16.604

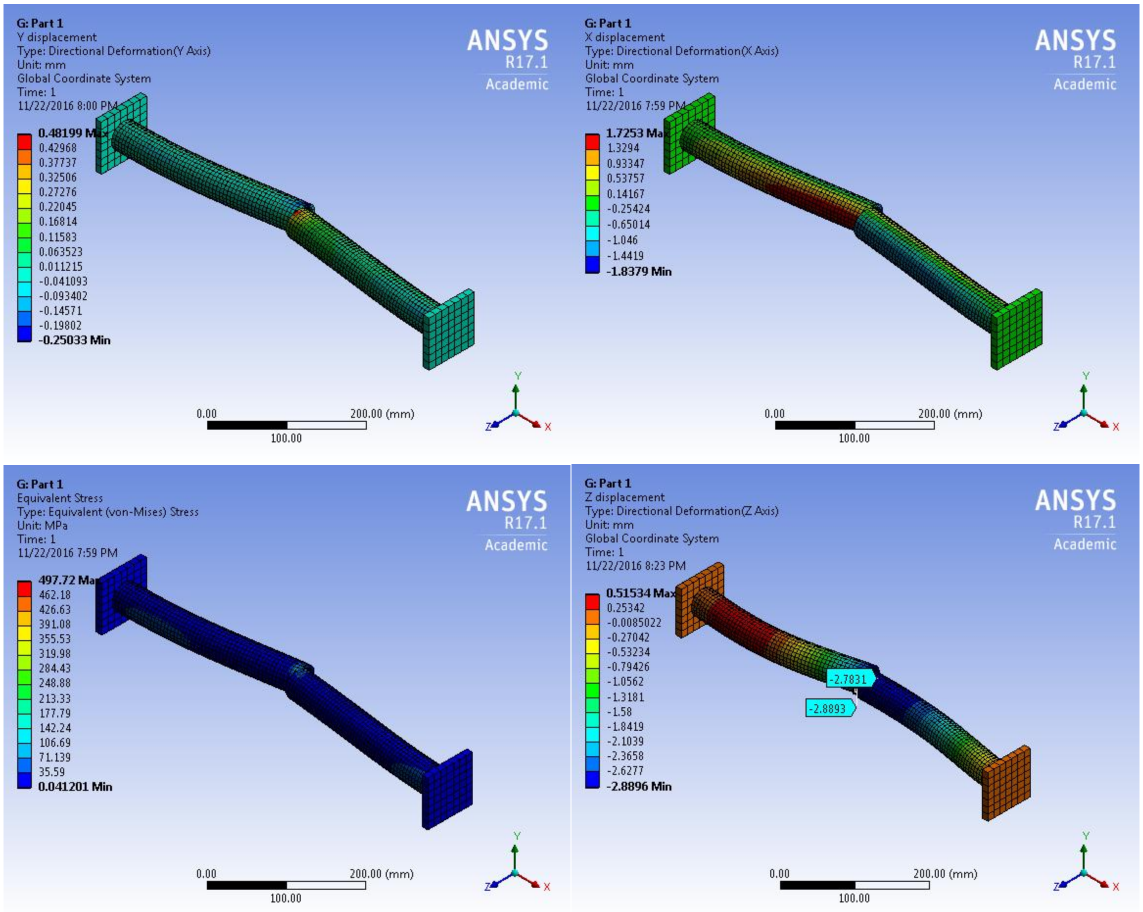
G: Part 1
Y displacement
Type: Directional Deformation(Y Axis)
Unit: mm
Global Coordinate System
Time: 1
11/22/2016 8:00 PM
ANSYS R17.1 Academic
0.48199 Max
0.42968
0.37737
0.32506
0.27276
0.22045
0.16814
0.11583
0.063523
0.011215
-0.041093
-0.093402
-0.14571
-0.19802
-0.25033 Min
0.00
200.00 (mm)
100.00
G: Part 1
X displacement
Type: Directional Deformation(X Axis)
Unit: mm
Global Coordinate System
Time: 1
11/22/2016 7:59 PM
ANSYS R17.1 Academic
1.7253 Max
1.3294
0.93347
0.53757
0.14167
-0.25424
-0.65014
-1.046
-1.4419
-1.8379 Min
0.00
200.00 (mm)
100.00
G: Part 1
Equivalent Stress
Type: Equivalent (von-Mises) Stress
Unit: MPa
Time: 1
11/22/2016 7:59 PM
ANSYS R17.1 Academic
497.72 Max
462.18
426.63
391.08
355.53
319.98
284.43
248.88
213.33
177.79
142.24
106.69
71.139
35.59
0.041201 Min
0.00
200.00 (mm)
100.00
G: Part 1
Z displacement
Type: Directional Deformation(Z Axis)
Unit: mm
Global Coordinate System
Time: 1
11/22/2016 8:23 PM
ANSYS R17.1 Academic
0.51534 Max
0.25342
-0.0085022
-0.27042
-0.53234
-0.79426
-1.0562
-1.3181
-1.58
-1.8419
-2.1039
-2.3658
-2.6277
-2.8896 Min
-2.7831
-2.8893
0.00
200.00 (mm)
100.00

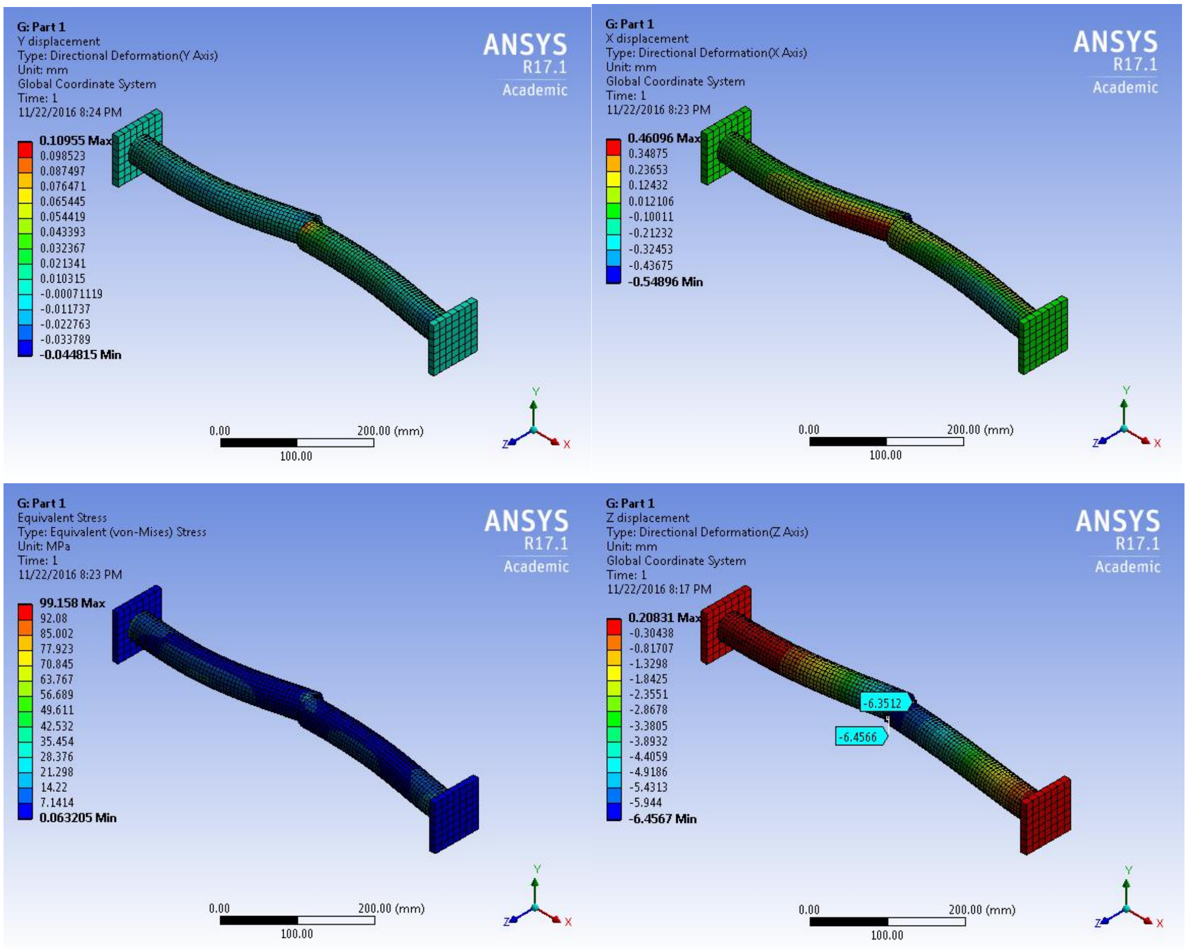
G: Part 1
Y displacement
Type: Directional Deformation(Y Axis)
Unit: mm
Global Coordinate System
Time: 1
11/22/2016 8:24 PM
0.10955 Max
0.098523
0.087497
0.076471
0.065445
0.054419
0.043393
0.032367
0.021341
0.010315
-0.00071119
-0.011737
-0.022763
-0.033789
-0.044815 Min
ANSYS
R17.1
Academic
0.00
200.00 (mm)
100.00
G: Part 1
X displacement
Type: Directional Deformation(X Axis)
Unit: mm
Global Coordinate System
Time: 1
11/22/2016 8:23 PM
0.46096 Max
0.34875
0.23653
0.12432
0.012106
-0.10011
-0.21232
-0.32453
-0.43675
-0.54896 Min
ANSYS
R17.1
Academic
0.00
200.00 (mm)
100.00
G: Part 1
Equivalent Stress
Type: Equivalent (von-Mises) Stress
Unit: MPa
Time: 1
11/22/2016 8:23 PM
99.158 Max
92.08
85.002
77.923
70.845
63.767
56.689
49.611
42.532
35.454
28.376
21.298
14.22
7.1414
0.063205 Min
ANSYS
R17.1
Academic
0.00
200.00 (mm)
100.00
G: Part 1
Z displacement
Type: Directional Deformation(Z Axis)
Unit: mm
Global Coordinate System
Time: 1
11/22/2016 8:17 PM
0.20831 Max
-0.30438
-0.81707
-1.3298
-1.8425
-2.3551
-2.8678
-3.3805
-3.8932
-4.4059
-4.9186
-5.4313
-5.944
-6.4567 Min
-6.3512
-6.4566
ANSYS
R17.1
Academic
0.00
200.00 (mm)
100.00

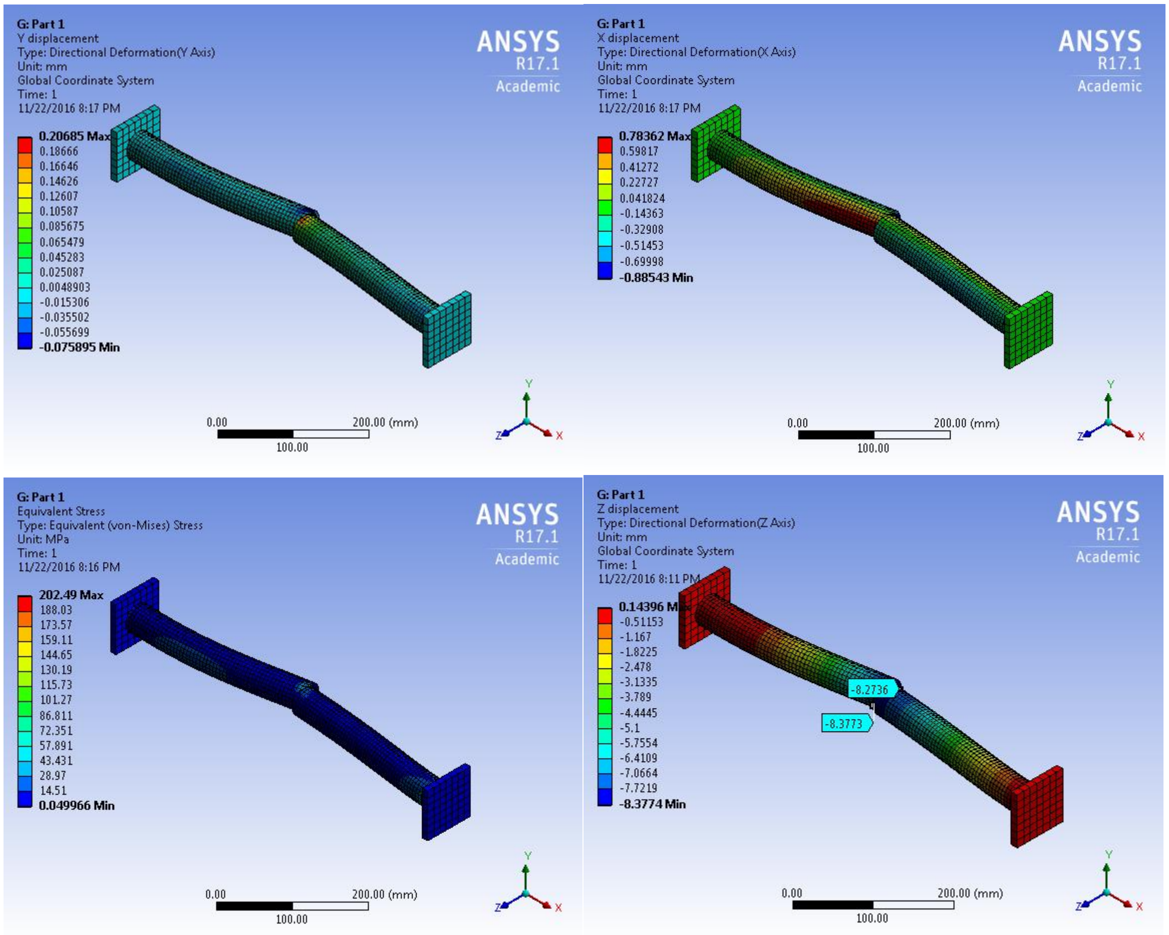
G: Part 1
Y displacement
Type: Directional Deformation(Y Axis)
Unit: mm
Global Coordinate System
Time: 1
11/22/2016 8:17 PM
ANSYS
R17.1
Academic
0.20685 Max
0.18666
0.16646
0.14626
0.12607
0.10587
0.085675
0.065479
0.045283
0.025087
0.0048903
-0.015306
-0.035502
-0.055699
-0.075895 Min
0.00
200.00 (mm)
100.00
Y
Z
X
G: Part 1
X displacement
Type: Directional Deformation(X Axis)
Unit: mm
Global Coordinate System
Time: 1
11/22/2016 8:17 PM
ANSYS
R17.1
Academic
0.78362 Max
0.59817
0.41272
0.22727
0.041824
-0.14363
-0.32908
-0.51453
-0.69998
-0.88543 Min
0.00
200.00 (mm)
100.00
Y
Z
X
G: Part 1
Equivalent Stress
Type: Equivalent (von-Mises) Stress
Unit: MPa
Time: 1
11/22/2016 8:16 PM
ANSYS
R17.1
Academic
202.49 Max
188.03
173.57
159.11
144.65
130.19
115.73
101.27
86.811
72.351
57.891
43.431
28.97
14.51
0.049966 Min
0.00
200.00 (mm)
100.00
Y
Z
X
G: Part 1
Z displacement
Type: Directional Deformation(Z Axis)
Unit: mm
Global Coordinate System
Time: 1
11/22/2016 8:11 PM
ANSYS
R17.1
Academic
0.14396 Max
-0.51153
-1.167
-1.8225
-2.478
-3.1335
-3.789
-4.4445
-5.1
-5.7554
-6.4109
-7.0664
-7.7219
-8.3774 Min
-8.2736
-8.3773
0.00
200.00 (mm)
100.00
Y
Z
X

REFERENCES

Beam deflection formulas. (2016, May 2). Retrieved from http://ruina.mae.cornell.edu/Courses/ME4735-2012/Rand4770Vibrations/BeamFormulas.pdf

Bingul, Z., & Karahan, O. (2012). *Dynamic Modeling and Simulation of Stewart Platform* . INTECH Open Access Publisher.

Christensen, S. (2014). *The design of a Stewart-Gough Platform as a Test Setup.* Aalborg University.

Craig, J. J. (1986). *Introduction to Robotics: Mechanics and Control.*

Dasgupta, B., & Mruthyunjaya, T. (2000). The Stewart platform manipulator: A review. Mechanism and Machine Theory. 15-40.

Dept. of Energy. Office of Scientific and Technical information. (2005). *The importance of Motor Shaft Alignment.* Washington.

Dimiter Zlatanov, I. B. (2002). *Constraint Singularities as C-Space Singularities.* International Symposium on Advances in Robot Kinematics . Retrieved from http://www.parallemic.org/Reviews/Review008.html

Ding, B. (2014). *A Study of a Gough-Stewart Based Manipulator for Applications in Biomechanical Testing.*

Doug, S. (1965, June). A platform with six degrees of freedom. *Proceedings of the Institution of mechanical engineers*, pp. 371-380.

Duffy, J., & Crane, C. (1997). *Research proposal submitted to the National Science Foundation.* Gainesville USA: University of Florida.

Firgelli Automations. (2016, April 23). *Firgelli Automations*. Retrieved from Feedback rod linear actuators: https://www.firgelliauto.com/products/feedback-rod-actuator

Furqan, M., & Suhaib, M. (2014, October). Some Studies on Parallel Manipulator – A Review. *Journal of Basic and Applied Engineering Research*, *1*(3), 99-104.

Ganem, F. (2000). *Bone Fixing Device in particular for Fixing to the Sacrum during Osteosynthesis of the Backbone.*

Gao, X.-s., Lei, D., Liao, Q., & Zhang, G.-f. (2003). Generalized Stewart platforms and their direct Kinematics. *IEEE Trans.Robotics, 2(2)*, 141-151.

Gitlin, D. (2010, June 30). Retrieved from Tech Briefs: http://contest.techbriefs.com/2010/entries/medical/1018

Gong, Y. (1992). *Design Analysis of a Stewart platform.*

Hanieh, A. A. (2003). *Active isolation and damping of vibrations via stewart platform.* Active Structrue Laboratory, ULB, PH.D. Thesis.

Hartt, B., Gilchrist, B., & Truman, V. (2012). *Hexapod linear actuators.*

Hopkins, B. R., & Williams II, R. L. (2002). Kinematics, design and control of the 6-PSU Platform. *Industrial Robot: An International Journal, 29*(5), 443-451.

Houdek II, P. J. (1997). *Design and Implementation Issues for Stewart Platform Configuration Machine Tools.* Massachusetts Institute of Technology.

Howland, R. S., Richard, S. M., & Kenneth, P. (1996). *Interspinous Segmental Spine Fixation Device.*

Jaffe, D. L., Nelson, D., & Thiemer, J. (2012). *Assistive Robotics.* Stanford University.

Jakobovic, D., & Budin, L. (2002). *Forward Kinematics of a stewart platform mechanism.* Faculty of Electrical Engineering and Computing.

Khalil, W., & Guegan, S. (2004). Inverse and Direct Dynamic Modeling of Gough-Stewart Robots. *IEEE Transactions on Robotics and Automation*, 754-761.

Kumar, V. (1992, September). Characterization of workspaces of parallel manipulators. *Transactions of the ASME, journal ofMechanical Design*, *114*, 368-375.

Lazarevic, Z. (1997). *Feasibility of a stewart platform with fixed actuators as a platform for CABG surgery device.*

Lopes, A. M. (2009). Dynamic modeling of a stewart platform using the generalized momentum approach. *Communications in Nonlinear Science and Numerical Simulation, 14*(9), 3389-3401.

Madsen, A. L., & Kristensen, S. G. (2012). *Design of Stewart Platform for wave compensation.* Aalborg University.

Majid, M., Huang, Z., & Yao, Y. (2000). Workspace analysis of a six-degrees of freedom, three-prismatic-prismatic-spheric-revolute parallel manipulator. *The international Journal of Advanced Manufacturing Technology, 6*, 441-449.

Mcmaster-carr. (2016, April 23). Retrieved from Ball Joint Rod Ends: http://www.mcmaster.com/#spherical-ball-joints/=11yrcbe

Merlet, J. (1994). Parallel manipulators: state of the art and perspectives. *Advanced Robotics, 8*(6), 589-596.

Mikrolar. (2016, May 2). Retrieved from The Hexapod: http://mikrolar.com/hexapod.html

Nguyen, C. C., Antrazi, S. C., Zhou, Z.-L., & Campbell Jr, C. E. (1991). Analysis and implementation of a 6 DOF stewart platform-based robotic wrist. *Computers & Electrical Engineering, 17*(3), 191-203.

Paley, D. (2011). History and Science Behind the Six-Axis CorrectionExternal Fixation Devices in Orthopaedic Surgery. *Operative Techniques in Orthopaedics*, 125-128.

Plessis, L. J. (1999). *An optimization approach to the determination of manipulator work spaces.* University of Pretoria.

Raymond, L. W. (n.d.). *Pediatric Orthopaedic Surgery*. Retrieved from External Fixator: http://www.raymondliumd.com/Conditions_External_Fixation.html

Skorrogan. (2009, January 25). Retrieved from Wikimedia: https://commons.wikimedia.org/wiki/File:Adam_Frame.jpg

Szatmari, S. (1999). GEOMETRICAL ERRORS OF PARALLEL ROBOTS. *43*(2), 152-162.

Szufnarowski, F. (2013). *Stewart platform with fixed rotary actuators: A low cost design study*. Advances in Medical robotics.

Thondel, E. (2010). *Electric motion platform for use in simulation technology–design and optimal control of a linear electromechanical actuator.* Proceedings of the World Congress on Engineering and Computer Science.

Wang, J., & Gosselin, C. (1997). Kinematic analysis and singularity representation of spatial. *Journal or robotic systems, 14*(12), 851-869.

Zhang, B. (2005). *DESIGN AND IMPLEMENTATION OF A 6 DOF PARALLEL MANIPULATOR.*

Zhang, D., & Gosselin, C. M. (2000). Kinetostatic Modeling of N-DOF Parallel Mechanisms With a Passive Constraining Leg and Prismatic Actuators. *Journal of Mechanical Design, 123*(3).